

## LEXNET Low EMF Exposure Future Networks

# D4.3: Final validation and recommendations for smart low exposure index

Contractual delivery date: M36 Actual delivery date: M36

#### **Document Information**

Version	V1.1	Dissemination level	PU						
Editor	Y. Fernández (T1	Y. Fernández (TTI)							
Other authors	Fang (FLE), M. A.Sánchez (TTI),	S. Bories (CEA), A. De Domenico (CEA), A. Clemente (CEA), Y. Fang (FLE), M. Lalam (SAG), Y. Pinto (TPT), X. Begaud (TPT), A.Sánchez (TTI), P. Chambers (UNIS), T. Brown (UNIS), E. Kocan (UoM), M. Pejanovic-Djurisic (UoM), D. Dragomir (UPB), A. Voinescu (UPB)							
Abstract	evaluation. It cor methodology for consolidated resi shown. WP4 and attempt to position	D4.3 presents the final absolute pletes the 5-steps common extracted and participations are deligated as a second conclusions are deligated as a second conclusion and participation and conclusions on a second conclusion and conclusions on a second conclusion and conclusions on a second conclusion and conclusions are deligated as a second conclusion.	posure evaluation d solutions. The nk techniques are vered and notably common EI axis in						

#### PROPRIETARY RIGHTS STATEMENT

This document contains information, which is proprietary to the LEXNET Consortium. Neither this document nor the information contained herein shall be used, duplicated or communicated by any means to any third party, in whole or in parts, except with prior written consent of the LEXNET consortium.





2

Key words	Down-selection,	common	evaluation	methodology,	validation
	framework, Expo	sure Index	improvement	Ĭ	

#### **Project Information**

Grant Agreement n°	318273
Dates	1 <sup>st</sup> November 2012 – 31th October 2015

#### Document approval

Name	Position in project	Organisation	Date	Visa
Joe Wiart	Coordinator	Orange	09/11/2015	OK

#### **Document history**

Version	Date	Modifications	Authors
V1.0	06/11/15	Final edition version	Y. Fernández
V1.1	09/11/15	Final review	S. Bories

Version: V1.1



## Table of contents

1	INTRODUCTION	12
2	EVALUATION FRAMEWORK: THE EI EVALUATION COMMON METHOD ANALYSIS	
2.1	REMINDS ON THE PROPOSED COMMON EVALUATION METHODOLOGY	
	2.1.1 STEP-1: SUB-SCENARIOS DESCRIPTION	
	2.1.3 STEP-3: EL RATIO EVALUATION	
	2.1.4 STEP-4: CAPACITY/QOS IMPROVEMENTS CONVERTION INTO EI REDUCTION	
	2.1.5 STEP-5: GLOBAL EI REDUCTION ASSESSMENT	
2.2	REMINDER ON THE GENERAL CONCEPTS OF ABSOLUTE EI CALCULATION	16
2.3	ADVANTAGES AND LIMITATIONS FOR DOWN-SELECTION PURPOSE	17
3	LOW EMF TECHNOLOGIES CONSOLIDATED RESULTS	19
3.1	Rural scenario	19
	3.1.1 SCENARIO INPUTS	
	3.1.2 SOLUTION A - LOW EXPOSURE COOPERATIVE COMMUNICATION TECHNIQUES EVALUATIO	N 19
3.2	Purban scenario	
	3.2.1 SCENARIO INPUTS	
	3.2.2 SOLUTION B- SMALL AND DIRECTIVE ANTENNA FOR LOW EXPOSURE INDEX	
	3.2.3 SOLUTION C —ENHANCED DTX FOR LOW EMF COMMUNICATIONS	
	3.2.4 SOLUTION D - LOW NOISE RECEIVER ARCHITECTURE	
3 3	3.2.3 SOLUTION E- ENHANCED EFFICIENCY IN REFERENCE SYMBOLS USAGE	
3.3	3.3.1 WI-FI SCENARIO INPUTS	
	3.3.2 WSN SCENARIO INPUTS	
	3.3.3 SOLUTION F - ANTENNA ON TERMINAL FOR LOW EXPOSURE INDEX	
	3.3.4 SOLUTION G – BEAMFORMING TECHNIQUES	58
	3.3.5 SOLUTION H - SLEEP/IDLE MODE IN A MESH GATEWAY DEPLOYMENT	65
	3.3.6 SOLUTION I – INTERFERENCE MITIGATION IN ZIGBEE & WI-FI	76
	3.3.7 SOLUTION J – RADIO LINK ALLOCATION	78
4	WP4 TECHNOLOGIES POSITIONING ON ABSOLUTE EI (STEP 5)	86
5	CONCLUSIONS AND RECOMMENDATIONS FOR SMART LOW EXPOSURE INDEX	90
6	REFERENCES	92
7	APPENDIX 1: INTERNAL REVIEW	95
8	APPENDIX 2: FLEORMULA & ASSOCIATED INPUT DATA	96



4

## List of acronyms

Abbreviation	Meaning
3GPP	Third generation partnership project
ACK	Acknowledgement
ADC	Analog to Digital Converter
AF	Amplify-and-forward
AMC	Artificial Magnetic Conductor
AP	Access point
BCH	Broadcast channel
BER	Bit error rate
BPF	Bandpass filter
BS	Base Station
BSS	Basic service set
CDF	Cumulative distribution function
COMP	Coordinated multipoint transmission
CP	Closing period
CQI	Channel quality indicator
CRS	Cell specific reference signal
CSI	Channel state information
CSMA/CA	Carrier sense multiple access with collision avoidance
CSRS	Cell specific reference signal
D	Destination terminal
DAC	Digital to Analog Converter
DBDC	Dual-band dual-concurrent
DDC	Digital Down Converter
DF	Decode-and-forward
DL	Downlink
DMRS	Demodulation reference signals
DTX	Discontinuous Transmission
DUC	Digital Up Converter
EBG	Electromagnetic Band Gap
EE	Energy efficiency
El	Exposure Index
EM	Electromagnetic
EMF	Electromagnetic field
eNB	Evolved Node B
FQL	Fuzzy Q-learning
HA	High affluence
HetNet	Heterogeneous Network
HIS	High Impedance Surface

Version: V1.1

FP7 Contract n°318273



**HPF** Highpass filter

I/Q In-phase and Quadrature components

**ICT** Information and communications technologies **IEEE** Institute of electrical and electronics engineers

Intermediate frequency IF **IFA** Inverted F Antenna

**IFFT** Inverse fast fourier transformation

ILA Inverted L Antenna InH **Indoor Hotspot** ISD Inter-site distance

ISM industrial, scientific and medical KPI **Key Performance Indicator** 

Low noise amplifier LNA

LOS Line of sight LPF Lowpass filter

LTE Long term evolution

LTE-A Long term evolution advanced

MA Middle affluence

MAC Medium access control

MC Macro cell

**MCS** Modulation and coding scheme

MeNB Macro eNB

MIMO Multiple Input Multiple Output Negative acknowledgement **NACK** 

NF Noise figure **NLOS** Non line of sight

**OFDM** Orthogonal frequency division multiplexing

PCB Printed Circuit Board

**PDSCH** physical downlink shared channel

PR Primary receiver

**PRB** Physical resource block PRR Packet reception rate

**QAM** Quadrature amplitude modulation

QoS Quality of service R Relay station

RAT Radio access technology

RB Resource block RE Resource element RF Radio frequency

Resistive High Impedance Surface RHIS

Reinforcement learning RL

**RMC** Reference measurement channel

RS Reference symbol

Version: V1.1

5

FP7 Contract n°318273



6

RSRP Reference signal received power
RSSI Received signal strength indicator

Rx Receiver

S Source of information SAR Specific absorption rate

SC Small Cell

SCeNB Small Cell eNB

SCM Subcarrier mapping

SINR Signal to interference plus noise ratio

SIR Stepped Impedance Resonator

SISO Single Input Single Output

SNR Signal to noise ratio

SotA State of the art

SSS Secondary synchronization signal

STA Station

TAS Transmit antenna selection
TCP Transmission control protocol

TDD Time division duplex

Tx Transmitter

TXOP Transmit opportunity
UE User Equipment

UL Uplink

UMTS Universal mobile telecommunications system

VoLTE Voice over LTE WAN Wide area network

WCDMA Wideband code division multiple access

Wi-Fi Wireless fidelity

WiMAX Worldwide interoperability for microwave access

WLAN Wireless local area network WMN Wireless mesh network

WP Work package

WSN Wireless sensor network WWAN Wireless wide area network

Version: V1.1



## List of figures

FIGURE 1. COMMON EI EVALUATION METHODOLOGY FOR WP4 SOLUTIONS
FIGURE 3. AVERAGE ACHIEVABLE RATES PER SUBCARRIER FOR THE ANALYSED OFDM RELAY SYSTEMS
OUTDOOR USER2
FIGURE 4. AVERAGE ACHIEVABLE RATES PER SUBCARRIER FOR THE ANALYSED OFDM RELAY SYSTEMS
INDOOR USER
FIGURE 5. A) BLOCK DIAGRAM OF A CONVENTIONAL DIGITAL BEAM-FORMING TRANSMITTER/RECEIVER SYSTEM
AND B) ARCHITECTURE BASED ON ELECTRONICALLY RECONFIGURABLE PARASITIC ARRAY ANTENNA 2
FIGURE 6. UL AND DL CUMULATIVE DISTRIBUTION FUNCTIONS OF THE DAILY AVERAGE EI AT UES FOR
DIFFERENT ANTENNAS
FIGURE 7. CUMULATIVE DISTRIBUTION FUNCTIONS OF THE DAILY AVERAGE EI AT UES FOR DIFFEREN
ANTENNAS
FIGURE 8. CUMULATIVE DISTRIBUTION FUNCTIONS OF THE AVERAGE ULSINR AT SCS WITH RESPECT TO
DIFFERENT ANTENNA PATTERNS
FIGURE 9. CUMULATIVE DISTRIBUTION FUNCTIONS OF THE AVERAGE DL SINR AT UES WITH RESPECT TO
DIFFERENT ANTENNA PATTERNS
FIGURE 10. LTE DL RADIO FRAME SHOWING CSRS FOR ONE ANTENNA PORT, DL CONTROL REGION (PDCCH
WITH A SIZE OF ONE OFDM SYMBOL, PRIMARY AND SECONDARY SYNCHRONIZATION SIGNALS (PSS AN
SSS), AND BROADCAST CHANNEL (BCH)[14].
FIGURE 11. EMF GAIN VS NUMBER OF ACTIVE UES FOR DIFFERENT DTX CONTROLLER
FIGURE 12. USER LATENCY VS. THE NUMBER OF ACTIVE UES
FIGURE 13. BLOCK DIAGRAM OF THE RECONFIGURABLE LOW NOISE RECEIVER
FIGURE 14. THE RECONFIGURABLE BPF DESIGN: A) BLOCK DIAGRAM AND B) PROTOTYPE
FIGURE 15. MEASURED RESULTS IN THE BPF PROTOTYPE: A) INSERTION LOSS AND B) RETURN LOSS
FIGURE 16. ANTENNA PORT 1 CONFIGURED FOR DMRS IN THE 2 CRS PORTS CASE
FIGURE 17. DMRS CONFIGURED ON 3 CRS ANTENNA PORTS IN THE 4 CRS PORTS CASE IN LTE RBs 48
FIGURE 18. A NEW DMRS PATTERN CONFIGURED ON 2 CRS ANTENNA PORTS IN THE 4 CRS PORTS CASE 49
FIGURE 19. STUDYING CASES: A) REFERENCE CASE, MONOPOLE ANTENNA AT THE CENTER. B) REALISTIC
CASE, IFA ANTENNA AT THE MIDDLE OF THE EDGE
FIGURE 20. SPATIAL DISTRIBUTION OF SAR 10G FOR THE CASE WITH MONOPOLE ANTENNA IN FRONT OF TH
FLAT PHANTOM
FIGURE 21. SPATIAL DISTRIBUTION OF SAR 10G FOR THE CASE WITH MONOPOLE ANTENNA ON THE OTHER
SIDE OF THE PCB
FIGURE 22. SPATIAL DISTRIBUTION OF SAR 10G FOR THE CASE WITH IFA ANTENNA IN FRONT OF THE FLA
PHANTOM
FIGURE 23. SPATIAL DISTRIBUTION OF SAR 10G FOR THE CASE WITH IFA ANTENNA ON THE OTHER SIDE O
THE PCB
Figure 24. Top-row: Histograms of the phase offset between Tx samples, $\Delta \theta Tx$ , for various
ANGLES, $\theta Null$ , for the case of null steering. Bottom-row: Histograms of the phase offse
BETWEEN TX SAMPLES, $\Delta \theta Tx$ , FOR VARIOUS ANGLES, $\theta SAR$ , FOR THE CASE OF SAR CODES
FIGURE 25. HISTOGRAMS OF THE PHASE OFFSET BETWEEN TX SAMPLES, $\Delta \theta Tx$ , FOR THE HYBRID TECHNIQUE
WHERE $\theta SAR$ IS SET $\theta SAR = \{450\}$ AND VARIOUS ANGLES, $\theta Null$ , ARE APPLIED
FIGURE 26. BASEBAND NULL STEERING: RECEIVED POWER AT CHEST FROM THE FIRST PAIR OF MIMO
ANTENNAS, 'PROBE PAIR 1'
•
PAIR 1'. 62
FIGURE 28. FIRST ORDER STATISTICS OF $\theta min$ , the angle that minimises exposure
FIGURE 29. THE EFFECT OF NULL STEERING (LEFT) AND THE HYBRID TECHNIQUE (RIGHT) ON THE AP POWER
GAIN IN THE UL BASED ON TWO CHANNELS, 'AP PAIR 1' AND, 'AP PAIR 2'
FIGURE 30. THE EFFECT OF NULL STEERING (LEFT) AND THE HYBRID TECHNIQUE (RIGHT) ON NEIGHBOURING
USERS FOR 6 POSITIONS, 1-6 DEPICTED.
FIGURE 31. ITU-R INH-BASED LAYOUT WITH 3 APS
FIGURE 32. DAY SEGMENTATION
FIGURE 33. STA DROP POSITIONS (WHITE CIRCLE)
FIGURE 34. GROWTH OF CONNECTED WEARABLE DEVICES

Version: V1.1 Dissemination level: PU



FIGURE 35. GROWTH OF EI VALUES FOR WSNS	. 82
FIGURE 36. EXAMPLE OF SENSOR NODES USED IN SOLUTION EVALUATION	. 84
FIGURE 37. POWER DENSITY THROUGHOUT THE DAY	. 84
FIGURE 38. SYNTHESIS OF THE WP4 SOLUTIONS TO REDUCE EMF POSITIONED ON A COMMON ABSOLUTE	ΞΕ
AXIS FOR 4 SCENARIOS BASED ON 2014-2015 ICT LISAGES DETAILED IN LEXNETD2.8	80

Version: V1.1



## List of tables

TABLE 1.	EI RATIO FOR THE ANALYSED OFDM RELAY SYSTEMS - OUTDOOR USER	22
TABLE 2.	EI RATIO FOR THE ANALYSED OFDM RELAY SYSTEMS - INDOOR USER	23
TABLE 3.	EI VALUES FOR OFDM DF RELAY SYSTEM AND EI REDUCTION IN PER CENTS ATTAINED WITH	THE
PROP	OSED SOLUTIONS	24
TABLE 4.	El reduction in per cents attained with the proposed solutions	
TABLE 5.	MAIN SIMULATION PARAMETERS	29
TABLE 6.	SIMULATION PARAMETERS	37
TABLE 7.	SYSTEM LEVEL ANALYSIS IN THE REFERENCE RECEIVER (LTE BAND 20)	41
TABLE 8.	SYSTEM LEVEL ANALYSIS IN THE REFERENCE RECEIVER (LTE BAND 3)	41
TABLE 9.	NF EVALUATION IN THE REFERENCE RECEIVER	41
	SYSTEM LEVEL ANALYSIS IN THE RECONFIGURABLE RECEIVER (LTE BAND 20)	
TABLE 11.	SYSTEM LEVEL ANALYSIS IN THE RECONFIGURABLE RECEIVER (LTE BAND 3)	43
TABLE 12.	NF EVALUATION IN THE RECONFIGURABLE RECEIVER	43
TABLE 13.	NF EVALUATION IN THE REFERENCE RECEIVER AND THE RECONFIGURABLE RECEIVER	43
TABLE 14.	POTENTIAL EI REDUCTION AS FUNCTION OF THE RECEIVER NF IMPROVEMENT	44
TABLE 15.	ABSOLUTE EI IN THE REFERENCE RECEIVER AND THE RECONFIGURABLE RECEIVER	45
TABLE 16.	NUMBER OF RES ANALYSIS ON PROPOSED SCHEMES ON 2 CRS PORTS CONFIGURATION	49
TABLE 17.	NUMBER OF RES ANALYSIS ON PROPOSED SCHEMES ON 2 CRS PORTS CONFIGURATION	50
TABLE 18.	El reduction on different RS settings	50
TABLE 19.	WSN SCENARIO INPUTS	51
TABLE 20.	RELATIVE EXPOSURE INDEX CALCULATION	55
TABLE 21.	EI GLOBAL FOR MONOPOLE ANTENNA WITH RHIS IN FRONT TO THE PHANTOM	57
TABLE 22.	EI GLOBAL FOR MONOPOLE ANTENNA WITH RHIS BACK TO THE PCB	57
TABLE 23.	EI GLOBAL FOR IFA ANTENNA WITH RHIS IN FRONT TO THE PHANTOM	57
TABLE 24.	EI GLOBAL FOR IFA ANTENNA WITH RHIS BACK TO THE PCB	57
TABLE 25.	Els for null steering and hybrid techniques. The absolute El is when no techniques.	JE IS
APPLI	ED 65	
TABLE 26.	% EI REDUCTION FROM ABSOLUTE EI FOR THE NULL STEERING AND HYBRID TECHNIQUES	65
	AVERAGE ARRIVAL TIME PER PERIOD OF DAY	
TABLE 28.	IEEE 802.11N PHYSICAL THROUGHPUT FOR ONE SPATIAL STREAM ON 20MHz	68
	MAIN SIMULATION ASSUMPTIONS	
TABLE 30.	MID-AFFLUENCE SCENARIO RESULTS (1 <sup>ST</sup> APPROACH)	71
	HIGH-AFFLUENCE SCENARIO RESULTS (1 <sup>ST</sup> APPROACH)	
TABLE 32.	MID-AFFLUENCE SCENARIO RESULTS (2 <sup>ND</sup> APPROACH)	72
TABLE 33.	HIGH-AFFLUENCE SCENARIO RESULTS (2 <sup>ND</sup> APPROACH)	72
TABLE 34.	El EVALUATION (STEP 5) (1 <sup>ST</sup> APPROACH)	74
TABLE 35.	El EVALUATION (STEP 5) (2 <sup>ND</sup> APPROACH)	75
TABLE 36.	SCENARIO BREAKDOWN	77
TABLE 37.	EI PERCENTAGE IMPROVEMENT CONSIDERING WI-FI	78
TABLE 38.	EI PERCENTAGE IMPROVEMENT CONSIDERING WSN	78
TABLE 39.	PERCENTAGE OF POPULATION AFFECTED BY WSNs	79
TABLE 40.	POWER DENSITY WITHOUT LEXNET SOLUTION	81
TABLE 41.	EXPOSURE INDEX FROM WSNs WITHOUT LEXNET	81
TABLE 42.	POWER DENSITY WITH LEXNET SOLUTION	82
TABLE 43.	EXPOSURE INDEX FROM WSNs WITH LEXNET	82
TABLE 44.	POTENTIAL EI IMPROVEMENT AS A FUNCTION OF BUFFER SIZE AND UPDATE RATE	83
	OVERVIEW OF ABSOLUTE AND RELATIVE EI EVALUATION FOR THE DIFFERENT SOLUTIONS	



10

## **Executive Summary**

The goal of the low EMF exposure future networks (LEXNET) project is to provide means of reducing human exposure to electromagnetic fields (EMF) that emanate from radio frequency (RF) communications devices. In the frame of "Smart Low EMF Radio" work package (WP), innovative solutions both on components and radio transmission techniques were proposed demonstrating their quantitative impacts on the exposure reduction and on the quality of service (QoS). The overall contribution of this deliverable is to present the final performance assessment of different examined solutions that optimize exposure, all conducted in accordance to an adopted common evaluation methodology.

This report presents the final performance assessment in terms of exposure index (EI) reduction of the evaluated components and radio transmission techniques in their associated scenario taking into account population ICT usages. To compare all of them in a fair manner, a common EI evaluation methodology using a five-step approach was adopted to unified EI reduction results. Each solution was examined following the same methodology to compare its effectiveness. However, it should mention that different proposed solutions do not compete among each other, and cannot be compared in completely fair conditions, as they may be solutions for different communications systems, in different communications scenarios, for different traffic types, etc., and at least different parameters may be taken as the QoS performance measures. Thus, many of the analysed innovative solutions may be actually complementary and can be combined to achieve higher global EI reduction.

Before presenting individual final results, the deliverable describes the evaluation framework related to the EI evaluation common methodology. It briefly reminds the five-step approach, focusing on the last step dedicated to the absolute EI evaluation. Following different solutions are grouped by scenarios defined in WP2. Three different scenarios were considered to merge all WP4 solutions: rural scenario, urban scenario, and WiFi and WSN scenario.

The global analysis of absolute EI figures can only be carried out by knowing the details of the EI evaluation context. Nevertheless this kind of analysis is able to point out the absolute exposure for a given situation that corresponds in the current case, to the population ICT usages in 2014. From an absolute point of view, the most promising solutions to reduce exposure are those which both present a hight level of absolute EI before the LEXNET implementation even if their relative reduction is low. That concerns the technologies which addresses the WiFi and LTE rural scenario. However this last point could change in future years while LTE penetration will have reached a dominant position among the different RATs.

The WP4 innovation beyond the state of the art (SotA) is twofold. On the one hand, the novelty of this work is in the analysis itself of a global assessment of the exposure (UL and DL, over a population). By considering the daily ICT usages, WP4 studies have evaluated the impact of a given technological solution in a given scenario. Before LEXNET, works that presented exposure reduction only showed one performance indicator (e.g. SAR) without taking into account both UL & DL, or any

Version: V1.1



ICT usage dilution effect. On the other hand some of the proposed solutions for El reduction present the cutting edge of research in their domain, while the other analysed radio components and transmission solutions adapted their mechanisms to reduce El.

The different examined solutions were positioned on a common EI axis following the same methodology. However their ranking is delicate because one should ensure that the input parameters and the evaluations of all these technologies are homogeneous. The impact of scenario inputs and the ICT usages is crucial. Therefore it suggests simplifying the ICT scenario with only 2 or 3 input parameters that could be play with (for instance the ratio between voice and data, the ratio between UL/DL,...).

Finally, the proposed EI evaluation methodology should be disseminated in the Telecom R&D community. This has been initiated through scientific communications but also thanks to inter-projects collaboration, particularly with FP7 MiWaves project. The proposed methodology could be reuse to evaluate the impact on EI of coming low frequency LTE bands (below 700 MHz) known to present higher SAR values.

Version: V1.1



12

#### 1 Introduction

The LEXNET project aims at reducing human exposure to EMF originated from RF communication devices. Innovative solutions both on components and radio transmission techniques were proposed demonstrating their quantitative impacts on the exposure reduction and on the QoS. To quantify EI, a global EI formula was defined evaluating relevant parameters which influences on EI such as the type of RF technology, or the RF device. Into WP4 a common EI evaluation methodology was adopted to unified El reduction results from the different proposed solutions. This enables fair comparisons among the various solutions on components and radio transmission techniques. Each of the technologies developed in the project were examined by similar criteria and therefore making it possible to compare their effectiveness. However, it should mention that different proposed solutions do not compete among each other, and cannot be compared in completely fair conditions, as they may be solutions for different communications systems, in different communications scenarios, for different traffic types, etc., and at least different parameters may be taken as the QoS performance measures. Thus, many of the analysed innovative solutions may be actually complementary and can be combined to achieve higher global EI reduction.

This deliverable presents the consolidated results of the three solutions for RF components and the seven solutions at the radio transmission techniques, which reduce the EI. One of the main objectives is to complete the common exposure evaluation methodology presented partially in D4.2 [1]. Previously the promising solutions were evaluated up to step-3 or step-4 of the methodology showing relative EI reduction; while preserving QoS. This document completes the evaluation methodology up to step-5 presenting absolute EI results, which includes the usage of the population over a 24h period.

The content of the deliverable is as follows. Chapter 2 illustrates the evaluation framework related to the EI evaluation common methodology. Initially it gives an update on the exposure evaluation process. It briefly reminds the five steps, focusing on the last step (step-5) dedicated to the absolute EI evaluation. Furthermore, it introduces the general formula to calculate the absolute EI [3] which takes into account a set of technical parameters: the time period (day and night), the population segmented in different categories (children, young people, adults and seniors), the different user load profiles (heavy, medium, light and non-user), the environment (home, office, outdoor or moving), the different available radio access technologies (RATs) (2G, 3G, 4G and Wi-Fi), the different cell types (macro, micro, pico and femto), the posture (standing and sitting) and the usage (voice and data). It presents the k coefficient matrices calculated in order to simplify the absolute EI computation for each scenario [3]. Moreover the advantages and the limitations of the down-selection process among WP4 solutions are presented, adding feedbacks from first implementations.

Chapter 3 presents the consolidated results of low EMF technologies grouped by scenarios. Three different scenarios were considered which include all solutions: rural scenario, urban scenario, and WiFi and WSN scenario. The main input

Version: V1.1



parameters for each scenario were described. For rural scenario, there is one solution which proposes low exposure cooperative communication techniques. The urban scenario comprises four solutions: small and directive antenna, low noise receiver architecture, enhanced efficiency in reference symbol usage and cell discontinuous transmission (DTX). The WiFi and WSN scenario covers five solutions: antenna on terminal for low EI, beamforming techniques, sleep/idle mode in a mesh gateway deployment, interference mitigation in Zigbee & WiFi and radio link allocation. The concept is reminded for each solution describing the specific scenario input parameters. Moreover the consolidated results related to step-5 are presented considering the advantages and the drawbacks regarding technology maturity, energy efficiency or deployment cost.

In Chapter 4, the different solutions are positioned on a common EI axis in order to compare the exposure reduction into a dedicated usage and a given scenario. Finally, Chapter 5 contains the conclusions of the whole WP4 and provides recommendations for future smart low EI technologies.

Version: V1.1



## 2 EVALUATION FRAMEWORK: THE EI EVALUATION COMMON METHODOLOGY ANALYSIS

#### 2.1 Reminds on the proposed common evaluation methodology

This section gives an update on the exposure evaluation process regarding the previous one detailed in Chapter 1 of deliverable D4.2[1]. It briefly reminds the four first steps mainly adressed by WP4 partners in Chapter 2 of deliverable D4.2[1] and it focuses on the last step (step-5) dedicated to the absolute EI evaluation.

Despite a large diversity of technical domains, whatever the scenario or the Radio Access Technologies (RAT), a single strategy to organize and align the different WP4 exposure evaluations has been presented. This 5-step approach (Figure 1) has been established in order to evaluate and harmonize the overall exposure improvement for each technology in the future. These steps also attempt to provide the basis for global exposure reduction evaluation in order to determine the most promising WP4 techniques based on fair and relevant comparisons.

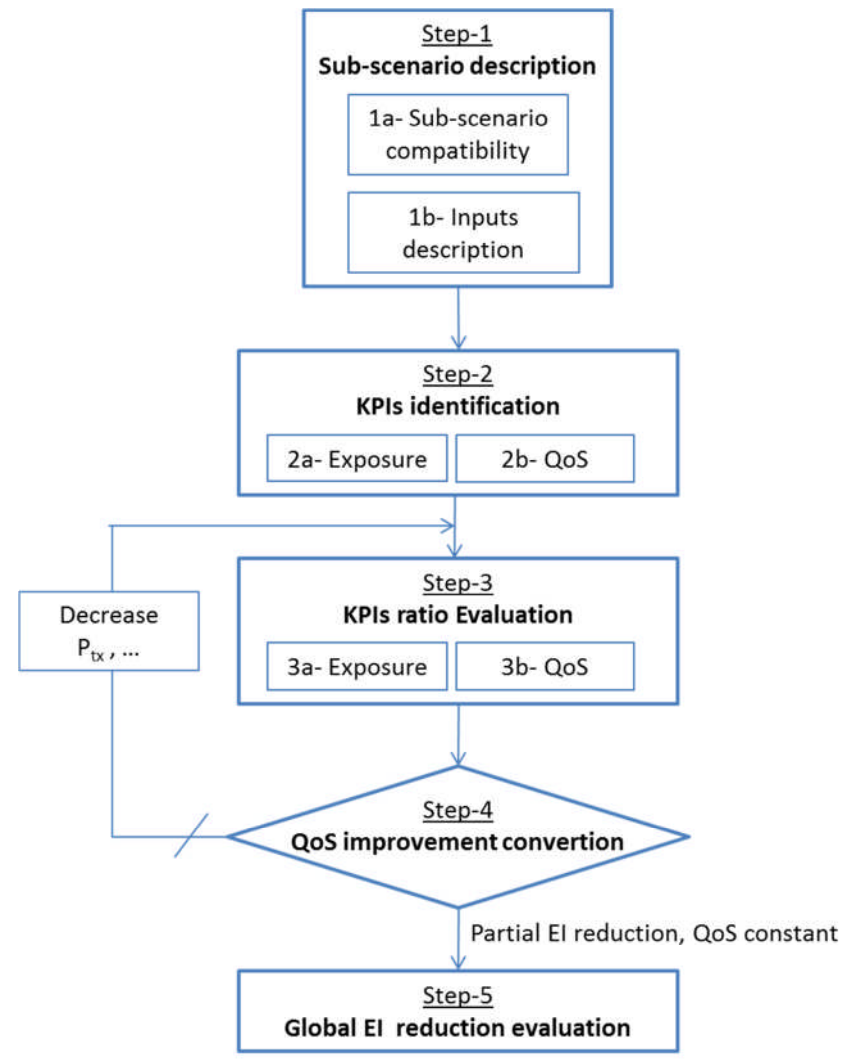


Figure 1. Common El evaluation methodology for WP4 solutions



#### 2.1.1 Step-1: Sub-scenarios description

The step-1 identifies how the individual WP4 techniques contribute towards the overall LEXNET use case scenarios from WP2. Specifically to WP4 evaluations, we have introduced four sub-scenarios to assist in separating the different techniques under investigation. WP4 studies have been structured based on those sub-scenario highlighting which ones are complementary and which ones will require further analysis to determine potential conflicts. Thus, the four 'sub-scenarios' have been defined and their inputs parameters are reminded in the beginning of each section. Thus, the WP4 sub-scenarios are: Rural, Small Cell (SC), Macro Cell (MC), and Wi-Fi &Wireless Sensor Network (WSN). Notice that for sake of coherence these WP4 sub-scenarios are now associated with WP2 scenarios. This concerns the Small Cell (SC), Macro Cell (MC) sub-scenarios which are associated with the more global urban scenario defined in D2.3 [2].

#### 2.1.2 Step-2: Exposure and QoS metrics identification

The step-2 clearly identifies the Key Performance Indicators (KPIs) being addressed by individual technique investigation. To facilitate this process, a limited numbers of KPIs for the exposure and for the QoS are used in the evaluation of each technique (see section 1.2 of D4.2[1]).

#### 2.1.3 Step-3: EI ratio evaluation

The step-3 (see section 1.3 of D4.2[1]) concerns the evaluation itself of a partial EI ratio, in comparison with a baseline scenario without implementing the studied solution. This can be seen as a relative improvement of the introduction of an evaluated solution. The exposure reduction is evaluated through the calculation of an EI ratio ( $Ratio_{EI}(\%)$ ) by comparing the 'with LEXNET' versus the 'without LEXNET' (i.e., SotA or standard) baseline configurations as shown in Eq. (2.1).

Ratio<sub>EI</sub> (%) = 
$$\frac{\text{EI}_{\text{partial}} (\text{w LEX}) - \text{EI}_{\text{partial}} (\text{wo LEX})}{\text{EI}_{\text{partial}} (\text{wo LEX})} \times 100$$
 (2.1)

Where  $\mathrm{EI}_{\mathrm{partial}}$  is the EI for a specific sub-scenario. The subscript 'w LEX' corresponds to the LEXNET solution implementation, and the subscript 'wo LEX' corresponds to the SotA or baseline (without the solution implementation).

The three KPIs detailed in section 1.2 of D4.2 [1] are variables independent of each other. This means that if a solution succeeds in decreasing one of the three KPIs, the two others will stay constant. Thus, all other things being equal, the EI ratio is thus equal to the identified KPI ratio as shown in Eq. (2.2). This approach brings a major advantage to simplify exposure reduction evaluation because it is easily matched with a typical RF front-end or PHY layer evaluation studies. By convention the EI ratio is negative when a reduction of exposure is reached. The equation (2.1) is simplified when a specific sub-scenario is considered:

$$Ratio_{EI}(\%) = \frac{KPI_{partial}(w LEX) - KPI_{partial}(wo LEX)}{KPI_{partial}(wo LEX)} \times 100$$
(2.2)



Where KPI<sub>nartial</sub> is the metric identified in step-2 calculated in the sub scenario context.

#### 2.1.4 Step-4: Capacity/QoS improvements convertion into EI reduction

The step-4 (see section 1.4 of D4.2[1]) aims to ensure that capacity or QoS improvements are converted into exposure reduction or at least that the EI reduction is obtained by preserving the QoS level. An objective of our research is to reduce exposure without impacting QoS.

#### 2.1.5 Step-5: Global EI reduction assessment

At last the step-5 (section 1.5 of D4.2[1]) estimates the global EI in a absolute way and no more a relative improvement like in step-4. This can be carried on both with and without the introduction of a given technology,through the 24 hours LEXNET reference scenario and Information and Communications Technologies (ICT) usages delivered by WP2 in deliverable D2.8[3].

The calculation process can be summarized as follow. WP2 introduces a series of weighting coefficients that take into account the population usages through sociological parameters (age, user profile, voice communication duration, location...) associated with technical telecom parameters (SAR, transmit data volume, throughput, UL/DL ratio...) for a given scenario. These series of coefficients are weighting a mean transmit power in the UL case and a mean power density in the DL one. Unlike in step-4, WP4 partners have, here, to assess absolute value of the transmit power or receiving power density. This can be done whether through large scale system-level, by measurements campaign in a given scenario, by reusing statistical distributions from the literature, or even by using a mere mean value of these two variables. At last the averaging on the different categories (population, period of the day; UL EI and DL EI...) is done to bring to a scalar value.

The step-5 and the absolute EI assessment are detailed in this document for each individual solution.

#### 2.2 Reminder on the general concepts of absolute El calculation

This section presents a short description of the general formula of EI, defined in D2.8 [3], and the role of the so-called k coefficients which role is explained hereafter.

The EI takes into account the global EMF exposure of a population from a given wireless telecommunication network (or set of networks). It covers the exposure of a population over a 24h period in a given area, incurred from the wireless telecommunication networks as a whole, aggregating the downlink (DL) exposure induced all day long by base stations and access points and the uplink (UL) exposure incurred by individual wireless communication devices. The UL exposure can be subdivided in exposure due to the UL of the user's own device and the UL of devices operated by other users nearby. This last contribution is neglected in the deliverable due to its low contribution in the selected scenarios.

In a nutshell, the LEXNET EI is a function transforming a highly complex set of data into a single parameter: the EI.In order to assess the realistic exposure of a population, many parameters influencing the exposure need to be taken into account

Version: V1.1



in the El. Some of them come from sociological data: age, posture, usage, user profile, density of population, life segmentation, and other are driven by the technical aspects: transmitted power, SAR, throughput, infrastructure density (base station or gateways) etc.

The general formula of the EI is reported in Appendix 2 for sake of brevity. It is important to notice how WP2 reduced the complexity of handling the absolute EI assessment. A major part of the sociological and constant technical (normalised SAR) inputs are integrated into a series of scalar coefficient called *k* coefficients.

The coefficients  $k_i$  for i from 1 to 4 are weighting the mean transmit power for UL exposure of voice calls. The coefficients  $k_i$  for i from 5 to 8 are weighting the mean transmit power normalised by the mean throughput for UL exposure of data transmission. And at last the coefficients  $k_i$  for i from 9 to 12 are weighting the mean received power density corresponding to the DL exposure. The k coefficients tables (one table per scenario) are reported in Appendix 2. These 12 coefficients stand for the 12 configurations considered in the presented example (Eq. 2.3) for both indoor and outdoor locations and two time period day (day and night slot). Notice that the distribution of typical values for both  $\overline{P}_{TX}$  and  $\overline{S}_{RX}$  can be estimated with usual telecom engineer tools.

$$EI_{adults} = EI_{in_{day}} + EI_{out_{day}} + EI_{in_{night}} + EI_{out_{night}} = k_1 * \bar{P}_{TXindoordayvoice} + k_2 * \\ \bar{P}_{TXoutdoordayvoice} + k_3 * \bar{P}_{TXindoornightvoice} + k_4 * \bar{P}_{TXoutdoornightvoice} + k_5 * \frac{\bar{P}_{TXindoordaydata}}{Th_{indoordaydata}} + k_6 * \frac{\bar{P}_{TXindoornightdata}}{Th_{outdoordaydata}} + k_7 * \frac{\bar{P}_{TXindoornightdata}}{Th_{indoornightdata}} + k_8 * \frac{\bar{P}_{TXoutdoornightdata}}{Th_{outdoornightdata}} + k_9 * \bar{S}_{RXindoorday} + k_{10} * \\ \bar{S}_{RXoutdoorday} + k_{11} * \bar{S}_{RXindoornight} + k_{12} * \bar{S}_{RXoutdoornight}$$
 (2.3)

In Eq. (2.3),  $\overline{P}_{TX}$  is the mean TX power transmitted by the users' devices (in W), $\overline{S}_{RX}$  is the mean incident power density on the human body (in W/m²) and Th... is the mean throughput (in kB/s).

Finally, the El of other population categories are calculated and the population distribution is integrated using Eq. 2.4 to derive the global EI:

$$EI_{global} = 0.139 * EI_{children} + 0.328 * EI_{youngpeople} + 0.382 * EI_{adults} + 0.151 * EI_{seniors}$$
 (2.4)

#### 2.3 Advantages and limitations for down-selection purpose

The WP4 goal is to propose techniques that achieve the best absolute EI reduction taking into account the absolute EMF exposure dose per day for the 'typical' individual of a population. The impact of proposed solution has to be evaluated regarding the 24h activities breaking down. The usage statistics are used to weight the calculated partial EI reduction in order to assess the global EI reduction for a given solution. Notice that the usage contains the information related to the SAR, the volume of transmitted data. Thus each individual solution evaluation is twofold: an EI ratio that quantifies the relative improvement (step-4), and an absolute EI evaluation taking into account the so-called dilution factor [3] (step-5) that positions on a

Version: V1.1 Dissemination level: PU



common absolute EI axis the level of exposure of a given technology compared to another one.

As explained in section 2.1.5, the evaluation of transmit power and receiving power density have to be done by WP4 partners who use different ways with different input parameters. As a consequence this heterogeneity leads to some difficulties in order to compare the results and improvements of the different solutions. This makes any down-selection or ranking quite delicate.

Version: V1.1



19

#### 3 Low EMF technologies consolidated results

#### 3.1 Rural scenario

#### 3.1.1 Scenario Inputs

The R station in LTE-A systems are primarily adopted as the solution for base station (BS) coverage extension, assuming that the complete communication process between BS (or source of information – S) and end-user (or destination terminal – D) is performed through the R station. The implementation of R stations in LTE-A systems will cause a decrease in the mean transmitted power (PTX) on UL, due to a shorter distance between D and R station compared with the distance between D and S. This will result in significant exposure reduction, as the same QoS level in UL transmission will be achieved with much lower power transmitted by end-user device. However, on the other side, closer position of R stations to end-users will cause a certain level of exposure increase on DL, compared to scenario with no relays. Therefore, we have been working on a solution for reducing public exposure to EMFs generated by R stations in DL communication process.

We analysed only one-cell scenario, i.e. the considered users are in the coverage range of a single relay station, so no other sources of DL exposure are taken into account. Population distribution for the rural area in France is used, given in [3], which assumes that 16.1% of the population are children, 28.1% are young people, 38.8% are adults and 17% are seniors. Also, we assumed that users are uniformly distributed, regarding their distance from R station.

A LTE-A relay system operating at 2GHz, with 5MHz channel bandwidth is considered. We assumed that BS transmit power is equal to 43dBm, while RS transmit power is 30dBm [4]. In the considered scenario we assumed direct line-of-sight (LOS) between base station and R station. In the simulated scenario, we took that base station - relay station (S - R) distance is equal to 10km, while relay station – end-user (R - D) distances range from 0.25km up to 2.5km, with the step of 0.25km. For outdoor environment, only pedestrian users are analysed, assuming extended pedestrian A (EPA) fading model [4]. In case when the user is in indoor environment, we took that in-building penetration loss is equal to 18dB [4]. Other relevant parameters specifying the scenario analysed, as well as simulation parameters can be found in D4.2 [1].

## 3.1.2 Solution A - Low exposure cooperative communication techniques evaluation

#### 3.1.2.1 Remind on solution concept

The focus of this work is on data traffic in an LTE-A network. We considered solutions for human exposure reduction in rural scenario, where the source of EMF is LTE-A relay station. Thus, the DL communication process is taken into account, and it is assumed that end-users (D) are not in the range of base station (S). The complete communication process on DL between S and D is performed through the R station, which operates in half-duplex mode. Such a communication system is denoted as dual-hop relay system. OFDM (Orthogonal Frequency Division

Version: V1.1



Multiplexing) based R station is considered, which implements decode-and-forward (DF) relaying, as it is defined in adopted relay solution for LTE-A systems.

We propose and analyse three different solutions for exposure reduction on DL in LTE-A relay systems. Each of these solutions brings capacity enhancement to OFDM DF relay system, which we use as a reference system. Moreover, choosing the system capacity as a QoS measure, which is preserved at the same level in all the systems, it is shown that all analysed solutions actually enable decrease of power transmitted by R on DL, i.e. enable lower EMF level at an end-user position (EI decrease). The first considered solution is OFDM DF system with ordered SCM performed at R station, presented in D4.2 [1]. The second solution assumes that the R station has more than one antenna for transmitting information on DL, and it implements transmit antenna selection (TAS) on subcarrier basis [5]. TAS is realized through comparison of the corresponding subcarriers from multiple branches on R-D link and on each subcarrier position subcarrier selection is performed based on the best channel transfer function. The third solution represents combination of SCM and TAS implemented at R station of dual-hop OFDM DF relay system (Figure 2).

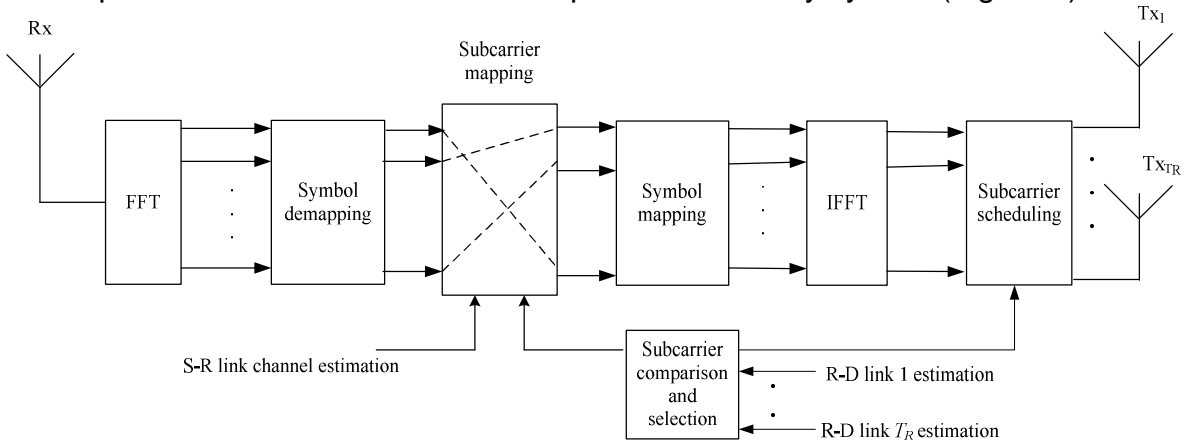


Figure 2. Block scheme of OFDM DF relay station implementing TAS and SCM

In the proposed relay system R station implementing both TAS and SCM, after OFDM demodulation, realized through FFT (Fast Fourier Transformations), symbol de-mapping is performed. Based on the feedback from D terminal, sub-band Channel Quality Indicator (CQI) is obtained (or equivalently, channel estimation on  $T_R$ DL channels), which is used for subcarrier selection on DL. This process assumes that subcarriers with the best channel transfer functions, among the  $T_R$  possible ones on each subcarrier position, are selected. Information about channel transfer functions of the selected subcarriers is fed into block for SCM. This block maps subcarriers from the first hop to the set of the selected subcarriers on the second hop, all in accordance to their instantaneous signal-to-noise ratios (SNRs). After symbol mapping block and OFDM modulation, realized through IFFT (Inverse Fast Fourier Transformations), there is a block for subcarrier scheduling to corresponding transmit antennas. This block also uses the information on the set of the selected subcarriers from the block for subcarrier comparison and selection.

If Subcarrier mapping block is omitted in the described R station, then it would be OFDM DF relay station with TAS. On the other hand, by omitting Subcarrier scheduling block, and if R station implements only one transmit antenna, then it would be OFDM DF relay station with SCM.

Version: V1.1 Dissemination level: PU



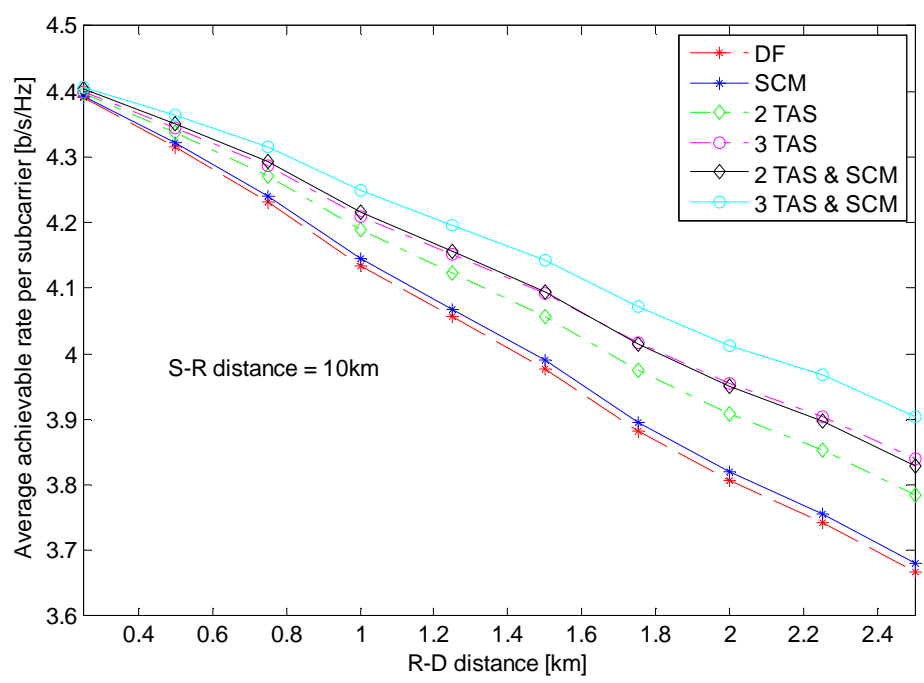
21

#### 3.1.2.2 Specific scenario inputs

By using a simulation model with parameters for LTE-A relay system in rural reference scenario given in [4], we obtained average achievable rate per subcarrier for the reference OFDM DF relay system, as well as for each of the systems implementing the three proposed solutions. In D4.2 [1], we explained how the achieved capacity improvements are converted to EI reduction, when capacity is preserved on the same level as in the reference OFDM DF relay system. Detailed description of the used simulation parameters are given in D4.2 [1]. In the simulations we assumed that R has channel knowledge of the S-R link and sub-band Channel Quality Indicator (CQI) for the TR R-D links, which is used for performing TAS and SCM. The same simulation model is then used for calculating the average received signal power density at D (end-user) terminal. Using this, and EI formula, as well as the corresponding coefficients for LTE network in rural scenario given in [3], we completed EI calculation for radiation originating from LTE-A relay station in rural area.

#### 3.1.2.3 Evaluation on exposure reduction

Before explaining the step 5 in our 5-step approach for EI evaluation, we first provide simulation results on average achievable rates per subcarrier ( $\bar{C}$ ) of the analysed three solutions for EI reduction in OFDM DF relay systems, for the cases of end-user in outdoor (Figure 3) and in indoor environment (Figure 4). When the TAS solution is considered, we analysed possibilities for performance improvement through the implementation of 2 and 3 transmit antennas, i.e., 2 TAS and 3 TAS. A similar approach was taken for the solution where TAS is combined with SCM, i.e. 2 TAS & SCM and 3 TAS & SCM. For the sake of comparison, average achievable rate per subcarrier of OFDM DF relay system is also given (denoted as "DF" in figures' legends).



Average achievable rates per subcarrier for the analysed OFDM relay systems -Figure 3. outdoor user



From the average achievable rates results, we calculate "equivalent SNR" values for each of the 6 considered systems using:

$$SNR_{eq_i} = 2^{(2\cdot \bar{C}_i)} - 1$$
 (3.1)

Where the index i=1,...,6 denotes different considered systems and  $\overline{C}_i$  is average rate per subcarrier of the considered system i. If we want to keep QoS at the same level, then all the proposed solutions should have the same equivalent SNR as the OFDM DF relay system. By comparing equivalent SNRs of each of the proposed solutions with the equivalent SNR of OFDM DF system, the possible value of signal level decrease at end-user site is calculated for the corresponding system. This value of signal level decrease is equal to EI ratio, a metric which describes the percentage of EI decrease attained with any of the proposed solutions, with respect to the more conventional OFDM DF relay system [1]. For the scenario with the user in outdoor environment, the EI ratio values are given in Table 1, while the corresponding values for the scenario of indoor user are presented in Table 2. Ten different distances between end-user (D) and R station are considered, starting from 250m, up to 2.5km.

Table 1. El ratio for the analysed OFDM relay systems – outdoor user

R-D distance [km]	0.25	0.5	0.75	1	1.25	1.5	1.75	2	2.25	2.5
EI ratio - SCM [%]	0.31	0.71	1.07	1.31	1.52	1.65	1.73	1.81	1.86	1.91
EI ratio - 2 TAS [%]	1.02	2.93	5.29	7.21	8.96	10.52	12.09	13.29	14.47	15.28
EI ratio - 3 TAS [%]	1.33	3.94	7.22	9.94	12.43	14.64	16.94	18.65	20.32	21.50
EI ra 2 TAS & SCM [%]	1.79	4.80	8.17	10.73	12.99	14.92	16.73	18.10	19.42	20.31
EI ra 3 TAS & SCM [%]	2.29	6.33	10.99	14.59	17.75	20.46	23.08	25.04	26.93	28.18

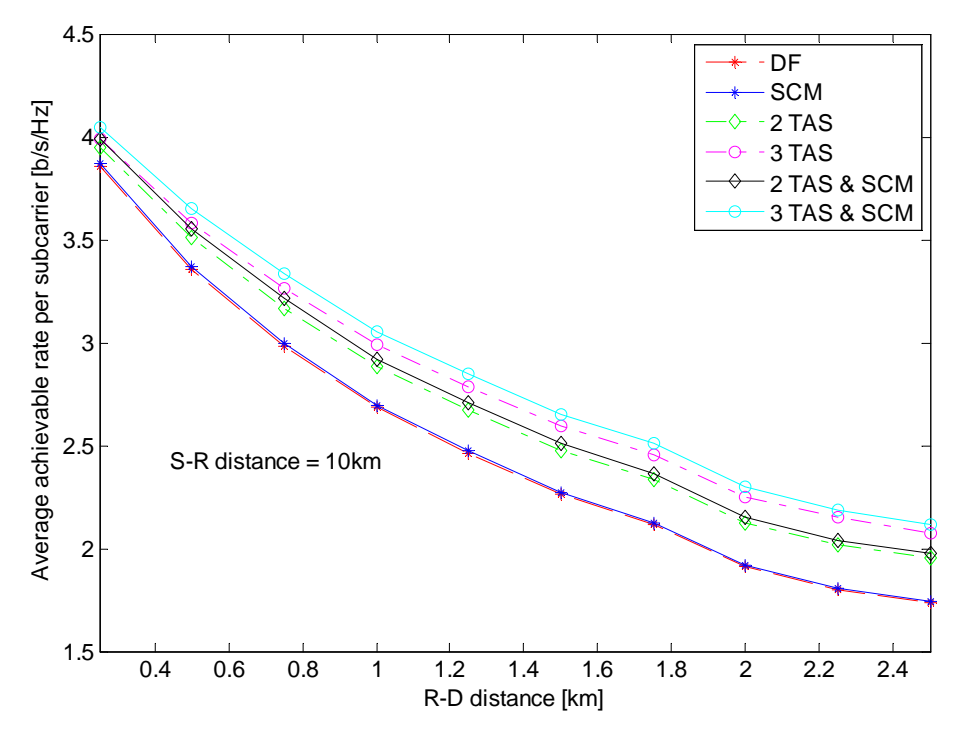


Figure 4. Average achievable rates per subcarrier for the analysed OFDM relay systems – indoor user

Version: V1.1 Dissemination level: PU



Table 2. El ratio for the analysed OFDM relay systems – indoor user

R-D distance [km]	0.25	0.5	0.75	1	1.25	1.5	1.75	2	2.25	2.5
EI ratio - SCM [%]	1.67	1.90	1.86	1.60	1.42	1.37	1.21	1.02	0.86	0.94
EI ratio - 2 TAS [%]	11.95	19.08	22.85	24.40	25.79	26.36	27.05	27.46	28.03	27.63
EI ratio - 3 TAS [%]	16.79	26.98	32.48	34.97	36.97	37.83	38.99	39.66	40.57	39.87
EI ra 2 TAS & SCM [%]	16.36	24.19	27.63	28.46	29.55	30.03	30.23	30.20	30.36	30.11
EI ra 3 TAS & SCM [%]	22.73	33.84	38.86	40.45	42.13	42.82	42.32	43.57	44.00	43.48

From Table 1 and Table 2, we can see that all the proposed solutions bring greater EI ratio in indoor environment. Also, we can conclude that higher EI ratio is achieved for the users which are further from R station, than for users closer to R. Furthermore, implementation of TAS solution brings significant EI decrease. For example, maximal EI ratio is equal to 21.5%, for the 3 TAS solution in outdoor environment and for R-D distance of 2.5km. The corresponding EI ratio value attained with this system in indoor environment is equal to 39.87%. In the considered scenarios, implementation of only SCM brings very small EI decrease (less than 2%) for all D positions. However, when combined with TAS solution, it can bring additional up to 7% EI decrease.

The previous analysis provides an insight in the effectiveness of the proposed solutions for EI reduction, in the specified environment, and at the given distance between end-user and R station. However, in order to derive DL EI values for OFDM based relay systems analysed, and to attain mean daily value of EI in rural scenario, we had to complete the step 5 of the adopted 5-step approach for EI assessment.

We wanted to keep unified approach in all the solutions proposed in WP4, and thus we used statistical data and k coefficients given in [3]. Such an approach assumes adoption of the hypothesis that in 2016, 48% of the connections will be 3G connections, 44% will be 2G and 8% 4G (LTE) connections. Moreover, as the existence of four telecom operators in France is taken into account, then, only 25% of total users are users of the assumed operator.

El for the considered rural scenario is obtained through [3]:

$$EI_{global}[w/kg] = [\%children \times EI_{children} + \% young\_people \times EI_{young\_people} + + \%adults \times EI_{adults} + \% seniors \times EI_{seniors}] / (24 \times 3600)$$
(3.2)

where population distribution for the rural area in France is used, thus having: %children = 0.161; %young\_people = 0.281; %adults = 0.388 and %seniors = 0.17.

El for each of the population category is obtained through simulations, using the formula given in D2.8 [3]. For example, El for adults is calculated through:



$$EI_{adults} = \left(k9 \times S_{RX\_indoor\_day} + k10 \times S_{RX\_outdoor\_day} + k11 \times S_{RX\_indoor\_night} + k12 \times S_{RX\_outdoor\_night}\right) / \left(24 \times 3600\right)$$
(3.3)

The terms related to voice communications are omitted as the focus is on data traffic. Also, we consider only DL data transmission from R station. SRX denotes received power density. As mentioned, in our simulated models, only one-cell scenario is considered and we did not differentiate among received power densities between the day and the night but only between different types of environments where user is situated (indoor and outdoor). The values corresponding to LTE network in rural scenario for coefficients k9, k10, k11 and k12, for each population category, are given in [3]. Using Eq. (3.3) and the simulation results for average received power densities in indoor and outdoor environment, we calculated EI for adults, where the only source of radiation is assumed to be the OFDM DF relay station.

Then, for each of the solutions proposed for EI reduction in OFDM DF system, using Eq. (3.3) and calculated EI ratio values for indoor and outdoor users (Table 1andTable 2)we obtained corresponding EI values for the considered population category. For example, EI for adults for the 2 TAS system is calculated through:

$$EI_{adults\_2TAS} = \left[ \left( k9 + k11 \right) \times S_{RX\_indoor\_day} \times \left( 1 - 0.01 \times EI_{ratio\_ind\_2TAS} \right) + \left( k10 + k12 \right) \times S_{RX\_outdoor\_day} \times \left( 1 - 0.01 \times EI_{ratio\_out\_2TAS} \right) \right] / \left( 24 \times 3600 \right)$$
(3.4)

The relation among the coefficients k9 and k10, as well as among the k11 and k12 includes the assumption that 80% of the users are placed indoor, while 20% are outdoor users. For each population category we have calculated EI using the same described approach, but implementing corresponding k9 – k11 coefficients, which we have found in [3]. Substituting the obtained EI results in Eq. (3.2), global EI for rural scenario in LTE-A relay system, for each of the considered solutions, is obtained.

Table 3 compares the EI values of the proposed solutions with the EI values for OFDM DF relay system at each of 10 examined end-user positions (0.25 m - 2.5 km).

Table 3. El values for OFDM DF relay system and El reduction in per cents attained with the proposed solutions

R-D distance [km]	0.25	0.5	0.75	1	1.25	1.5	1.75	2	2.25	2.5
EI (·10 <sup>-6</sup> ) for DF [W/kg]	7.62	1.91	0.58	0.26	0.25	0.18	0.07	0.07	0.07	0.06
EI reduction - SCM [%]	0.48	0.83	1.22	1.33	1.50	1.60	1.66	1.74	1.65	1.78
EI red 2 TAS [%]	2.29	4.68	8.13	10.30	10.27	12.15	14.42	16.52	16.49	16.79
EI red 3 TAS [%]	3.11	6.43	11.32	14.46	14.30	17.15	20.37	23.39	23.40	23.70
EI red 2 TAS & SCM [%]	3.54	6.98	11.40	13.86	14.34	16.34	18.74	21.03	20.88	21.61
EI red 3 TAS & SCM [%]	4.75	9.40	15.59	19.26	19.67	22.65	26.09	29.42	29.29	30.16

Version: V1.1 Dissemination level: PU



From the results presented in Table 3, conclusions can be derived similar to the ones derived for data provided in Table 1andTable 2. Namely, each of the proposed solution brings higher EI reduction for the higher distances between R and D. TAS solutions bring significant EI reduction and it ranges from 3.11% (for R-D distance of 0.25 km) up to 23.70% (for R-D distance of 2.5 km) for the case of R station with 3 transmit antennas. At the other side, the SCM solution alone achieves very small EI reduction (less than 1.8%) for all the presented distances between R-D. However, when it is combined with TAS, it can bring an additional 6.5% exposure reduction in certain cases.

In order to calculate mean daily EI in rural scenario for the OFDM DF relay station, we assumed that users are uniformly distributed around the R station. For the examined case of 10 users positioned at distances from 0.25km up to 2.5km from R station, with a step of 0.25km between two adjacent user positions, we obtained the mean values of EI for each analysed system. Thus, for example, mean daily EI in rural scenario caused by OFDM DF relay station is equal to 1.1072·10<sup>-6</sup> W/kg. Based on this, we were able to calculate absolute reduction and of mean daily EI attained by the proposed solutions, as well as to express it in percentage (Table 4).

Table 4. El reduction in per cents attained with the proposed solutions

	SCM	2 TAS	3 TAS	2 TAS & SCM	3 TAS & SCM
Mean EI (•10 <sup>-6</sup> ) [W/kg]	1.0988	1.0643	1.048	1.0446	1.0222
EI reduction (·10 <sup>-8</sup> ) W/kg]	0.7388	4.2878	5.9132	6.2574	8.4933
EI reduction [%]	0.67	3.87	5.34	5.65	7.67

The final results given in Table 4approve that applying jointly TAS & SCM at OFDM DF relay station can be considered as an interesting solution for EI reduction in LTE-A relay systems. Namely, we have shown that, in average, on daily basis, it can bring 7.67% of EI reduction in rural scenario.

#### 3.1.2.4 Conclusions, analysis

Through the conducted analysis we have shown that the proposed solution, combining both TAS and SCM in LTE-A relay system can achieve up to 7.67% El reduction in rural environment. The proposed solutions for decrease of radiation of LTE-A relay stations bring exposure reduction not only to active users, but to everyone being in the coverage area of R station. Besides lower EMF exposure on DL, the analysed systems improve energy efficiency of both R and base station. Namely, due to the nature of DF relaying, the power transmitted from R and base station in the proposed solutions should be decreased for El ratio per cents, in order to keep the achievable capacity on the same level like in OFDM DF relay system. The nature of UL communication, the level of power transmitted, as well as duration of UL communication slot remain the same as in OFDM DF relay system.

When practical implementation of TAS and SCM is considered, then adjacent subcarriers (or resource blocks) should be grouped based on the coherent channel bandwidths and TAS, as well as SCM, should be realized on chunk basis. In this way, the amount of signalling between R and D would be decreased. Finally, the practical implementation of the proposed 2 and 3 TAS & SCM systems should be considered and would be valuable for system testing. It should be stressed that only



26

minor additions to the signal processing effort are required and as such the additional system complexity is not thought to be prohibitive.

#### 3.2 <u>Urban scenario</u>

#### 3.2.1 Scenario Inputs

Thanks to the popularity of smartphones and tablets going into people's lives, with most of the data usage happens indoors, the extensive indoor cellular mobile coverage becomes absolute necessary. The indoor small cells are seen to be an integral part of the modern cellular networks, working together with the macrocells to provide data coverage, seamless mobility experience and enrich people's lives.

Specially, the small cells inside-out deployment means that the targeted serving devices are no longer limited to be only indoors but also the outdoor terminals. Heterogeneous network (HetNet) is the envisaged scenario where macro base stations (MeNBs) are complemented with small cell eNBs (SCeNBs) to extend the cellular network coverage in both (indoor and outdoor environment). Given this reason, the urban LTE scenario is defined as the reference scenario for three different low EMF solutions: small and directive antenna for low EI, low noise receiver architecture and enhanced efficiency in reference symbols usage. These techniques are described below showing their impact on exposure reduction.

The transmission bandwidth for these applications is at a typical setting of 10 MHz. The maximum allowed transmitted power from the small cells is set to be 1 W.

#### 3.2.2 Solution B- Small and directive antenna for low exposure index

#### 3.2.2.1 Remind on solution concept

The proposed antenna solution is based on super directive compact parasitic arrays [6] with beam-steering capability. The key of our approach is the optimization of the compact antenna array using the spherical modal expansion [7] and introducing the optimal amplitude and phase weight by integration of complex loads on each array elements. Compared to classical omnidirectional (360° angular resolution) antenna solutions available commercially, a directive antenna introduces spatial selectivity. In our proposition, a directivity around 10 dBi (-3dB beamwidth around 60°) is specified. This directivity level can be obtained using a three-element array separated by a distance of  $0.1\lambda_0$  (where  $\lambda_0$  is the wavelength calculated at the operational frequency). In order to achieve 360° beam-steering capability, a planar array composed of six electric dipoles will be designed.

In our case, the radiation efficiency degradation due to the super directivity is balanced thanks to the antenna spatial filtering properties. Thus, the interference level decreases. In conclusion, our approach consists in keeping the same QoS of classical network architecture while reducing the transmitted power level thanks to the higher antenna angular selectivity. This power reduction will lead to an efficient decrease of the electromagnetic exposure at the UL that is at the UE (User Equipment).

Version: V1.1



#### 3.2.2.1.1 Super directive compact antenna arrays for small cells

A simple block diagram of a conventional digital-beam forming system is presented in Figure 5(a). The signal received from each antenna is digitalized (ADC) and combined with the signals received from the others antennas in order to form a desired beam pattern. Generally, the antennas are separated by a distance  $\lambda_0/2$  in order to reduce the mutual coupling effects. The conventional digital beam-forming system is composed of four principal blocks: i) the antenna and the radiofrequency front-end (Tx/Rx), ii) the digital-analog or analog-digital converter (DAC/ADC), iii) the digital up or down conversion (DUC/DDC) system, and iv) the adaptive algorithm. It is important to notice that each antenna has a dedicated radiofrequency module, a DAC/ADC system, and a DUC/DDC.

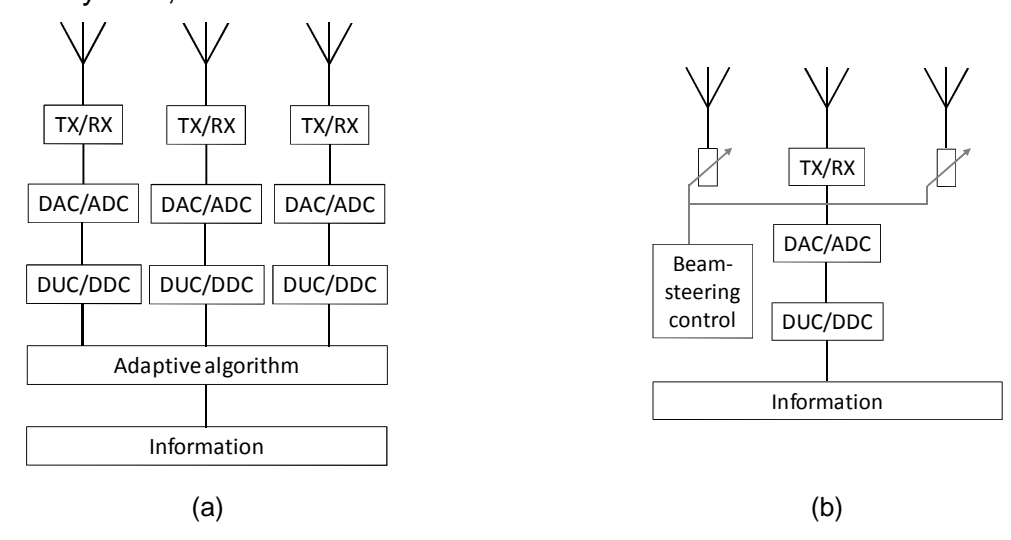


Figure 5. a) Block diagram of a conventional digital beam-forming transmitter/receiver system and b) architecture based on electronically reconfigurable parasitic array antenna.

The proposed solution is to integrate a super directive compact parasitic antenna array with beam-steering capability on the small cell (Figure 5(b)). In this case, the antenna is composed of one fed element and a number of parasitic elements loaded by complex impedance loads. The elements are separated by a distance of  $\lambda_0/10$  and the beam-steering is achieved by controlling the input impedance of the parasitic elements. Our approach limits the antenna size (reduction of the total surface of a factor five as compared to the digital beam-forming architecture with same angular resolution) and the system complexity compared to the classical beam-forming architecture, which is beneficial for the small cell design.

The proposed antenna design is based on super directivity theory which makes theoretically possible to reach any desired directivity for a given antenna array volume at the cost of a degradations on the bandwidth and efficiency. As consequence, a trade-off between electrical size (physical size regarding the wavelength), directivity, efficiency, and bandwidth must be done.

For a correct understanding, it is important to recall the some antenna parameter definitions. The antenna gain (G) takes into account the directional properties and the antenna total efficiency  $\eta$  ( $G = \eta D$ , where D is the antenna directivity), while the directivity takes into account only the antenna directional properties.

Version: V1.1 27



A super directive compact antenna array has been designed and optimized using an *ad-hoc* procedure developed at CEA-LETI [8],[1]. Then, the super directive array radiated gain pattern is calculated with an EM simulator or assed by measurement of a prototype. The spatial filtering is thus evaluated within a system-level simulation at the small-cell scale which is detailed in the following section.

#### 3.2.2.2 Specific scenario inputs

Here we investigate Heterogeneous Network (HetNet) operating at 2 GHz [11]-[12] and we propose the use of super directive [6] compact parasitic antenna array with real-time beam-steering capability for small cells (SC) to enable low EMF wireless communications. In this HetNet architecture, classical macro base stations (MeNBs) are complemented with low-power low-cost Small Cell eNBs (SCeNBs) to extend the cellular network coverage in both (indoor and outdoor environment) and improve performance experienced at end users by shortening the distance between mobile terminals and access nodes.

In our analysis six different antenna radiation patterns have been considered: the omnidirectional patterns with 5 and 2 dBi of directivity, the 10 dBi directivity ideal pattern with 100% of efficiency ( $G_{max}$ = 10 dBi), 15% of efficiency ( $G_{max}$ = 2 dBi), 8% of efficiency ( $G_{max}$ = -1 dBi), and the radiation pattern obtained by full-wave electromagnetic simulation of a three-dipole super directive compact antenna arrays optimized at 2 GHz. The ideal patterns have been calculated considering the equation:

$$D(\theta, \phi) = 2(n+1)\cos^n(\theta), \tag{3.13}$$

In Eq. (3.13), by varying the n order, it is possible to control the directivity and the angular aperture of the desired synthetic pattern. Imposing n=4 we obtain a directivity of 10 dBi and an angular aperture of 65.5°. The three-dipole compact parasitic array has been optimized using the proposed design procedure based on spherical wave expansion, and simulated using CST microwave studio (3D EM simulator). The antenna is composed of three electrical dipoles of length  $\lambda_0/2$  and inter-element distance of  $\lambda_0/10$  (total size  $0.2\lambda_0\times0.5\lambda_0$ ,  $30\times75$  mm² at 2 GHz). A directivity of 9.1 dBi, a gain of -2.46 dBi (total efficiency 7%) and an angular aperture of 62.2° have been obtained. It is important to notice that in this preliminary investigation, we have considered an ideal beam-steering. In fact, we have assumed that with our antennas it is possible to steer the beam in any possible direction with the same maximum gain.

Coherently with the 3GPP study on small cell enhancement [11], our research focuses on HetNets where small cells are densely deployed. We consider a trisectorial macro cell (MC) and we assume that the SCs form a 3 × 3 cluster located inside each MC sector. In each MC sector, 30 UEs are dropped in the MC area: following the 3GPP guidelines [11], 2/3 of the overall UEs are distributed inside the SC cluster and the remaining UEs are uniformly located in the macro cell area. Moreover, 80% of the UEs are deployed indoor and 20% outdoor. Relevant key simulation parameters are detailed in Table 5. The results are averaged over 10<sup>3</sup> independent runs. At the beginning of each run, the clusters of SCs and UEs are randomly deployed in the MC area. The association between the UEs and eNBs is based on the DL reference signal received power (RSRP) [13].



**Table 5.** Main Simulation Parameters

Parameter	Value
Cellular layout	Hexagonal grid
Macro sector/site	3
SCeNBs/macro sector	9
UE dropping	2/3 UEs within the clusters, 1/3 UEs throughout the macro area. 80% UEs are indoor.
Min. dist. SC-UE	10 m
Min. dist. MeNB-UE	35 m
Dist. SC-SC	40 m
Macro cell path loss	ITU UMa (Table B.1.2.1-1[11])
Small cell path loss	ITU Umi (Table B.1.2.1-1[11])
Carrier frequency	2.0 GHz
MeNBTx power	46 dBm
MeNB max. antenna gain	13 dB
SCeNBTx power	30 dBm
MeNB antenna pattern	2D Three-sectorized
Shadowing distribution	Log-normal
Macro/SC LOS Prob.	See Table A.2.1.1.2-3 [11]
Thermal noise density	<i>N</i> 0=-174 dBm/Hz

#### 3.2.2.3 Evaluation on exposure reduction

To evaluate the performance of our network we evaluate the SINR associated to the UE transmissions in both the DL and UL. On the contrary, in order to assess the impact of the EMF radiation in HetNets, we use a simplified version of the EI defined in the LEXNET project [3] where only LTE data traffic is assumed. With these assumptions, the EI can be computed as the sum of the DL/UL contributions in the considered time periods (day and night).

```
EI_{category} = k5 x PTx_indoor_day_data / Th_indoor_day_data + K6 x PTx_outdoor_day_data / Th_indoor_day_data + k7 x PTx_indoor_night_data / Th_indoor_night_data + k8 x PTx_outdoor_night_data / Th_indoor_night_data + k9 x SRx_indoor_day + k10 x SRx_outdoor_day + k11 x SRx_indoor_day + k12 x SRx_outdoor_night;
```

Where PTX\_... indicates the UL power [W], Th\_... stands for the related throughput [kB/s], SRX\_... represents the SAR value [W/m2], and the k coefficients are weights that take into account the usage and population statistics.



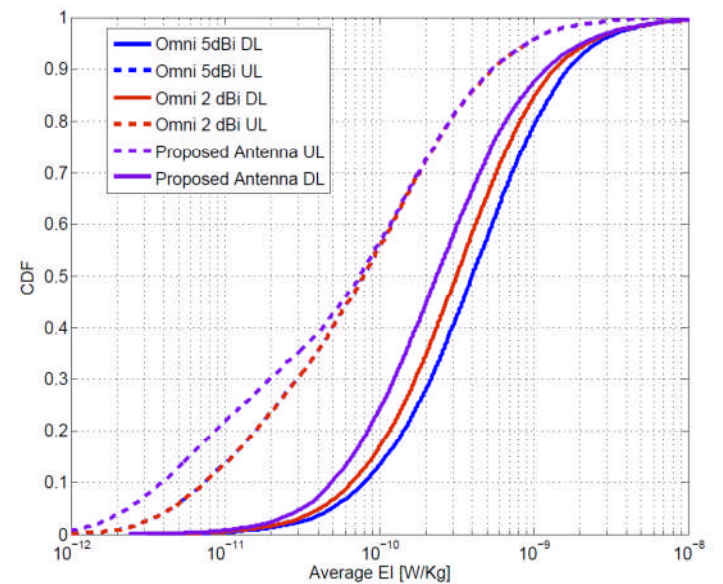


Figure 6. UL and DL Cumulative distribution functions of the daily average El at UEs for different antennas.

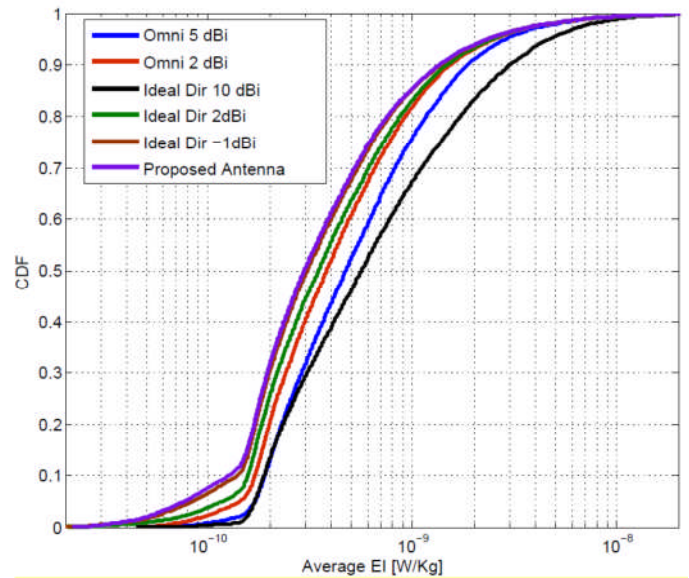
Figure 6 separately shows the UL and DL cumulative distribution function (CDF) of the measured EI at UEs for different antennas at the small cells. In particular, the blue and red lines correspond to the performance of the omnidirectional antennas with 5 and 2 dBi of gain respectively. Additionally, the performance of the proposed solution is described by the violet line. Simulation results show that the UL omnidirectional antennas are characterized by the same performance since the same gain variation applies both in the strength of the received signal as well as on the interference. On the contrary, in the DL a reduction on the antenna gain directly leads to an EI reduction.

However, the proposed solution results in notable EI reduction, especially in the DL where it leads up to 41% gain in terms of the EI with respect to the omnidirectional antenna with 5dBi of antenna gain. On the other side, from the UL perspective, our solution is beneficial for a half of the population without any other negative effect on the other half of the end-users. The latter is composed by cell edge users for which the advantage due to the usage of directive antennas does not compensate the losses in terms of antenna gain.

Figure 7 shows the CDF of the simulated EI at UEs for different antennas at the small cells. The black, green, and brown correspond to the EI related to the ideal directive antennas with gain equal to 10, 2 and -1 dBi respectively.



31



Cumulative distribution functions of the daily average El at UEs for different antennas.

First of all, we can say that larger value of the EI (in the right side of the figure) are associated to indoor UEs, which are characterized by high propagation and penetration losses and make large use of wireless data connections. On the other hand, outdoor UEs located close to small cells are characterized by a limited UL power, which in turns reduces the El. Additionally, results confirm that antennas characterised by limited gain may reduce the user experienced EI, i.e., directive antennas with large gain are not beneficial from the EI perspective, and lead to worse performance than omnidirectional ones.

Accordingly, our simulations show that the proposed antenna design leads up to 22%, 37%, and 47% of gain in terms of EI (measured at the median value of the CDF) with respect to the omnidirectional antenna with 2 dBi of gain, the omnidirectional antenna with 5 dBi of gain, and the ideal directive antenna with 10 dBi of gain. The analysis of global (UL+DL) shows a 3.0 10<sup>-10</sup> W/kg absolute EI at the median point (Figure 7) for the miniature and directive proposed antenna to be compared to the 4.0 10<sup>-10</sup> W/kg absolute EI of the standard 2 dBi omnidirectional antenna.

Figure 8 shows the CDF of the average UL Signal to Noise plus Interference Ratio (SINR) measured at the SCs with respect to the investigated antenna patterns. Our results show that the SCs characterized with an omnidirectional antenna experience the worst performance: with this solution the SC does not distinguish amongst interference signals and useful signals. On the contrary, the small cells with ideal directive antennas achieve the best performance since only the signals originated into the same direction of the useful signal are received at the SC, and most of the interference is rejected.



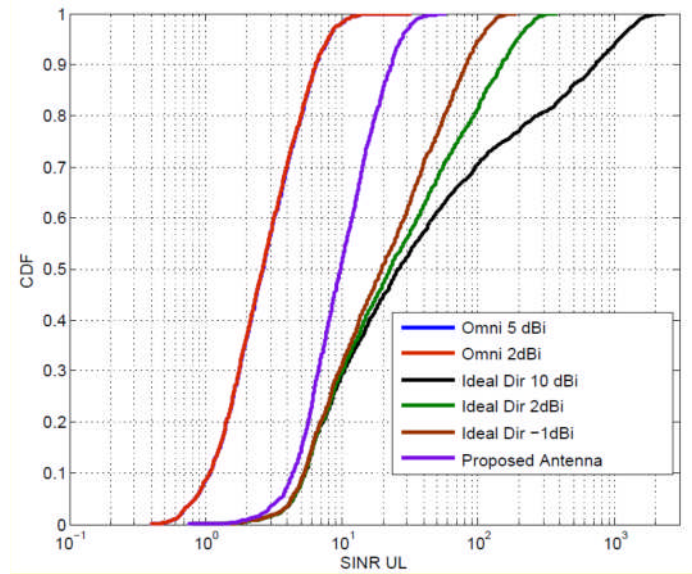


Figure 8. Cumulative distribution functions of the average ULSINR at SCs with respect to different antenna patterns.

Our simulations show that the small cells achieve a 9.3 gain factor with respect to the standard omnidirectional antennas when using ideal directive antennas with  $G_{\rm max}$  equals to 10dBi. Finally, when considering the proposed (realistic) directive antennas, most of the interference is only mitigated and not completely cancelled at the receiver. However, this solution achieves notable improvements with respect to the classic omnidirectional antenna and lead to a 2.77 factor gain. It is important to note that the gain related to the proposed antenna design can be either used to improve the cell data rate or to reduce the UL user power to further reduce the EI.

Figure 9 shows the CDF of the average DL Signal to Noise plus Interference Ratio (SINR) measured at the UEs with respect to the investigated antenna patterns. Results show that using directive antennas has a double effect on the DL SINR, both on the strength of the useful received power as well as the received interference. This can be explained by the following. On the left side of the Figure 9, we can observe the performance of the cell edge UEs, whose received signal is limited when using an antenna with limited gain (negative impact of the proposed antenna). On the contrary, the UEs on the right side of the picture benefit of a reduced interference, which characterise all the directive antennas (positive impact of the proposed antenna).



33

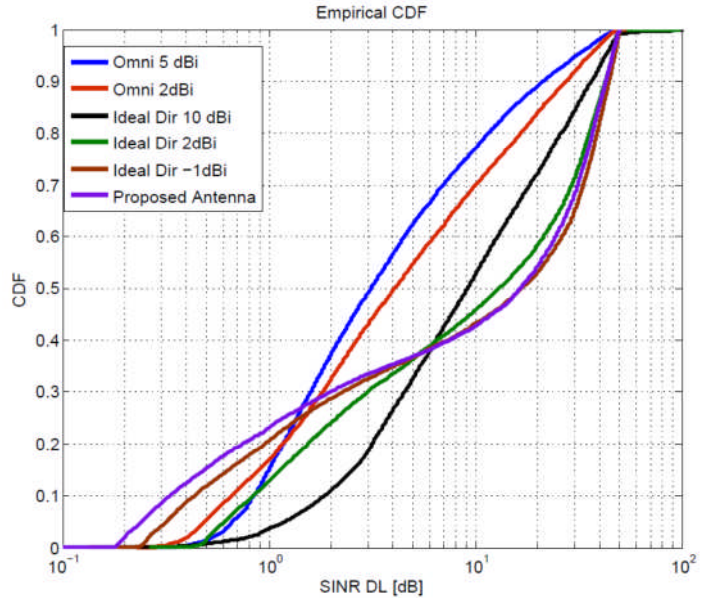


Figure 9. Cumulative distribution functions of the average DL SINR at UEs with respect to different antenna patterns.

Our results (measured at the median value) show that the proposed antenna achieves 1.53 and 2.1 factor gain with respect to the omnidirectional antennas with 2dBi and 5dBi gain.

#### 3.2.2.4 Conclusions, analysis

In this report, a small and directive antenna design to reduce the EM exposure has been presented. It is demonstrated that in such dense environment, the budget link is no more critical point compared to the interference constraint. Thus despite the proposed antenna presents a lower gain, the QoS (here the SINR) is improved by a factor 2.77 and simultaneously the absolute EI is decreased from 4 10<sup>-10</sup>W/kg (2 dBi omnidirectional case) to 3 10<sup>-10</sup> W/kg (miniature and directive antenna case) which corresponds to 25% EI ratio.

#### 3.2.3 Solution C - Enhanced DTX for low EMF communications

#### 3.2.3.1 Remind on solution concept

Today cellular networks are designed to be "always on" to guarantee ubiquitous coverage and backward compatibility. To achieve these goals, most current cellular systems, mandate that the base stations transmit certain control signals, even when there are no active users in the cell. Examples of such signals are cell specific reference signals (CSRS), primary and secondary synchronization signals (PSS and SSS, respectively), and physical broadcast channel (BCH) information (see Figure 10).

The consequence of this approach is that there can be a significant of useless EMF radiations, which are not directly related to UEs accessing the network. De-activating the transmission chain and avoiding the transmission of signaling in absence of data would introduce important EMF reduction and also avoid detrimental interference on the control channel.

Version: V1.1



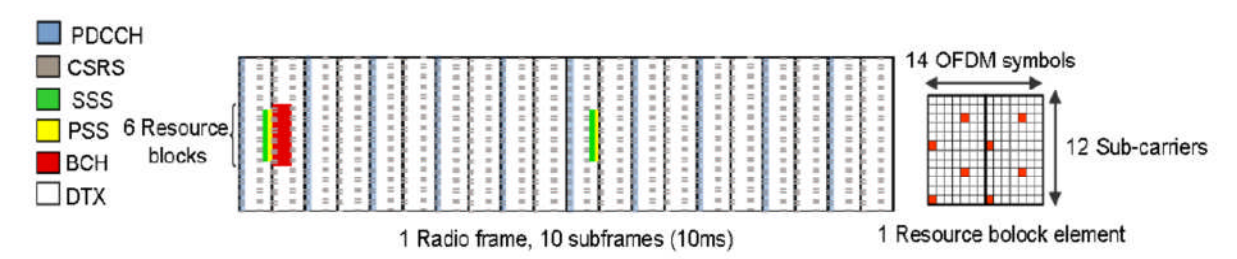


Figure 10. LTE DL radio frame showing CSRS for one antenna port, DL control region (PDCCH) with a size of one OFDM symbol, primary and secondary synchronization signals (PSS and SSS), and broadcast channel (BCH)[14].

From a hardware perspective, it is possible to enable fast activation and de-activation at the eNB if Discontinuous Transmission (DTX) is prioritized in the hardware design process. In particular, modern systems may enter in DTX mode with zero delay and wake up with a delay in the order of 30µs (less than an OFDM symbol) [15], which is basically instantaneous and cost-free [16]. From Figure 11 it can be concluded that it is possible to put the radio into DTX during the OFDM symbols only between cell specific reference signals (CSRS). This mode is denoted in literature as micro DTX [15][14], and it is fully compliant with the 3GPP LTE as it does not require any changes in the control signals. However, it results in limited energy saving because the RF unit is switched off for periods that last less than 1ms, and it does not induce any gain from the EMF reduction perspective as it does not limit the transmitted signals.

To efficiently take advantage of the DTX to reduce the EMF exposure in wireless network, it is necessary 1) to reduce the number of time slot where the small cells are activated and 2) to subsequently limit the control signal overhead. In the next section, we will present a controller based on Fuzzy Q-learning (FQL) tool to achieve the first goal; however, with respect to the second target, it is necessary to exploit an innovative frame structure, where signalling can be adapted according to the cell load.

This approach is in line with a new trend in 3GPP that aims to replace cell specific control channel with more flexible UE specific signals [17]. The main characteristic of these UE specific signals is that they are transmitted only in Physical Resource Blocks (PRBs) used for data transmitted: this reduces the overhead and results in lower inter-cell interference on the control channel.

Integrating all these functionalities enables to switch-off an eNB up to 4 subframes, since each 5 subframes the synchronization signals (PSS/SSS) have to be broadcast to enable coarse time/frequency synchronization and cell (re)selection functions.

Further enhancements can be introduced by consider the concept of dual connectivity, where a UE is simultaneously connected to both a macro cell and a small cell [18]. In this case, small cells are not conventional cells but rather a transmission point, since they are not configured with the conventional cell specific signals, and are used only to carry user traffic. On the contrary, the macro is in charge of all the functionalities related to the Radio Resource Control protocol, such as mobility and connection establishment, it has to send system information and to enable the small cell discovery.

Version: V1.1
Dissemination level: PU



This framework results in a functional split between the user and the control planes. Practically, a UE served by a small cell exploits an inter-eNB Carrier Aggregation approach, which allows to receive the control plane by the macro on a lower band (that provides high coverage), while the data plane is transferred on a higher band (that permits higher data rate) [14].

#### 3.2.3.1.1 DTX Controller based on Fuzzy Q-Learning

Let consider a wireless network where data to be transmitted by small cell is stored in dedicated buffers. When required, a logical controller, activates a given small cell and forwards to it part of the associated traffic. Thereafter, the activated small cell will autonomously manage available radio resources to efficiently transmit the data received according to a first-in-first-out policy.

In our model we consider N buffers of size M packets, each one dedicated to a specific small cell. Let S be a finite set referred to as the small cell state set and defined as  $S = Q \times R \times UE$ , where Q, R, and UE are the composite state sets, which describe the buffer state, the cell capacity, and the number of active UEs per small cell. In particular, at each time step, the small cell queue is described through the couple  $q_t = (l_t, n_t) \in Q$ , where  $n_t$  indicates the size of each packet presents in the queue and  $l_t$  the packet time-to-live.

Moreover,  $r_t \in R$  and  $u_t \in UE$  describe the expected cell capacity (in bits) and the number of served UEs, respectively. Accordingly, each small cell state can be represented through the state vector  $s_t = (q_t, r_t, u_t)$ . The controller observes the current state of each small cell and selects an action  $a_t \in A, \{0, 1\}$ , where  $a_t = 0$  corresponds to keep the small cell and the associated BH link idle, while  $a_t = 1$  indicates that the small cell is activated and  $min(r_t, \sum n_t)$  are transferred to the small cell. A cost is associated to each state-action pair given by

$$C(\mathbf{s}_t, a_t) = P(\mathbf{s}_t, a_t) + \beta d(\mathbf{s}_t, a_t), \tag{3.14}$$

where  $P(s_t, a_t)$  describes small cell radiated power,  $d(s_t, a_t)$  indicates the number of bits dropped due to the latency constraints, and  $\beta$  is a constraint that prioritizes amongst QoS and power consumption. The goal is to find an optimal policy, i.e., a state-action mapping that minimizes the expected cumulative cost of the agent when visiting the state space S. However, in general, it is difficult to define appropriate state and action spaces for RL problems. The discretization of the state space has to be rather fine to cover all possibly relevant situations and there can also be a wide variety of actions to choose from. As a consequence, there exists a combinatorial explosion problem when trying to explore all possible actions from all possible states.

#### **Fuzzy Q-Learning**

To solve dimensionality problems, the fuzzy inference system (FIS) is a suitable candidate. In fact, it aims to perform as a control system considering that, many times, real problems cannot be efficiently expressed through mathematical models. The FIS relies on fuzzy logic in which, unlike standard conditional logic, the truth of any statement is a matter of degree. In other words, the statement "x is a member of X" is not necessary true of false and the degree to which any fuzzy statement is true is denoted by a value between 0 and 1.



In our model, the small cell state vector is represented by L=4 linguistic variables. Then by denoting as  $\bar{S}=\{\bar{s}_1,\dots,\bar{s}_n\}$  the set of fuzzy state vectors composed by the linguistic variables the fuzzy inference rule is:

IF input state vector  $\mathbf{s}$  is  $\bar{s}_i$ 

Then action  $a_0$  with  $q(\bar{s}_i, a_0)$ 

or action  $a_1$  with  $q(\bar{s}_i, a_1)$ ,

where  $a_j \in A$  is the j-th action candidate which is possible to choose for state  $\bar{s}_i$ , and  $q(\bar{s}_i, a_j)$  is the fuzzy Q-value for the state-action pair  $(\bar{s}_i, a_j)$ . The FQL has two outputs: one corresponds to the inferred action and the other represents the Q-value for the state-action pair (s, a):

$$a = \frac{\sum_{i}^{n} w_i \cdot a_i}{\sum_{i}^{n} w_i} \tag{3.15}$$

$$Q(\mathbf{s}, \mathbf{a}) = \frac{\sum_{i}^{n} w_{i} \cdot q(\bar{s}_{i}, a_{i})}{\sum_{i}^{n} w_{i}},$$
(3.16)

Where  $w_i$  represents the truth value (i.e., the output of fuzzy-AND operator) of the rule representation of FQL for  $\bar{s}_i$ , and  $a_i$  is the action selected for state  $\bar{s}_i$ . Q-values have to be updated after the action selection process according  $\log(\bar{s}_i,a_i)=q(\bar{s}_i,a_i)+\alpha\cdot\Delta q(\bar{s}_i,a_i)$ , where  $\alpha$  is the learning rate,  $\Delta q(\bar{s}_i,a_i)=(C(s,a)+\delta Q(y,a')-Q(s,a))\cdot\frac{w_i}{\sum_{i=1}^{n}w_i}$ , C(s,a) represents the cost obtained applying action a in state vector s, and Q(y,a') is the next-state optimal Q-value defined as:

$$Q(\mathbf{y}, \mathbf{a}') = \frac{\sum_{i}^{n} w_{i} \cdot q(\bar{y}_{i}, a_{i}^{*})}{\sum_{i}^{n} w_{i}},$$
(3.17)

and  $a_i^* = \frac{argmin}{a_j^* \in A} q(\bar{y}_i, a_j^*)$  is the optimal action for the next state  $\bar{y}_i$ , after the execution of action  $a_i$  in the fuzzy state  $\bar{s}_i$ .

The proposed FQL algorithm consists of a four layer Fuzzy Inference System (FIS), where the first layer has as input the four linguistic variables defined by the term sets:

 $T(l) = \{VeryHighUrgent, VeryUrgent, Urgent, Almosturgent, NotUrgent\},$ 

 $T(\mathbf{n}) = \{VeryHighlyLoaded, HiglyLoaded, MidLoaded, LightlyLoaded, UnLoaded\},$ 

 $T(r) = \{LowCapacity, MidCapacity, HighCapacity\},$ and

 $T(u) = \{FewUEs, SomeUEs, ManyUEs\}.$ 

In this layer, there are  $z = |T(\boldsymbol{l})| + |T(\boldsymbol{n})| + |T(r)| + |T(u)| = 16$  output nodes, each one describing (via a trapezoidal membership function  $\mu(x)$ , to which degree the small cell state variables belong to the appropriate fuzzy sets (fuzzification process). Let denote as  $O_{1,k}$  with  $1 \le k \le z$  the output of this layer.

The second Layer is named as the rule nodes layer and is composed by  $n = |T(\boldsymbol{l})| \cdot |T(\boldsymbol{n})| \cdot |T(r)| \cdot |T(u)| = 225$  nodes. Each node gives as output the truth value of the ith fuzzy rule  $O_{2,i}$  with  $1 \le i \le n$  which is the product of four membership values corresponding to the term set inputs.



The third layer is also composed of n=225 nodes named as action-selection nodes. The selection of the per node action a is based on the  $\epsilon$ -greedy action selection policy. Each node  $1 \le i \le n$  generates two output values as follows:

$$O_{3,i}^{A} = \frac{O_{2,i} \cdot a_{i}}{\sum_{i}^{n} O_{2,i}},\tag{3.18}$$

$$O_{3,i}^{Q} = \frac{O_{2,i} \cdot q(\bar{s}_{i}, a_{i})}{\sum_{i}^{n} O_{2,i}}$$
(3.19)

The fourth layer is has two output nodes, action node  $O_4^A$  and Q-value node  $O_4^Q$ , which represent the results of the defuzzification process.

$$O_4^A = \sum_{i}^{n} O_{3,i}^A \tag{3.20}$$

$$O_4^Q = \sum_{i}^{n} O_{3,i}^Q \tag{3.21}$$

#### 3.2.3.2 Specific scenario inputs

We consider a mobile wireless cellular network where user terminals and eNBs implement an OFDMA air interface based on 3GPP/LTE DL specifications. Coherent with the study on small cell enhancement, currently under investigation in 3GPP [11], our research focuses on HetNets where small cells operate in a dedicated carrier with respect to the macro cell. Here we assess our solution in a hotspot where a cluster of four small cells is deployed in each macro cell sector. Near Real Time Video traffic (average user rate and latency constraints equal to 64 Kbps and 100 ms, respectively) is simulated for the UEs located in the central macro cell, while other cells generate only additive interference. Moreover, since we focus on a small cell controller, we present here only results related to small cells. Results are averaged over 50 independent runs that simulate 10 seconds of network activity. At the beginning of a run, the small cell hotspots and the UEs are randomly deployed in the macro cell area. Additional simulation parameters are detailed in Table 6.

 Table 6.
 Simulation parameters.

Parameter	Value
Macro ISD	500 m
N <sub>iSC</sub> per sector	4
Users per sector	20-45
Traffic	NRTV 64 kps
Radio access channel	ITU UMi
Carrier	2GHz (macro),
	3.5GHz (small cells)
Bandwidth (RAN)	10MHz

#### 3.2.3.3 Evaluation on exposure reduction

To evaluate the performance of our network we evaluate the SINR associated to the UE transmissions in both the DL and UL. On the contrary, in order to assess the



impact of the EMF radiation in HetNets, we use a simplified version of the EI defined in the LEXNET project [3] where only LTE DL is considered. With these assumptions. the EI can be computed as the sum of the contribution due to control and data channels in the considered time periods (day and night)

```
EI \{category\} = k9 \times S_{RX} \text{ indoor day } +
                         k10 x S<sub>RX</sub> outdoor day +
                         k11 x S<sub>RX</sub>_indoor_day +
                         k12 x S<sub>RX</sub>_outdoor_night;
```

Where S<sub>RX</sub>... represents the SAR value [W/m<sup>2</sup>], and the k coefficients are weights that take into account the usage and population statistics.

Following results presented in the literature we assume that the control/data separation and the usage on user specific control channel can result in 75% reduction of pilot overhead [19].

Figure 11 show the achievable gains by using the proposed framework that combined an optimized DTX controller based on FQL jointly combined with the control signal of next generation cellular network. In particular, this approach is accessed with respect to the classic LTE control signal (circled line), with respect the classic DTX solution presented in [15] with (diamond-marked line) and without the new control signal (squared-dashed line). Additionally, the gain of the new control signal with respect to the baseline solution is accessed when using the classic DTX (plus-marked line). Results in Figure 11 show that the EMF gains are constant with respect to the number of UEs (i.e., the cell load). Furthermore our solution can achieve up to 80% of gain in terms of EMF reduction without affecting the user QoS.

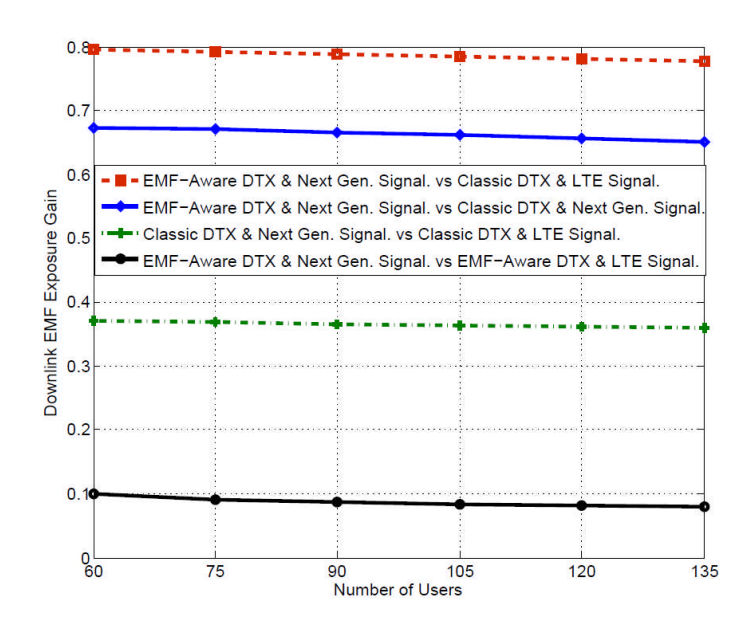


Figure 11. EMF Gain vs number of active UEs for different DTX controller.

Figure 12 shows the average perceived latency at the small cell UEs with and without the proposed EMF-aware controller. Note that classic DTX as well as the different control signal schemes have no impact on the latency. These results confirm that the



proposed DTX-controller takes into account the latency constraints of the video application (100 ms), thus avoiding packet losses.

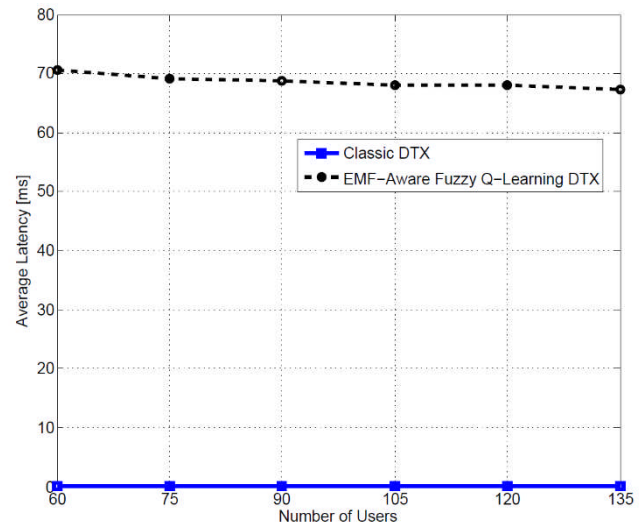


Figure 12. User latency vs. the number of active UEs.

### 3.2.3.4 Conclusions, analysis

In this study we have investigated optimized cell DTX controller with future generation of control signals, which adapt the pilot overhead to momentary cell load and avoid unnecessary transmission in absence of data.

The obtained results confirm that the proposed framework can introduce up to 80% of gains in term of EMF reduction in the DL with respect to baseline solutions.

#### 3.2.4 Solution D - Low noise receiver architecture

#### 3.2.4.1 Remind on solution concept

Nowadays multi-band receivers are demanded to fulfil the requirements of next generation wireless technologies. This study proposes reconfigurable multi-band low noise receiver architecture capable to improve the receiver sensitivity while keeping, or even improving specific requirements such as intermodulation, spurious rejection, channel selectivity or blocking response. Reconfigurability feature is applied using tuneable components in different receiver stages, avoiding multiple RF chains working in different operating bands presented in typical multi-band receivers.

Figure 13 presents the proposed reconfigurable low noise receiver architecture focusing on improving noise figure (NF) to reduce EMF exposure, and minimizing the size and the power consumption.



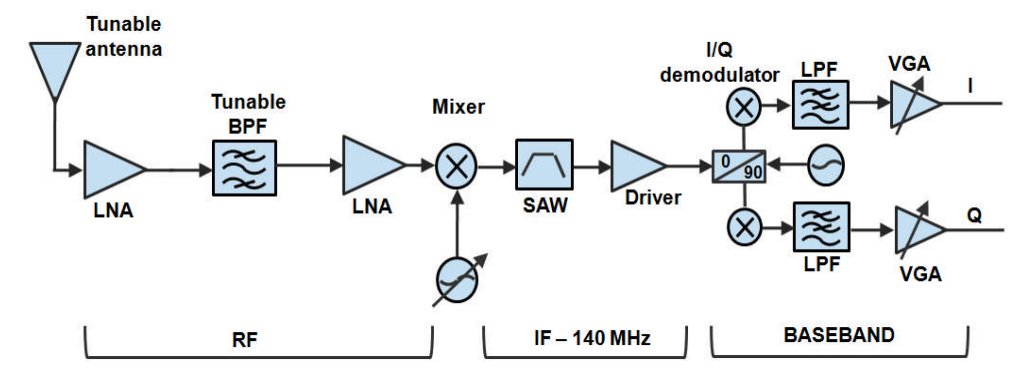


Figure 13. Block diagram of the reconfigurable low noise receiver

This low EMF solution refers to UL. By improving receiver NF, lower power is required at receiver input to ensure a given signal-to-noise ratio (SNR). Thus, if lower power should be received at base station, the required transmitted power at terminal can be reduced, thus lowering human exposure to EMF.

In this architecture, the most challenging block is the reconfigurable bandpass filter (BPF) whose design and results are presented below.

#### 3.2.4.2 Specific scenario inputs

This work proposes reconfigurable receiver architecture capable to operate at different operating bands tuning appropriately varactors. To validate multi-band operation, LTE band 20 (832 – 862 MHz) and LTE band 3 (1710 – 1785 MHz) were selected.

The proposed architecture is compared to a reference multi-band receiver supporting also both LTE frequency bands.

#### 3.2.4.3 Evaluation on exposure reduction

El evaluation consists on the assessment of the reconfigurable low noise receiver compared to the reference multi-band receiver, basically in terms of NF as it was described in D4.2 [1]. Nevertheless, other parameters were also considered to fulfil 3GPP receiver requirements [20].

For the evaluation, typical commercial components were selected to build up the reference receiver and the reconfigurable receiver taking into account 3GPP receiver requirements.

A system level analysis was done in each receiver describing each component with its main RF parameters such as NF, gain, output third-order intercept point or output power at 1dB compression point. The evaluation results should be considered as estimation, because slight variations can appear depending on the selected components. Furthermore, in the analysis two results are highlighted, one is related to NF for the block up to demodulation stage and another refers to the NF of the complete receiver. The scope of the WP6 hardware demonstrator is limited up to demodulation stage due to lab equipment constraints.

In the reference receiver, specific components as the low noise amplifier or the BPF were selected for each operating band. Narrowband components are usually

-90.3

dBm

-92.0



implemented because they have better performance than broadband components. Table 7 and Table 8 show the system level analysis performed in the reference receiver in LTE band 20 and LTE band 3 respectively.

REFERENCE RECEIVER - LTE BAND 20 (832 - 862 MHz) STAGE DATA UNITS STAGE 1 STAGE 6 STAGE 7 STAGE 8 STAGE 2 STAGE 3 STAGE 4 STAGE 5 SPDT Switch I/Q Demodulator Component type SPDT Switch LNA LPF Input power: Æ -90dBm Manufacturer Macom TriQuint Freescale Minicircuits Macom **Analog Dev** TTI Analog Dev MASWSS0115 Part number 856932 MML09211H LFCN-800D+ MASWSS0115 ADL5380 ADA4857 AD8338 Noise Figure dB dB -0.3 -1.7 -1.0 -0.3 6.9 0.0 45.1 Output IP3 dBm 46,0 20,0 32,5 40,0 46,0 36,6 10,0 12,0 dBm 25.0 20.0 220 40.0 25.0 18.5 0.0 12.0 STAGE ANALYSIS 0,3 2,0 2,6 2,6 3,0 3,0 Noise Figure 2,6 Gain dB 19,3 18,3 18,0 24,9 70,0 Output IP3 46,0 20,0 30,4 30,0 33,8 10,0 12,0 dBm 32,0 19,2 17,8 P1dB dBm 18,3 20,9 12,0

Table 7. System level analysis in the reference receiver (LTE band 20)

Table 8. System level analysis in the reference receiver (LTE band 3)

-70.7

-71.7

-72.0

-65.1

-65.1

-20,0

REFERENCE RECEIVER - LTE BAND 3 (1710 - 1785 MHz)											
STAGE DATA	UNITS	STAGE 1	STAGE 2	STAGE 3	STAGE 4	STAGE 5	STAGE 6	STAGE 7	STAGE 8		
Component type	-	SPDT Switch	SAW filter	LNA	LPF	SPDT Switch	/Q Demodulator	BB LPF	BB VGA		
Input power: -90dBm		43	-[%]-	-[]-	-[%]-	# <del>**</del>		-[%]-	-123-		
Manufacturer	i i	Macom	TriQuint	Freescale	Minicircuits	Macom	Analog Dev	TTI	Analog Dev		
Part number		MASWSS0115	856654	MML20211HT1	LFCN-1575D+	MASWSS0115	ADL5380	ADA4857	AD8338		
Noise Figure	dB	0,3	2,0	0,7	1,0	0,3	11,7	3,0	3,0		
Gain	dB	-0,3	-2,0	19,7	-1,0	-0,3	6,8	0,0	47,1		
Output IP3	dBm	46,0	5,0	32,2	40,0	46,0	34,6	10,0	12,0		
P1dB	dBm	25,0	5,0	21,1	40,0	25,0	18,4	0,0	12,0		
STAGE ANALYSIS											
Noise Figure	dB	0,3	2,3	3,0	3,0	3,0	3,7	3,7	3,7		
Gain	dB	-0,3	-2,3	17,4	16,4	16,1	22,9	22,9	70,0		
Output IP3	dBm	46,0	5,0	24,0	22,9	22,6	28,2	9,9	12,0		
P1dB	dBm	25,0	4,9	19,5	18,5	17,4	17,4	-0,1	12,0		
Output power	dBm	-90,3	-92,3	-72,6	-73,6	-73,9	-67,1	-67,1	-20,0		

Table 9 summarizes NF results in the reference receiver before demodulation stage and its total performance. From these results, NF performance in a reference multiband receiver can be estimated around 3 to 4 dB.

Table 9. NF evaluation in the reference receiver.

NF results	LTE Band 20	LTE band 3
Before demodulation	2.6 dB	3 dB
Total NF	3 dB	3.7 dB

The reconfigurable BPF design is the most challenging block in the proposed architecture. Different hardware prototypes based on tuneable elements were realized [1]. All solutions have constraints in terms of insertion loss, wideband operation, high frequency operating range or manufacturing integration. In order to achieve appropriate reconfigurability feature of the BPF, varactors were considered as the most promising solution for the application.

Version: V1.1

**Output power** 



Firstly, a reconfigurable BPF based on varactor-tunable7-section Chebyshev lowpass filter (LPF) and varactor-tunable7-section Chebyshev highpass filter (HPF) was manufactured. The measured insertion loss was as high as 13dB at LTE band 20. The greater is the order of the filter, the higher would be the selectivity, but more insertion loss would be achieved.

Secondly, a stepped impedance resonator (SIR) topology was considered to reduce insertion loss. A varactor-tunable SIR prototype was manufactured. This solution has around 5dB insertion loss. However, the frequency selectivity was poor.

Finally, previous topologies were appropriately combined in order to achieve low insertion loss and better frequency selectivity. Figure 14 presents the block diagram and the manufactured prototype of the reconfigurable BPF design combining a varactor-tunable SIR topology and a varactor-tuneable 5-section LPF topology.

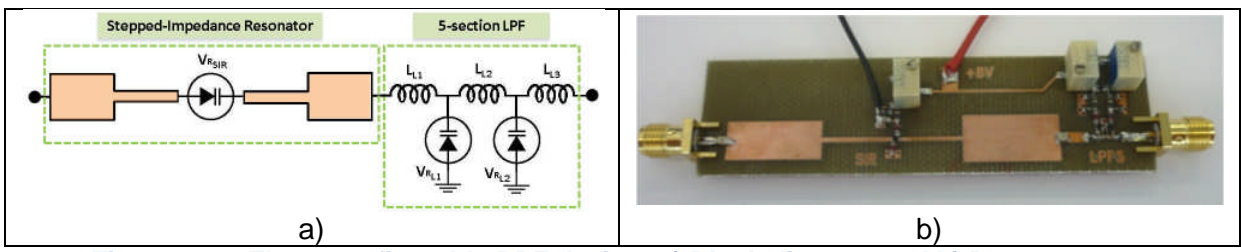


Figure 14. The reconfigurable BPF design: a) Block diagram and b) Prototype

Figure 15 shows that the measured insertion loss results are about 7.5 dB and 6 dB in LTE band 20 and LTE band 7 respectively, achieving good frequency selectivity. The linearity was also evaluated in the BPF prototype due to the implementation of active components (varactors). The output power at 1dB compression point in the BPF prototype is around 10 dBm which is considered appropriate for the application.

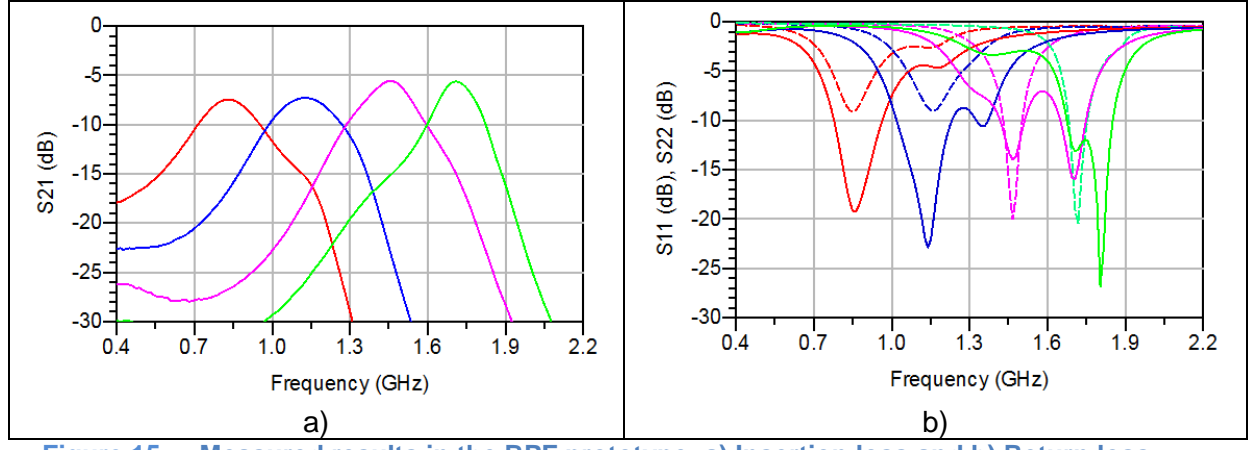


Figure 15. Measured results in the BPF prototype: a) Insertion loss and b) Return loss

This reconfigurable BPF design was integrated in the reconfigurable receiver prototype developed in WP6.

Considering the insertion loss and the output power at 1dB compression point results from the reconfigurable BPF, the reconfigurable receiver was analysed as the reference receiver. In this architecture, some components require wideband

Version: V1.1



operation in order to work at different operating bands. Table 10 and Table 11 present the system level analysis performed in the reconfigurable receiver in LTE band 20 and LTE band 3 correspondingly.

Table 10. System level analysis in the reconfigurable receiver (LTE band 20)

	RECONFIGURABLE RECEIVER - LTE BAND 20 (832 - 862 MHz)									
STAGE DATA	UNITS	STAGE 1	STAGE 2	STAGE 3	STAGE 4	STAGE 5	STAGE 6	STAGE 7	STAGE 8	STAGE 9
Component type		LNA	Tunable filter	LNA	Mixer	SAW filter	Driver	/Q Demodulator	BB LPF	BB VGA
Input power: -90dBm			-13%-	-[]			-[>-		-[%]-	
Manufacturer		Trquint	TTI	Triquint	Minicircuits	Golledge	Minicircuits	Linear	TTI	Analog Dev
Part number	i i	TQP3M9005	SMV1247	TQP3M9005	HJK-272H+	MA05918	GALI-3+	LT5517	ADA4857	AD8338
Noise Figure	dB	1,0	7,5	1,0	8,0	11,5	2,6	9,0	6,0	3,0
Gain	dB	19,4	-7,5	19,4	-8,0	-11,5	23,1	4,0	0,0	31,1
Output IP3	dBm	32,5	10,0	32,5	17,0	20,0	28,0	27,5	10,0	12,0
P1dB	dBm	22,0	10,0	22,0	12,0	20,0	13,2	14,0	0,0	12,0
STAGE ANALYSIS						3. /		50 60		
Noise Figure	dB	1,0	1,2	1,2	1,2	1,4	1,6	1,6	1,6	1,6
Gain	dB	19,4	11,9	31,3	23,3	11,8	34,9	38,9	38,9	70,0
Output IP3	dBm	32,5	9,9	27,6	15,1	3,5	24,2	24,8	9,9	12,0
P1dB	dBm	22,0	8,7	21,0	9,5	-2,0	12,5	12,1	-0,3	11,9
Output power	dBm	-70,6	-78,1	-58,7	-66,7	-78,2	-55,1	-51,1	-51,1	-20,0

Table 11. System level analysis in the reconfigurable receiver (LTE band 3)

	RECONFIGURABLE RECEIVER - LTE BAND 3 (1710 - 1785 MHz)										
STAGE DATA	UNITS	STAGE 1	STAGE 2	STAGE 3	STAGE 4	STAGE 5	STAGE 6	STAGE 7	STAGE 8	STAGE 9	
Component type		LNA	Tunable filter	LNA	Mixer	SAW filter	Driver	/Q Demodulator	BB LPF	BB VGA	
Input power: -90dBm		-[]	-28-	-[>]-		-[%]-	-[]-		-{%}-	-123-	
Manufacturer		Triquint	TTI	Triquint	Minicircuits	Golledge	Minicircuits	Linear	TTI	Analog Dev	
Part number		TQP3M9005	SMV1247	TQP3M9005	HJK-272H+	MA05918	GALI-3+	LT5517	ADA4857	AD8338	
Noise Figure	dB	1,0	6,0	1,0	8,0	11,5	2,6	9,0	6,0	3,0	
Gain	dB	16,7	-6,0	16,7	-8,0	-11,5	23,1	4,0	0,0	35,0	
Output IP3	dBm	33,0	10,0	33,0	17,0	20,0	28,0	27,5	10,0	12,0	
P1dB	dBm	22,0	10,0	22,0	12,0	20,0	13,2	14,0	0,0	12,0	
STAGE ANALYSIS											
Noise Figure	dB	1,0	1,2	1,3	1,3	1,8	2,1	2,2	2,2	2,2	
Gain	dB	16,7	10,7	27,4	19,4	7,9	31,0	35,0	35,0	70,0	
Output IP3	dBm	33,0	9,9	25,7	14,3	2,8	23,8	24,6	9,9	12,0	
P1dB	dBm	22,0	9,0	20,5	9,2	-2,3	12,5	12,1	-0,3	12,0	
Output power	dBm	-73,3	-79,3	-62,6	-70,6	-82,1	-59,0	-55,0	-55,0	-20,0	

NF results in the reconfigurable receiver before demodulation stage and its total performance are depicted in Table 12. In the reconfigurable receiver, NF performance is estimated to be around 1.5-2.5dB.

Table 12. NF evaluation in the reconfigurable receiver

NF results	LTE Band 20	LTE band 3
Before demodulation	1.6 dB	2.1 dB
Total NF	1.6 dB	2.2 dB

Comparing the results from the reference receiver and the reconfigurable receiver (Table 13), it shows around 1dB NF improvement before demodulation and around 1.5 dB in total.

Table 13. NF evaluation in the reference receiver and the reconfigurable receiver

NF	Before der	nodulation	Total performance		
improvement	Reference receiver	Reconfigurable receiver	Reference receiver	Reconfigurable receiver	



LTE band 20	2.6 dB	1.6 dB	3 dB	1.6 dB
LTE band 3	3 dB	2.1 dB	3.7 dB	2.2 dB
	≈ 1	dB	≈ 1. <del>.</del>	5 dB

In D4.2 [1], EI evaluation was performed up to the step 4 showing the potential EI reduction as function of the receiver NF improvement, which is evaluated through comparing the proposed receiver with the reference receiver. Table 14 presents the potential EI reduction as function of the receiver NF improvement:

Table 14. Potential El reduction as function of the receiver NF improvement

El reduction	El reduction as function of NF (%)		Reference receiver NF (dB)				
of NI			3.5 dB	4 dB			
able NF	1.5 dB	29.2 %	36.9 %	43.8 %			
figur ver dB)	2 dB	20.6 %	29.2 %	36.9 %			
Reconf recei	2.5 dB	10.9 %	20.6 %	29.2 %			

From the previous analysis, it has been shown that with 1.5 dB NF improvement, the expected relative EI reduction is around 29.2% using this low EMF solution. In all this analysis, the QoS maintains constant assuming the same conditions (channel bandwidth, processing gain, radio link, etc.) in both receivers. By improving NF performance in the reconfigurable receiver, SNR also improves in the same relation compared to the reference receiver. Therefore to maintain the same SNR as in the reference receiver, the required transmitted power at terminal can be reduced using the reconfigurable receiver, enhancing EMF exposure.

In order to calculate the absolute EI, the impact of the proposed solution on the absolute exposure level and dose per day should be evaluated. This refers to the step 5 of the EI evaluation common methodology analysis regarding the 24h activities breaking down.

Initially, one reference global scenario was defined to calculate the EI "before" LEXNET and for each solution the EI "after" LEXNET should be also evaluated. Details about the distribution of different input parameters such as population categories(children, young people, adults and seniors), time periods (day and night), environments (indoor and outdoor) or network usage (voice and data traffic) are required.All these parameters were defined and computed in order to generate k coefficient matrices for each scenario[3] which assist EI calculation. The current study refers to the urban macro LTE scenario and its corresponding k coefficient matrix is included in D2.8 [3].



Apart from the k coefficient matrix for the urban macro LTE scenario, other input parameters are required to calculate the global EI: the transmitted power, the received power density and the throughput.

For the urban LTE scenario, the mean transmitted power at mobile terminal is taken to be 0 dBm(1mW) and the mean received power at small base station in -60 dBm (1\*10<sup>-9</sup> W). Therefore considering LTE band 3, the received power density is about 4.5\*10<sup>-7</sup> W/m<sup>2</sup>.

Two different network usages are considered: voice and data traffic. Nevertheless, in the urban macro LTE scenario only data traffic usage is now considered. Assuming moderate usage, it is assumed that 66MB of data per day is the amount of data traffic for a user.

Taking into account these input parameters and the k coefficient matrix for the urban macro LTE scenario, the absolute EI can be calculated using the formula "EI\_global" defined in D2.8 [3]. Table 15 presents the absolute EI "before" LEXNET associated to the reference receiver and the absolute EI "after" LEXNET associated to the proposed reconfigurable receiver.

 Table 15.
 Absolute El in the reference receiver and the reconfigurable receiver

	Reference	Reconfigurable receiv	er – NF imp	provement
	receiver	0.5 dB	1 dB	1.5 dB
Absolute EI (10 <sup>-8</sup> ) [W/Kg]	3.28	2.95	2.62	2.29
El reduction (%)		9.9%	19.9%	29.9%

The absolute EI "before" LEXNET related to the reference receiver is 3.28\*10<sup>-8</sup> W/kg. Meanwhile, the absolute EI "after" LEXNET related to the reconfigurable receiver presenting around 1.5 dB NF improvement is 2.29\*10<sup>-8</sup> W/kg.

Furthermore, the relative EI reduction was calculated achieving 29.9% for 1.5 dB NF improvement in the reconfigurable receiver.

#### 3.2.4.4 Conclusions, analysis

The reconfigurable low noise receiver architecture can improve NF performance around 1.5 dB compared to the reference receiver, reducing the absolute EI from 3.28\*10<sup>-8</sup> W/Kg to 2.29\*10<sup>-8</sup> W/Kg, which implies 29.9% EI reduction.

To sum up, the most challenging block in the proposed architecture is the reconfigurable BPF. The tuning feature was obtained thanks to varactors. Along this study several solutions based on tuneable components were evaluated. However all of them have constraints in terms of insertion loss, wideband operation, high frequency operating range or manufacturing integration. The technology maturity of tuneable components is still underdeveloped to build reconfigurable BPFs, which would operate in wide frequency range at microwave frequencies. Nevertheless it is an attractive topic, and the obtained results have shown that it is possible to meet requirements from multi-band and multi-RAT devices.

Version: V1.1



# 3.2.5 Solution E- Enhanced efficiency in reference symbols usage

# 3.2.5.1 Remind on solution concept

The evolution of the wireless networks such as the LTE-A constantly involves increasing data throughput to meet the ever-increasing traffic demand, and at the same time aims for reduction of transmission power for green and low EMF radios. By considering the presence of the various reference symbols (RS) in the LTE systems, such as the common reference symbol (CRS), demodulation reference signals (DMRS), channel state information (CSI) RS, the solution we envisage is to reduce the "transmission overhead" for a specific amount of data, therefore to reduce to the overall data transmission time and hence user exposure

# 3.2.5.2 Specific scenario inputs

The evaluation is carried out over LTE band 20.

## 3.2.5.3 Evaluation on exposure reduction

The impact of the more efficient reference symbol usage on EI is mainly reflected through the reduction of DL transmission time. Such reduction in transmission time can be possible when more data OFDM symbols, in the form of a Resource Element in LTE, can be conveyed per LTE DL frame (with duration of 10ms) or sub-frame (with duration of 1ms). In order to allow for more data RE in a frame, some of the non-data related REs will need to be removed and then replaced with data REs. As mentioned previously in [1], the non-data REs investigated in this study are the DMRS and CRS. If designed properly, a new DMRS/CRS pattern will allow a reduced number of DMRS and CRS RE to be used a LTE frame and cause no apparent QoS loss.

There are two approaches to evaluate the effectiveness of the proposal. The first is on the basis of theoretical/numerical analysis, and by counting the number of REs of a LTE system's resource block (RB) being made available by using a newly designed RS patterns. With consideration to REs occupied by other RSs and control signalling employed in a LTE system, comparisons in a number of data REs available per subframe with or without the new RS pattern can be carried out. Subsequently, assuming the amount of data OFDM symbols for the transmission remain the same, a transmission time reduction can then be calculated. The second is through a simulation justification. This is a phase of evaluation that has been developed intensively and has generated a number of results. The following is an outline of the simulation set-up.

- 1. Reference Measurement Channel (RMC) 3GPP 36.101 Compatible.
- 2. Transmission simulated using extended pedestrian propagation channel model.
- 3. Channel noise is added to the received waveform which is then OFDM demodulated, resulting in a received resource grid
- 4. Calculate average frame throughput on various transmission configuration
- 5. Channel estimation is performed to determine the channel between the transmit/receive antenna pairs.
- 6. The PDSCH (Physical DL Shared Channel) data is then extracted and decoded from the received resource grid.



7. Using the result of the block CRC the throughput performance of the transmit/receive chain is determined.

The solution "Enhanced Efficiency in Reference Symbol Usage" is applicable to LTE DL and mainly designed for the Mean Tx duration reduction."

In this section, details of the numerical analysis will be given. As previously introduced, a new DMRS pattern will be designed to reuse part of the CRS REs. There are several ways of configuring the new DMRS patterns.

It is assumed in the small cell environment that, from the REs that may be reserved for the configuration of 4 CRS ports, a significant amount of these REs can be saved from being used by CRS, and instead to be used by the transmission of the DMRS. This is because the configuration of CRS does not always need to cover four antenna ports (In LTE, one antenna port correspond to one radio channel) in the small cells environment. This is as with small cells, it is likely that the channel conditions between the antenna ports may exhibit strong correlation, due to the fact that the antennas are closed placed together and exhibits very similar fading patterns. The layer 1 transmission is likely to be always or at least frequently used with high order modulation such as the 256-QAM.

The arrangement of reusing the CRS resources t create a new DMRS pattern will offer ample possibilities. Depending on the number of cells that will be considered for DMRS multiplexing and the number of DMRS REs desired in a RB, there are a number of possibilities available for the configuration of the new DMRS, which will be introduced as following.

Starting from the 2 CRS ports configuration case, the antenna port 0 will remain to be used by CRS, which is essential to maintain backward capability. Then the remaining antenna port 1 will be used by the DMRS as drawn in Figure 16. The shaded " $R_0$ " is the CRS port 0 and the shaded " $D_0$ " is the first DMRS port.

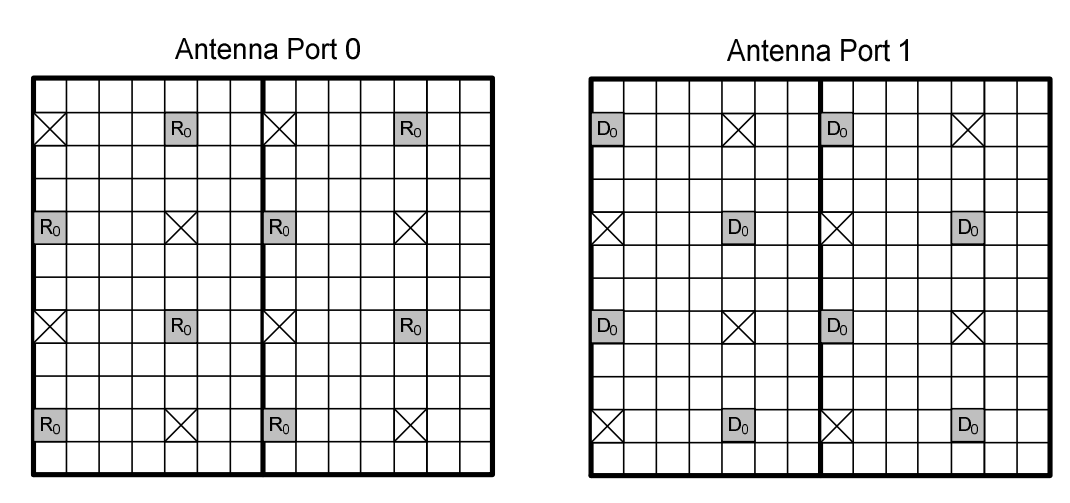
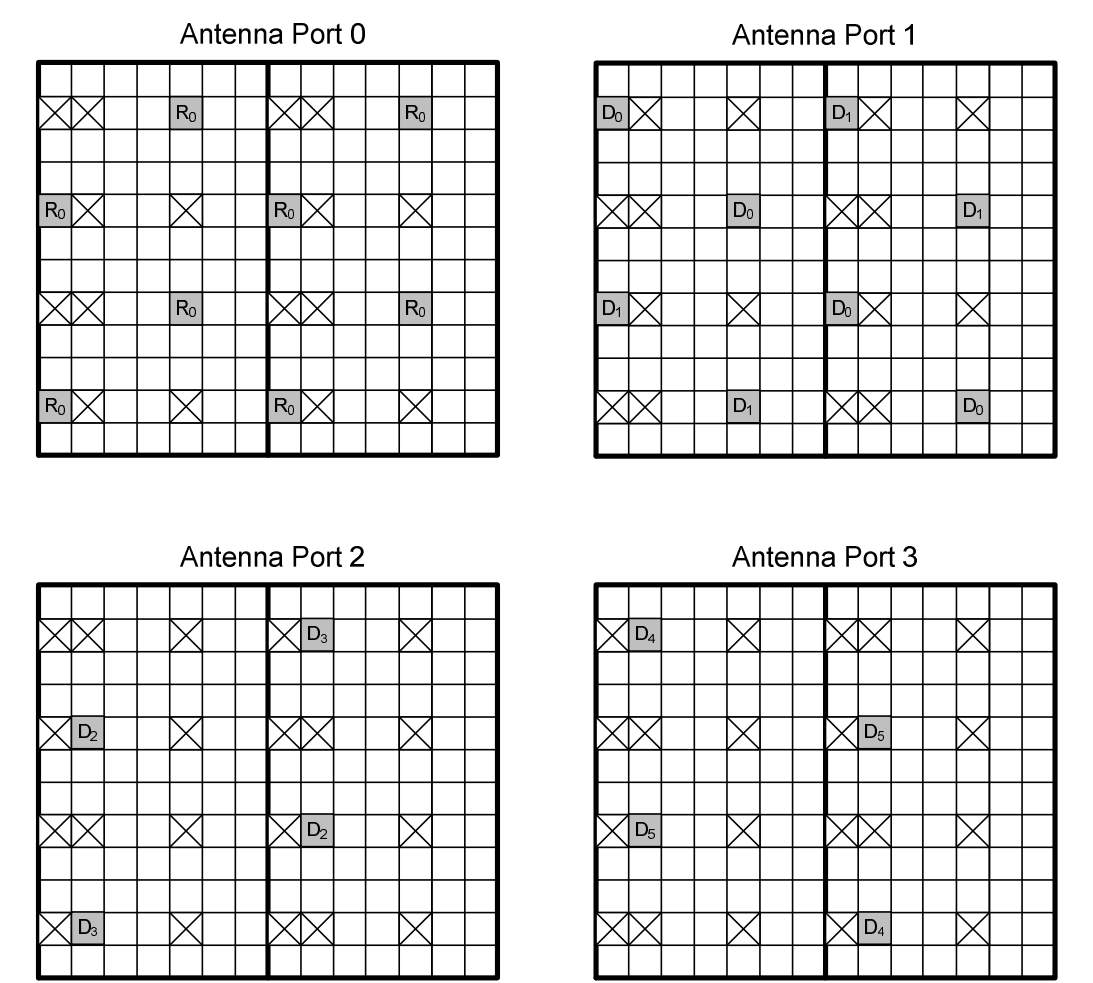


Figure 16. Antenna Port 1 configured for DMRS in the 2 CRS ports case

During the case of 4 CRS ports being available, similar to the 2 CRS ports case, the configuration of Antenna Port 0 CRS is essential to be reserved, and assuming only 1 CRS port is required, the other 3 CRS ports REs can be configured as DMRS. If



assuming 4 REs required for rank 1 DMRS in two of the neighbouring cells and 2 REs required for the rest of cells, the re-used REs from CRS port 1-3 will be to able host 6 new orthogonal DMRS patterns, as depicted in Figure 17.



DMRS configured on 3 CRS antenna ports in the 4 CRS ports case in LTE RBs.

This is only an example of the possible configuration of the DMRS use of the CRS ports. Depending on the scenario, there may be more or less REs required for a reduced DMRS pattern in a cell therefore the total number of REs saved from the CRS ports 1–3 will be able to host the orthogonal new DMRS pattern for a different number of cells, depending on configuration. In any of the configurations, to ensure a good spread of time and frequency, the DMRS REs for the same cell is likely to be located on different frequency and/or different time, but they do not have to be exactly as in Figure 18.

As in the case where 2 CRS ports are required to be configured, assuming those are ports 0 and 1 as indicated by areas labelled " $R_0$ " and " $R_1$ ", CRS port 2 and 3 may be reconfigured as DMRS. Figure 18illustrates an example. In this example, both CRS port 2 and port 3 are configured for the DMRS for one spatial layer in the same cell. This configuration will boost the total DMRS energy for that cell. The shaded areas indicated by " $D_0$ " represent these DMRS symbols.



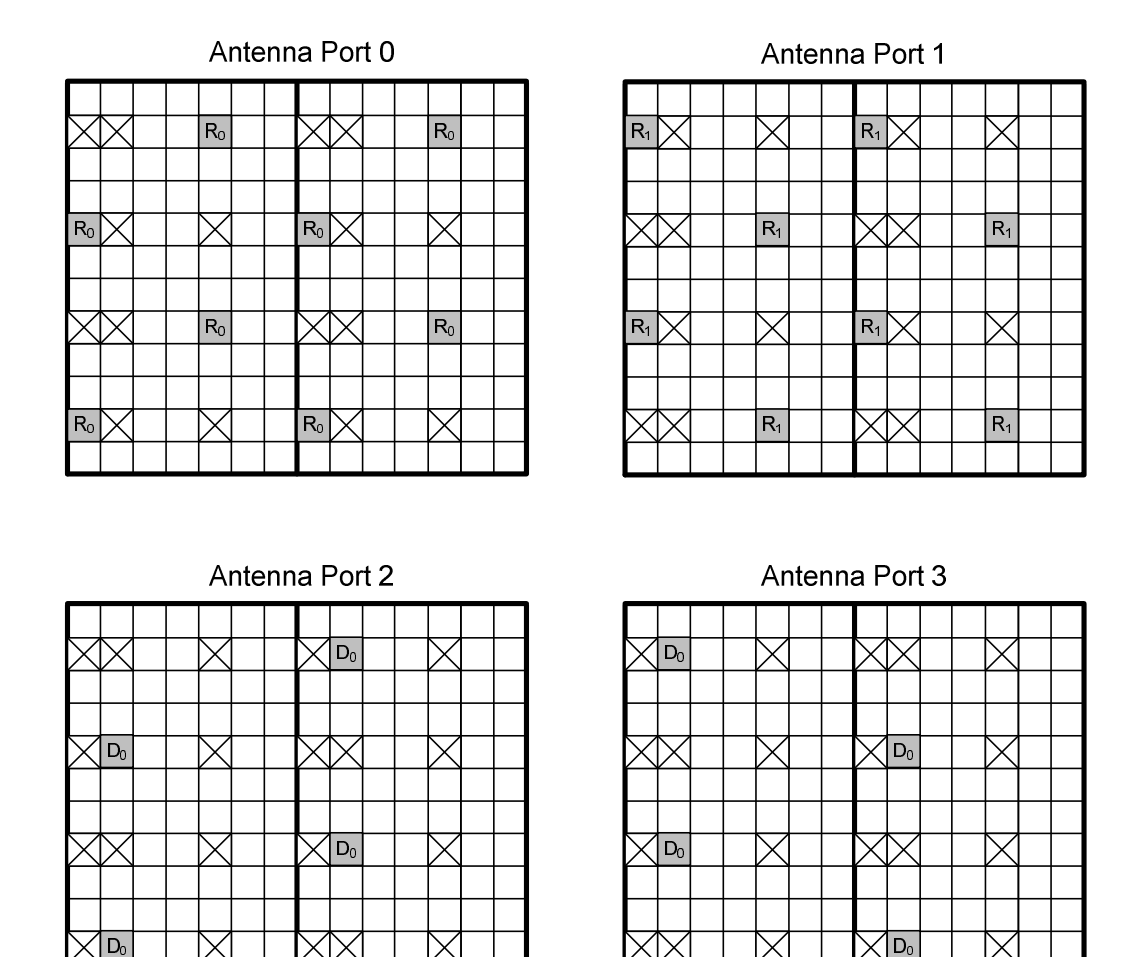


Figure 18. A new DMRS pattern configured on 2 CRS antenna ports in the 4 CRS ports case

The following is the numerical analysis on the performance improvement. Table 16introduces the comparison between 2 cases. The 1<sup>st</sup> is the baseline case where 2 CRS ports and 1 DMRS ports are configured. The 2<sup>nd</sup> case is when 2 CRS ports are configured and a third CRS port is being used a DMRS port. The results show when comparing the peak rate, the number of REs may be available for PDSCH transmission will be increased from 128 to 136 for a pair of LTE RBs, which is a 6% increase in available resources. This translates into a 5.7% reduction in number of sub-frames required for the same amount of OFDM symbols.

Table 16. Number of REs Analysis on Proposed Schemes on 2 CRS ports configuration

Comparison items	Total number of REs in a pair of LTE RB (normal CP)	Taken by CRs	Taken by Rel.9 DMRS	Taken by control channel (PDCCH)	Taken by CRS used for new DMRS	Remaining Res possible for PDSCH transmission
2 CRS ports + 1 DMRS port	168	16	12	12	0	128
2 CRS ports + 1 CRS port used for new DMRS	168	16	0	12	4	136

Version: V1.1



Table 17 provides comparison between the two configurations. The first is the baseline case where all 4 CRS ports plus 1 DMRS ports are configured. The second case is when a reduced DMRS pattern is applied and thus result in 3 CRS ports configured and the 4<sup>th</sup> CRS port is used by the new DMRS pattern. When comparing the peak average data rate, the number of REs may be available for PDSCH transmission will be increased from 120 to 132 for a pair of LTE RBs, which is a 10% increase in available resources. This translates into a 9.1% reduction in number of sub-frames required for the same amount of data symbols.

Table 17. Number of REs Analysis on Proposed Schemes on 2 CRS ports configuration

Comparison items	Total number of REs in a pair of LTE RB (normal CP)	Taken by CRs	Taken by Rel.9 DMRS	Taken by control channel (PDCCH)	Taken by CRS used for new DMRS	Remaining Res possible for PDSCH transmission
4CRS ports + 1 DMRS port	168	24	12	12	0	120
3 CRS ports + 1 CRS port used for new DMRS	168	20	0	12	4	132

The two cases above explains for a fixed amount of data can be achieved by using a more efficient RS design, under radio conditions which allow the new pattern to be deployed.

El reduction on different RS settings Table 18.

	Refer-	Proposed Reduced Reference Symbol Usage Reduction					
	ence	2 Port 50%	2 Port 75%	2 Port 100%	4 Port 50%	4 Port 75%	4 Port 100%
Absolute El [W/Kg]	2.02 e-7	1.96 e-7	1.93 e-7	1.90 e-7	1.93 e-7	1.88 e-7	1.83 e-7
El reduction (%)	N/A	2.9%	4.3%	5.7%	4.6%	6.8%	9.1%

# 3.2.5.4 Conclusions, analysis

The result shows depending on the configuration, a maximum of 9.1% of EI reduction can be achieved. This maximum radio is achieved when 4 CRS Port is configured and when for 100% of time, the reduced CRS port configuration is applicable. In practice, the change in percentage where the proposed reference symbol pattern is applicable is to be further examined, as this depends on the future 3GPP specification as well as the specific wireless network deployment.



# 3.3 Wi-Fi and WSN scenario

# 3.3.1 Wi-Fi Scenario Inputs

Wi-Fi operates mainly in the 2.4 GHz and 5 GHz unlicensed bands. These bands are subject to regulation which are given in Europe by the ETSI EN 300 328 and the ETSI EN 301 893 standards for the 2.4GHz and 5GHz, respectively. In particular, the equivalent isotropically radiated power (a.k.a the transmit power including the antenna gain) is limited to:

- 20 dBm from 2 400 to 2 500 MHz;
- 23 dBm from 5 150 to 5 350 MHz:
- 30 dBm from 5 470 to 5 725MHz.

With the latest IEEE 802.11 amendments, the channels to be used for transmission are defined on a 20MHz granularity.

The EI per population category can be computed as follows for the Wi-Fi scenario [3].

EI\_{category} = k5 x PTX\_indoor\_day\_data / Th\_indoor\_day\_data + k7 x PTX\_indoor\_night\_data / Th\_indoor\_night\_data + k9 x PTXWLAN\_indoor\_day + k10 x SRX\_outdoor\_day + k11 x PTXWLAN\_indoor\_night + k12 x SRX\_outdoor\_night;

(transmit power values in W, received power density values in W/m2and throughputs in kB/s).

The coefficients of interest in Wi-Fi scenario are in Appendix 2.

# 3.3.2 WSN Scenario Inputs

The WSNs we consider operate mainly in the same 2.4GHz ISM band as Wi-Fi and other unlicensed communication technologies. The IEEE 802.15.4 standard which governs most WSN installations imposes a channel bandwidth of 2MHz and typical maximum transmit powers for WSN hardware are around 3.5dBm.

The WSN scenario is based on the urban scenario defined in [3] with some additions necessary for deriving an EI for WSN solutions. The scenario inputs specific to WSN are defined in Table 19. The time period, population categories and environment are kept the same as in the urban scenario. Cell types are not applicable to WSN, same as usage and user profiles, the latter being because users do not directly interact with WSNs. The WSNs are monitoring indoor environments and periodically send data, irrespective of user behaviour. Lastly, only the standing posture is considered as there is insufficient user data for computing multiple postures and the respective SAR values are also very similar between different postures.

Table 19. WSN scenario inputs

Time	Population	Environment	RAT	Cell type	User profile	Posture	Usage
Day	Children	Indoor	WSN	N/A	N/A	Standing	N/A

Version: V1.1 51

Document ID: D4.3: Final validation and recommendations for smart low exposure index FP7 Contract n°318273



Night	Young	Outdoor			
	Adults				
	Seniors				

### 3.3.3 Solution F - Antenna on terminal for low exposure index

# 3.3.3.1 Remind on solution concept

Some studies based on the Specific Absorption Rate (SAR) analysis show that exposure can be reduced by applying some techniques to the antenna design. Main techniques are focused on increasing the distance or using an electromagnetic shield between the antenna and the user[21]-[23]. Despite the good performance of these techniques, these can be expensive and require complex manufacturing. Recent research, focused on alternative solutions, proposes the use of metamaterials[24]-[25] to reduce the exposure. Using metamaterials can be a low cost and easy implementation solution.

Our challenge is to prove the benefits to use a metamaterial structure to reduce the exposure without modifying the antenna performances. Metamaterials are usually composed of tailored and tiny (size about 0.1 wavelength) structures in metallic/dielectric materials. They have interesting properties when a sufficient number of metamaterials cells are used. So the objective is to prove that it is possible to reach an improvement even if the PCB and the number of metamaterial cells is small. Dimensions of the PCB are 12.5 cm x 6 cm (classical smartphone dimensions).

Three different structures of metamaterials have been studied: the AMC (Artificial Magnetic Conductor), the EBG (Electromagnetic Band Gap) and the RHIS (Resistive High Impedance Surface). These artificial materials have the capability to act as a magnetic conductor to reduce surface currents (AMC), to reduce surface waves (EBG) and to absorb currents (RHIS) [26]-[29].

The process is the following: first of all, the metamaterial structures are simulated and optimized. Second, the phone models with and without metamaterials are simulated. Then, the best metamaterial solution is selected: this solution is defined as the one where impedance matching and omnidirectional radiation are preserved.

In a previous document [1], two cases (antenna choice) have been proposed (Figure 19). The first case has been defined as a reference case, where a monopole antenna is associated with AMC, EBG and RHIS structures. The monopole is used because it has the radiation behaviour of a mobile phone antenna, and presents an omnidirectional radiation pattern. The antenna is located at the centre of the PCB. The second case represents a more realistic case where an IFA (Inverted F Antenna), located at the middle of the edge, is associated with AMC, EBG and RHIS structures. The IFA antenna was selected because this antenna is representative of the current mobile phone antennas.



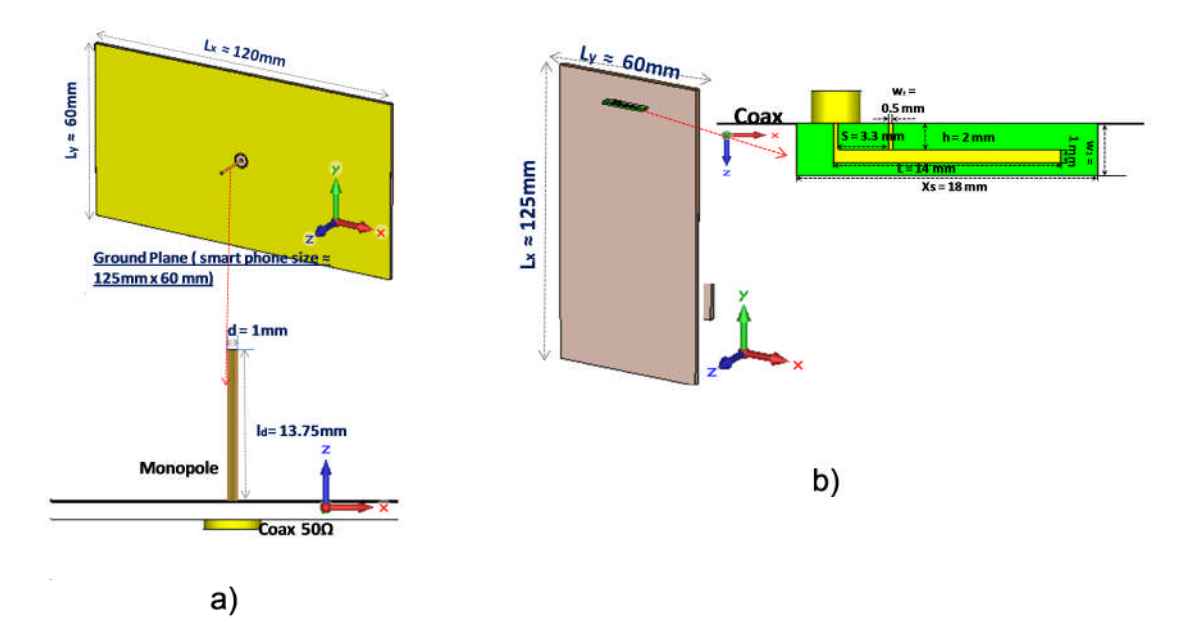


Figure 19. Studying cases: a) Reference case, monopole antenna at the center. b) Realistic case, IFA antenna at the middle of the edge.

Simulation and experimental results of the reference case were presented in [1] and [30]. For the realistic case, first simulation results have been also presented in previous document [1]. These results have been corrected to agree with the dimensions of the fabricated prototypes, in fact antenna dimensions was changed in order to take into account the realization limitations (e.g. the connector size). The corrected results are presented in[31].

#### 3.3.3.2 Specific scenario inputs

The scenario for the evaluation of the global EI for the metamaterial antenna solution is the Wi-Fi at 5 GHz. The hypotheses of the scenario have the same characteristics than those presented in the EI user manual document in [3].

We consider that population uses mobile phone or tablet for Wi-Fi connection, 100% of user are indoor (office, home) and their posture is sitting.

#### 3.3.3.3 Evaluation on exposure reduction

The exposure has been evaluated using a simplified phantom model. The flat phantom is illuminated by the mobile terminal antenna. The distance between the phantom and the phone model is 5 mm. The terminal is located at the centre and in front of the phantom. The model of the phantom consists on a homogeneous equivalent liquid with electrical properties:  $\varepsilon_r = 39.29$ ,  $\sigma = 3.48$  S/m and  $\rho = 1030$ Kg/m<sup>3</sup> at 5 GHz.

The exposure is evaluated for both solutions, with and without metamaterials. The SAR is calculated only for the best solutions: the RHIS optimized for oblique incidence (85°) in the case of the monopole antenna, and the RHIS optimized for normal incidence in the case of the IFA antenna. The exposure reduction is evaluated through the calculation of an EI ratio by a comparison of the SAR calculated with the antenna with best metamaterial solution versus the antenna without metamaterial.



In this document the results of two different configurations that are representatives of the phone uses are presented. In the first configuration, the antenna is located in front of the phantom, and in the second configuration the antenna is on the other side of the PCB. Figure 20 and Figure 21 show the spatial distribution of SAR 10g for both configurations of reference case. Figure 22 and Figure 23 show the case of the realistic antenna. The SAR 10g is plotted at 5mm from the model phone; it is calculated taking into account an accepted power of 1W. All the simulations have been done at 5 GHz.

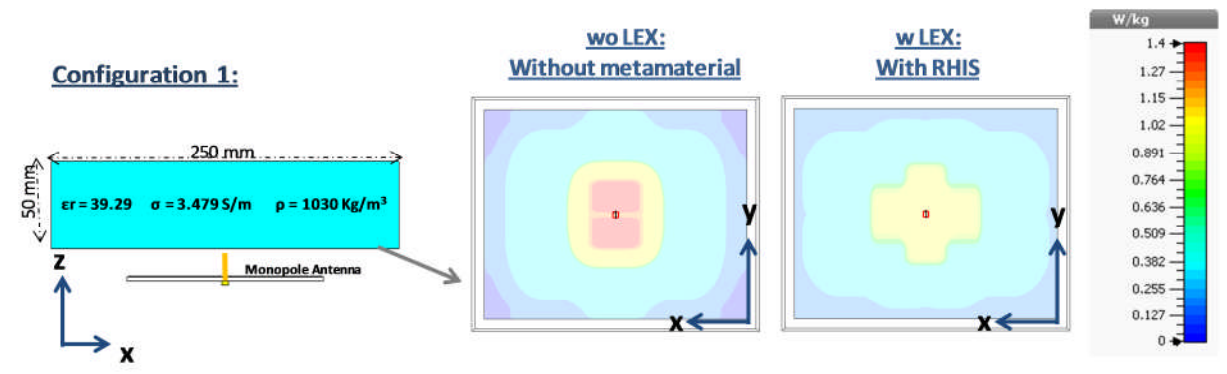


Figure 20. Spatial distribution of SAR 10g for the case with monopole antenna in front of the flat phantom

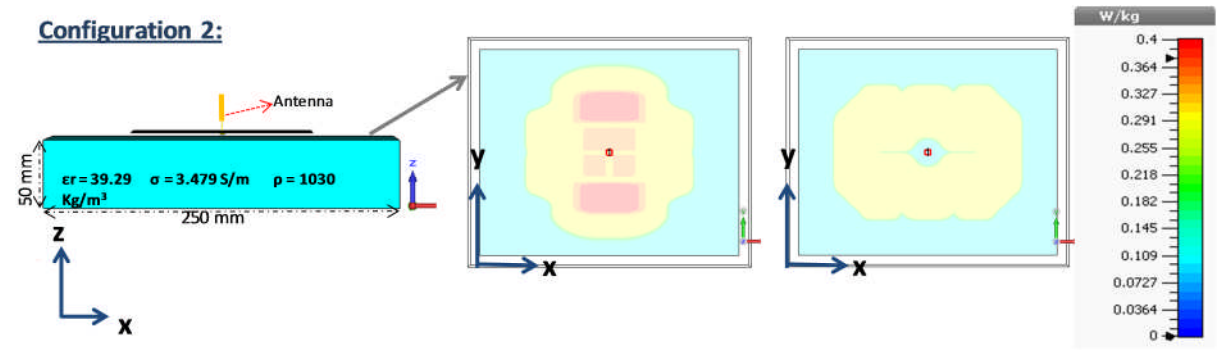


Figure 21. Spatial distribution of SAR 10g for the case with monopole antenna on the other side of the PCB

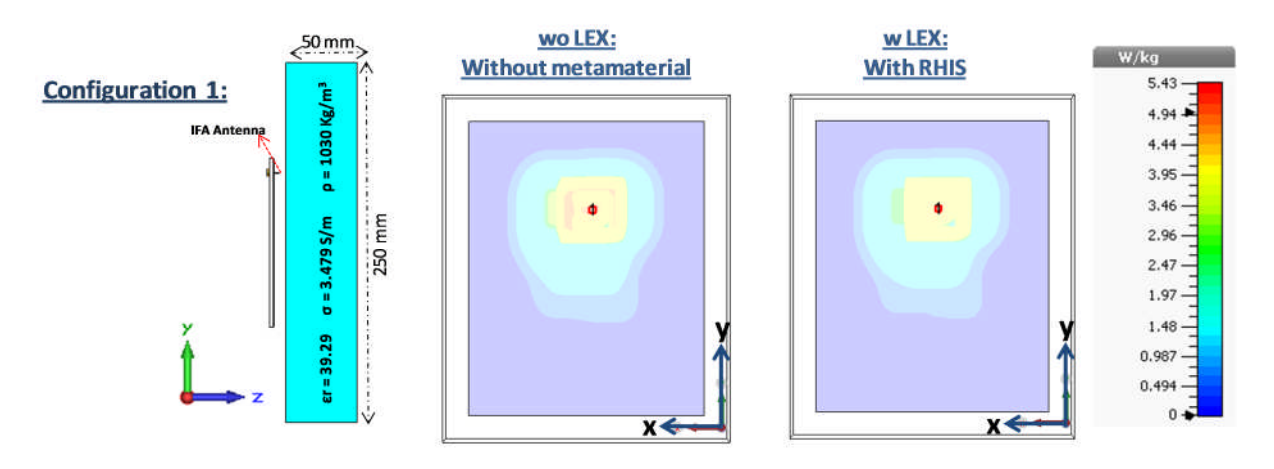


Figure 22. Spatial distribution of SAR 10g for the case with IFA antenna in front of the flat phantom



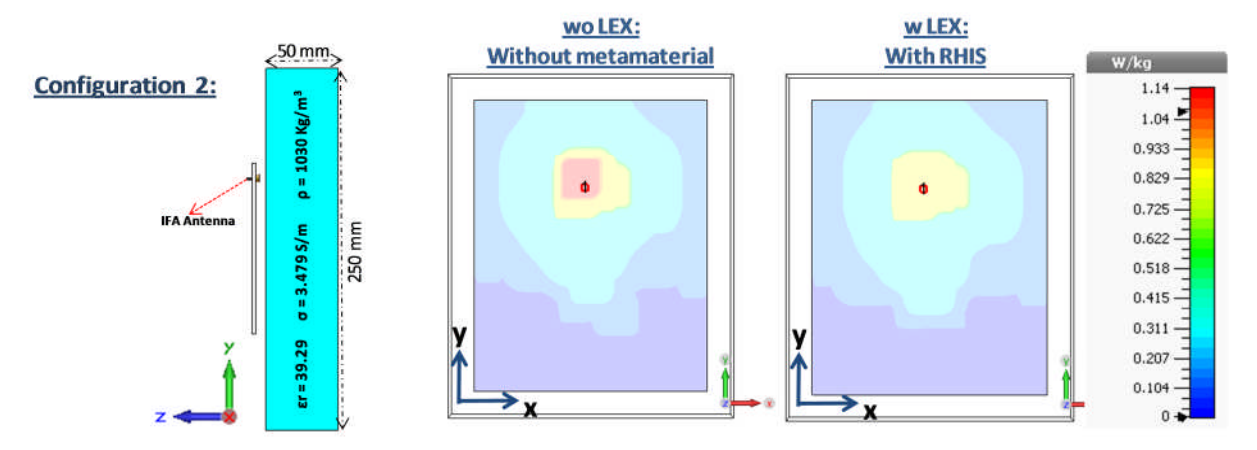


Figure 23. Spatial distribution of SAR 10g for the case with IFA antenna on the other side of the PCB

The Specific Absorption Rate (SAR) is the considered variable to be decreased in order to evaluate the EI in the case of the terminal mobile antennas. Table 20 presents the Maximum SAR 10g and the EI for the two cases (reference and realistic) in both configurations (front of the phantom and on the other side of the PCB).

**Table 20.** Relative Exposure Index Calculation

			Total SAR [W/kg]:	Maximum SAR (rms,10g) [W/kg]:
	Configuration	Without metamaterials	0.106	1.4
Reference case:	1	With metamaterials	0.094	1.07
Monopole antenna at the centre		Ratio El (%)	-11.3	-23.6
	Configuration 2	Without metamaterials	0.07	0.41
		With metamaterials	0.05	0.37
		Ratio El (%)	-28.7	-9.7
	Configuration	Without metamaterials	0.105	5.43
Realistic case: IFA	1	With metamaterials	0.100	5
		Ratio El (%)	-4.7	-7.9
antenna at the middle of edge	Configuration	Without metamaterials	0.39	1.13
	2	With metamaterials	0.38	1.06
		Ratio El (%)	-2.6	-6.2



Results show that using the RHIS, the exposure can be reduced preserving the antenna performances. In fact, the total efficiency of antennas with and without metamaterials is preserved.

#### 3.3.3.3.1 Global EI Evaluation

In this Wi-Fi scenario, only the UL inputs are considered and the EI for each population category is calculated as:

El\_population\_category = k5 x PTX\_indoor\_day\_data / Th\_indoor\_day\_data + k7 x PTX\_indoor\_night\_data / Th\_indoor\_night\_data

#### Where:

<u>k5</u> is related to the EI in UL during the day and <u>k7</u> is related to the EI in UL during the night. They are calculated as:

k5=0.25\*[(percentage\_user\_3Gtablet\*vol\_tablet\_day)\*WBSAR\_uplink\_data\_in]; k7=0.25\*[(percentage\_user\_3Gtablet\*vol\_tablet\_night)\*WBSAR\_uplink\_data\_in];

#### Where:

- 0.25 value is because only the 25% of the population is considering
- Only the user\_3Gtablet (We suppose that the 3Gtablet users are the same that use data applications via Wi-Fi, for example to call via skype):
  - For children → percentage\_user\_3Gtablet = 0.05
  - For young people → percentage user 3Gtablet = 0.08
  - For adults→percentage\_user\_3Gtablet = 0.07
  - For seniors -> percentage\_user\_3Gtablet = 0.02
- vol tablet day is: 1365kB
- vol\_tablet\_night is : 5490kB
- WBSAR\_uplink\_data\_in corresponds to values of Total SAR presented in Table 20.

<u>PTX indoor day data</u> is the transmitted power value in W during the day and <u>PTX\_indoor\_night\_data</u> is the transmitted power value in W during the night. The PTX\_indoor\_day\_data and PTX\_indoor\_night\_data are considered as 200 mW.

<u>Th indoor day data</u> and <u>Th indoor night data</u> are the throughputs in kB/s during the day and the night. We consider the throughputs max value of the 802.11a standard that is 54Mbits/s or 6912kB/s.

The results of the EI global for the antenna metamaterial solution are presented in Table 21, Table 22, Table 23 and Table 24.

Version: V1.1



Table 21. El global for Monopole Antenna with RHIS in front to the phantom

	k5		k7		El	
	Without	With	Without	With	Without	With
	metamaterials	metamaterials	metamaterials	metamaterials	metamaterials	metamaterials
Children	1.80	1.6	7.27	6.4	2.6 x 10E-4	2.3 x 10E-4
Young People	2.89	2.56	11.63	10.3	4.2 x 10E-4	3.7 x 10E-4
Adults	2.53	2.24	10.18	9.03	3.6 x 10E-4	3.2 x 10E-4
Senior	0.72	0.64	2.90	2.58	1.0 x 10E-4	9.3 x 10E-5
		3.83 x 10E- 9W/Kg	3.39 x 10E- 9W/Kg			
Ratio EI (%)					-13	1.3

Table 22. El global for Monopole Antenna with RHIS back to the PCB

	k5		k7		El	
	Without	With	Without	With	Without	With
	metamaterials	metamaterials	metamaterials	metamaterials	metamaterials	metamaterials
Children	1.19	0.85	4.8	3.43	1.7 x 10E-4	1.2 x 10E-4
Young People	1.91	1.36	7.68	5.49	2.7 x 10E-4	1.9 x 10E-4
Adults	1.67	1.19	6.72	4.8	2.4 x 10E-4	1.7 x 10E-4
Senior	0.47	0.34	1.92	1.37	6.9 x 10E-5	4.9 x 10E-5
El global					2.5 x 10E-9 W/Kg	1.8 x 10E-9 W/Kg
	Ratio EI (%)				-28	3.7

Table 23. El global for IFA Antenna with RHIS in front to the phantom

	k5		k7		El	
	Without	With	Without	With	Without	With
	metamaterials	metamaterials	metamaterials	metamaterials	metamaterials	metamaterials
Children	1.79	1.70	7.2	6.86	2.6 x 10E-4	2.4 x 10E-4
Young People	2.86	2.73	11.53	10.98	4.1 x 10E-4	3.9 x 10E-4
Adults	2.5	2.38	10.08	9.6	3.6 x 10E-4	3.4 x 10E-4
Senior	0.71	0.68	2.88	2.74	1 x 10E-4	9.9 x 10E-5
	El global					3.61 x 10E-9 W/Kg
	Ratio EI (%)					.7

Table 24. El global for IFA Antenna with RHIS back to the PCB

	k5		k7		El	
	Without	With	Without	With	Without	With
	metamaterials	metamaterials	metamaterials	metamaterials	metamaterials	metamaterials
Children	6.65	6.48	26.76	26.07	9.6 x 10E-4	9.4 x 10E-4
Young People	10.64	10.37	42.82	41.72	1.54 x 10E-3	1.5 x 10E-3
Adults	9.31	9.07	37.46	36.5	1.3 x 10E-3	1.3 x 10E-3
Senior	2.66	2.59	10.70	10.43	3.8 x 10E-4	3.7 x 10E-4
	El global					1.37 x 10E-8 W/Kg
	Ratio EI (%)					.6

Version: V1.1

Document ID: D4.3: Final validation and recommendations for smart low exposure index FP7 Contract n°318273



# 3.3.3.4 Conclusions, analysis

Studying the SAR reduction by using metamaterials is a challenge. On one side, metamaterial structures presents different topologies, and on the other side, SAR evaluation depends on different parameters as antenna type, antenna position, user position, morphology, etc. For that, this work has been concentrated in evaluating the effect of the metamaterials to reduce exposure in simplified cases, using basic metamaterials structures, with a simplified antenna and with a very simplified phantom model. In all cases, it has been demonstrated that the exposure can be reduced preserving the antenna performances by using an optimized structure of metamaterials. The El global is reduced by29 % when a RHIS optimized solution is associated with a monopole. A future study will be to study more realistic cases, by using a human phantom to be more compliant with realistic model.

# 3.3.4 Solution G – Beamforming techniques

This work presents null steering from an experimental point of view for the purpose of exposure reduction for a person using a Wi-Fi enabled laptop. The goal is to use experimental data to find a phase offset angle between a pair of transmit antennas that can allow for the implementation of null steering. While many works on the various types of null steering system models exist [32]-[35], these use geometrical analyses to derive equations that provide phase weights to steer the null. The focus of the null steering here is on low complexity form that need not be adaptive nor posses multiple nulls and requires merely an appropriate phase angle. This type of null steering has been explored in relation to exposure reduction in [36]-[39], where simulation software (electromagnetic solvers) has been used to derive the appropriate phase weight. In contrast to these simulation-based methods and also the above mentioned geometrical analyses to steer the null, a key strength of this work is its use of experimental data for the purpose of null steering.

Further to this, the work seeks to demonstrate that unlike many conventional null steering approaches, it is possible to transmit a second data stream from the second transmit antenna in the pair thus gaining some data throughput while also providing reduced EM exposure to the user.

#### 3.3.4.1 Remind on solution concept

In this work, a MIMO LTE system, i.e. MIMO-OFDM, is considered from the point-ofview of operating in channels based on channelmeasurementsat2.4 GHz. The scenario is a laptop making an UL connection wirelessly to a Wi-Fi access point. In brief, for the case of null steering, two identical signals are launched from two transmit RF chains but where, in the baseband digital domain, one of the transmit streams is rotated by an angle,  $\theta_{Null}$ , with respect to the other. At a certain,  $\theta_{Null}$ ,there will be a reduction in exposure as a null is steered to the user. A shortfall of this approach is the fact that the transmit sample streams are identical except for this rotation and thus only one information stream can be obtained at the receiver. In the case of the specific absorption rate (SAR) code technique, this concerns the engineering of modulation symbols coming from either RF chain also to form a null at the user. This is done such that, although there is an angle of rotation between them, in this case:  $\theta_{SAR}$ , the stream of samples from either Tx RF chain is not identical. This isbecause the second stream facilitates the demodulation of a pair modulation symbols:  $\exp\{j\theta_{SAR}\}$  and  $\exp\{j-\theta_{SAR}\}$ , that are defined relative to every modulated symbol that was transmitted on the first stream. As a result, this technique can exploit



a second transmit RF chain to enhance the throughput as well as reduce exposure. In the testing and implementing of SAR codes during this work, it was discovered that this technique has some issues.

- If  $\theta_{SAR}$  on the second stream must benear to  $0^{\circ}$  or  $180^{\circ}$  to steer the null to the user, then the quality of transmission on the second stream would be highly degraded due to the fact that the modulation alphabet used on the second stream is derived from symbols that arise from two rotations from a common point:  $\exp\{j\theta_{SAR}\}\$  and  $\exp\{j-\theta_{SAR}\}\$ . As a result, these symbols would be too close together for meaningful reception.
- The angular range over which a null can be steered using SAR codes is restricted due to the fact that SAR codes do not work satisfactorily in conjunction with the IFFT stage of an OFDM transmitter.

In order to address these issues, a third novel, 'Hybrid', technique is proposed where both null steering and the SAR code techniques are employed together. In order to explain this technique, the output of the Tx RF chains after the IFFT stage but before the channel is examined. The phase angle of each sample at the first transmit RF chain, i.e.  $\angle \theta_{Tx1}$ , and similarly for the second RF chain,  $\angle \theta_{Tx2}$ , is calculated. The difference between these phase angles,  $\Delta\theta_{Tx}$ , is then considered, i.e.  $\Delta\theta_{Tx}$  =  $\angle \theta_{Tx2} - \angle \theta_{Tx1}$ . Histograms of  $\Delta \theta_{Tx}$  for the case of null steering and SAR codes for various values of  $\theta_{Null}$  and  $\theta_{SAR}$  are given in Figure 24.

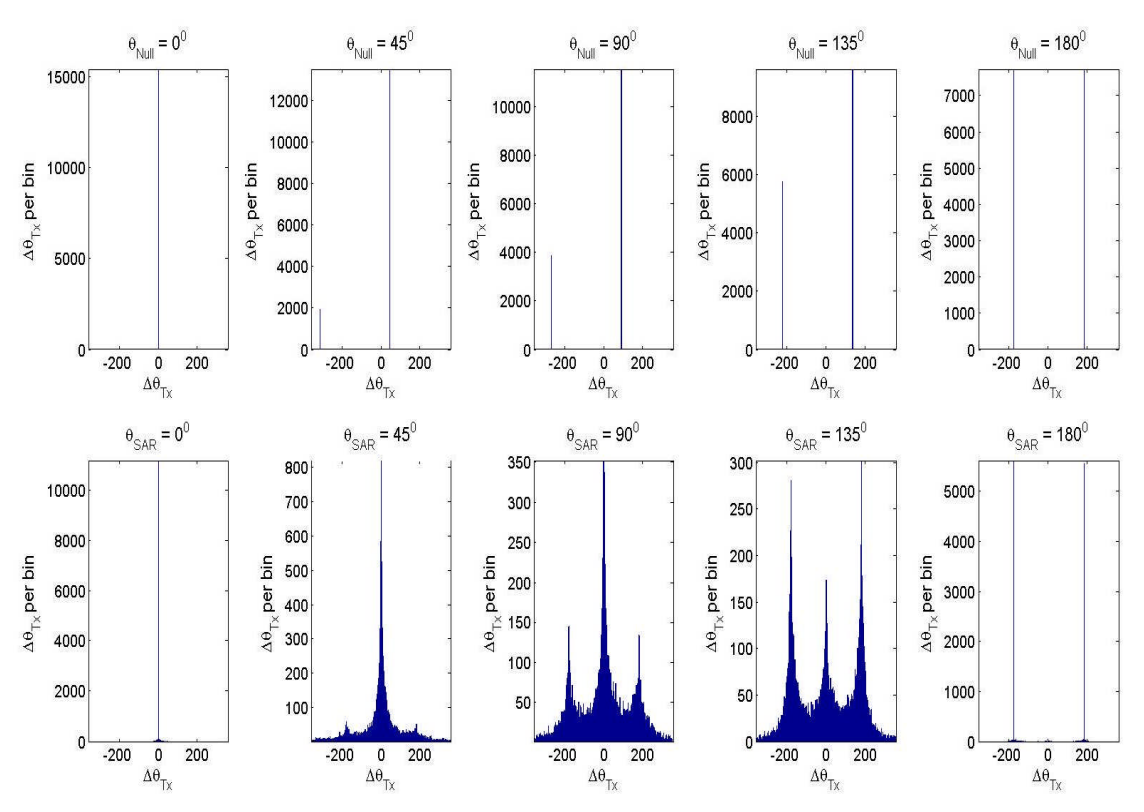


Figure 24. Top-row: Histograms of the phase offset between Tx samples,  $\Delta\theta_{Tx}$ , for various angles,  $heta_{\mathit{Null}}$ , for the case of null steering. Bottom-row: Histograms of the phase offset between Tx samples,  $\Delta\theta_{Tx}$ , for various angles,  $\theta_{SAR}$  , for the case of SAR Codes.



It is clear from this analysis that null steering presents a histogram of  $\Delta\theta_{Tx}$  that is appropriate to the angle,  $\theta_{Null}$  that has been applied. It should be noted that along with the appropriate bar in the histogram (positive value), there is a gradually increasing negative valued bar, which is merely the  $2\pi$  complement value, and is equally valid. However the same observation cannot be made regarding SAR Codes. In the case of SAR codes, the histogram of  $\Delta\theta_{Tx}$  does not represent the applied angle,  $\theta_{SAR}$ , as faithfully as is the case in null steering. This is particularly apparent when  $\theta_{SAR} = \{45^{\circ}, 90^{\circ}, 135^{\circ}\}$  and thus it can be concluded that trying to steer a null using these phase offsets will not be particularly effective since only a few of the angles in the histogram fulfil the necessary condition. This highlights a second issue with SAR codes when they are used with OFDM, which is that the SAR code system model is not viable with the IFFT stage of OFDM. However, what is of interest to note, is the fact that when  $\theta_{SAR} = \{45^0\}$ , many of the values of  $\Delta\theta_{Tx}$  are zero. Furthermore, it is on this basis that a hybrid system is proposed where essentially the SAR code angle is set:  $\theta_{SAR} = 45^{\circ}$  before applying null steering to the SAR code system model at various angles of  $\theta_{Null}$ . In order to verify the effectiveness of this approach, appropriate histograms of  $\Delta\theta_{Tx}$  are given in Figure 25based on this, 'hybrid', idea.

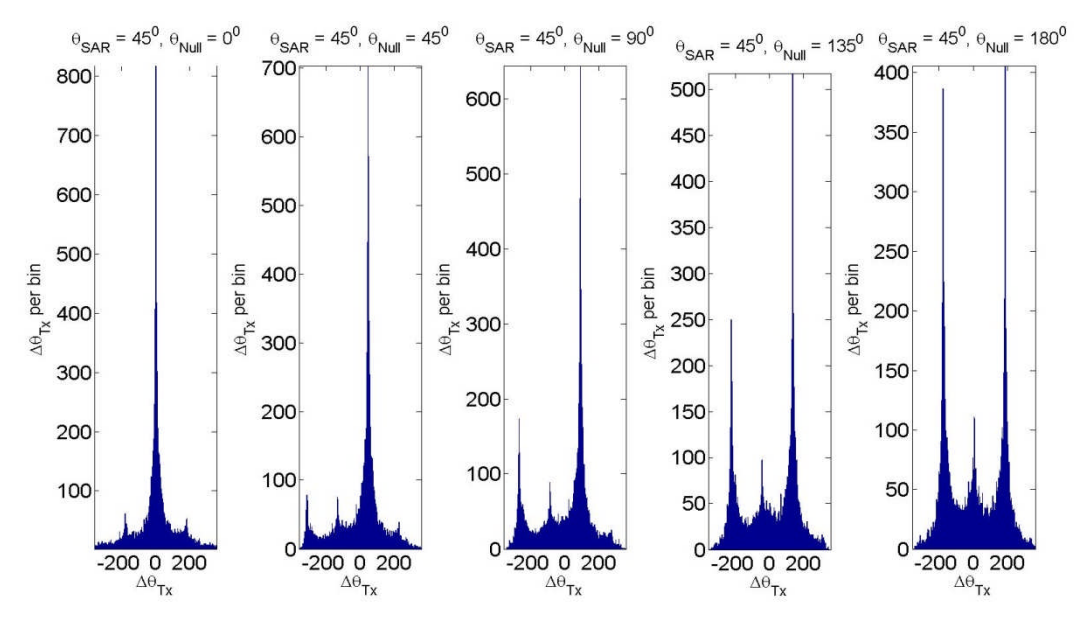


Figure 25. Histograms of the phase offset between Tx samples,  $\Delta \theta_{Tx}$ , for the hybrid technique where  $\theta_{SAR}$  is set  $\theta_{SAR} = \{45^0\}$  and various angles,  $\theta_{Null}$ , are applied.

Figure 25shows that the technique is effective. The main peak is shifting in a manner that would be expected with the increasing value of  $\theta_{Null}$ . There is also a negative valued peak that is mimicking the behaviour of that seen in on the top row of Figure 24and again, this angle should be equally valid for exposure reduction.

In order to assess the novel hybrid technique in terms of exposure reduction and compare with the simple null steering approach, simultaneous channel measurements of a transmitting laptop enabled with 2 pairs of 2 transmit antennas to receivers acting as human mounted chest probes as well as receivers acting as an access point were made. 2 pairs of these transmit antennas were used to evaluate repeatability over a relevant region of space, i.e. from two slightly different points of



transmission from the laptop screen. Furthermore, repeatability of the technique was also performed where the transmitting laptop was placed at 3 positions in a furnished laboratory. These three different positions are referred to as 'Desk', 'Bench' and 'Far Bench'. In each position, measurements were made with ('dynamic') and without ('static') a person walking in the access point channel, thus a total of 6 scenarios may be inferred. The result of applying these techniques in each of the six scenarios is compared in Figure 26and Figure 27and in either case, the phase offset,  $\theta_{Null}$ , is varied (y-axis) and the received power at the chest mounted probes is calculated. The term, 'Probe pair 1' refers to the average power in the MIMO channel between the first pair of Tx RF chains and the 4 chest mounted probes. Similar results were obtained for the case of 'Probe pair 2', which confirmed repeatability, but have been omitted here for brevity.

The results in Figure 26 and Figure 27 pertain to many channel measurements thus consider now,  $\theta_{min}$ , which is the angle,  $\theta_{Null}$ , that minimises the receive power at the probes and hence user exposure. Anappropriate PDF of  $\theta_{min}$  in respect of this is given in Figure 28. The behaviour of the hybrid technique is clearly similar to null steering but with the added benefits of being able to transmit more than one data stream, being able to function with OFDM and also being able to function when the phase offset to create a null could be near  $0^{\circ}$  or  $180^{\circ}$ .

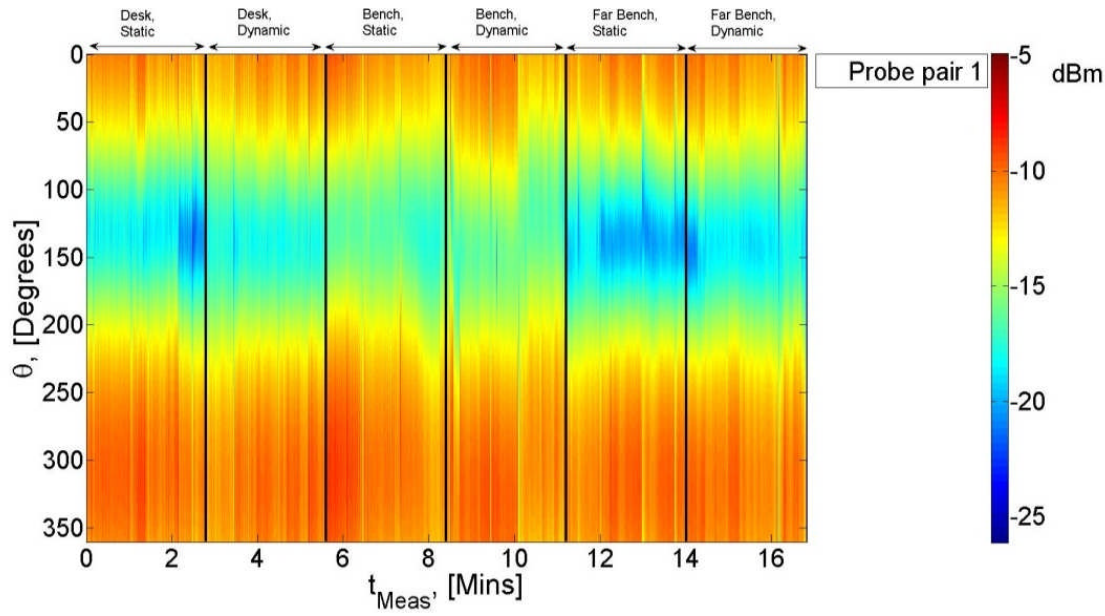


Figure 26. Baseband null steering: Received power at chest from the first pair of MIMO antennas, 'Probe pair 1'.



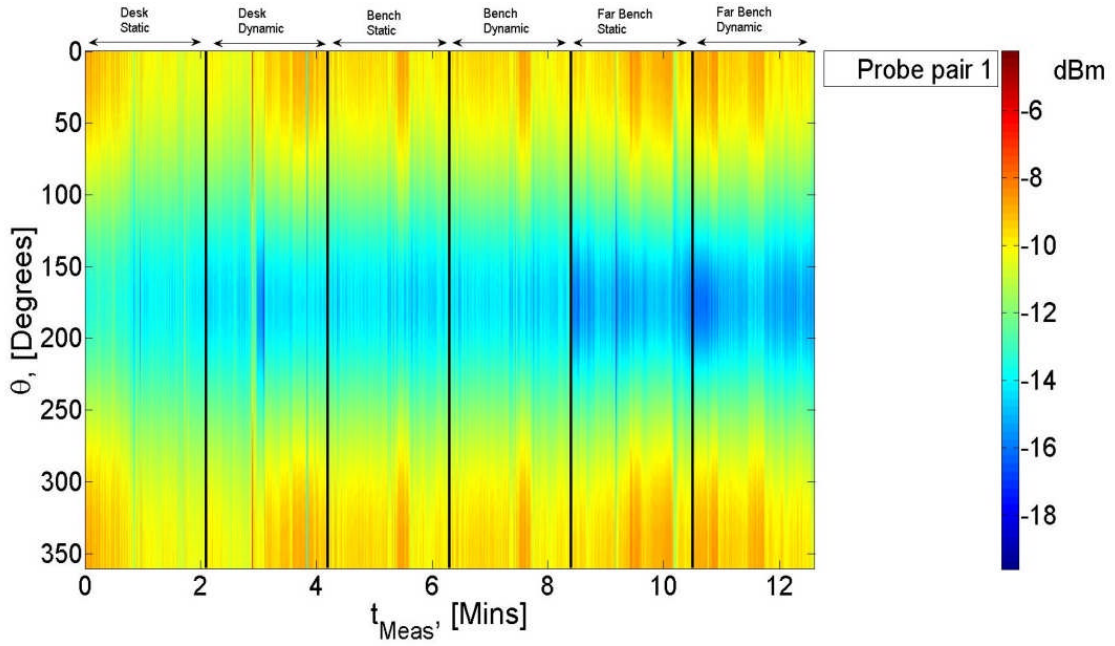


Figure 27. Hybrid technique: Received power at chest from first pair of MIMO antennas, 'Probe pair 1'.

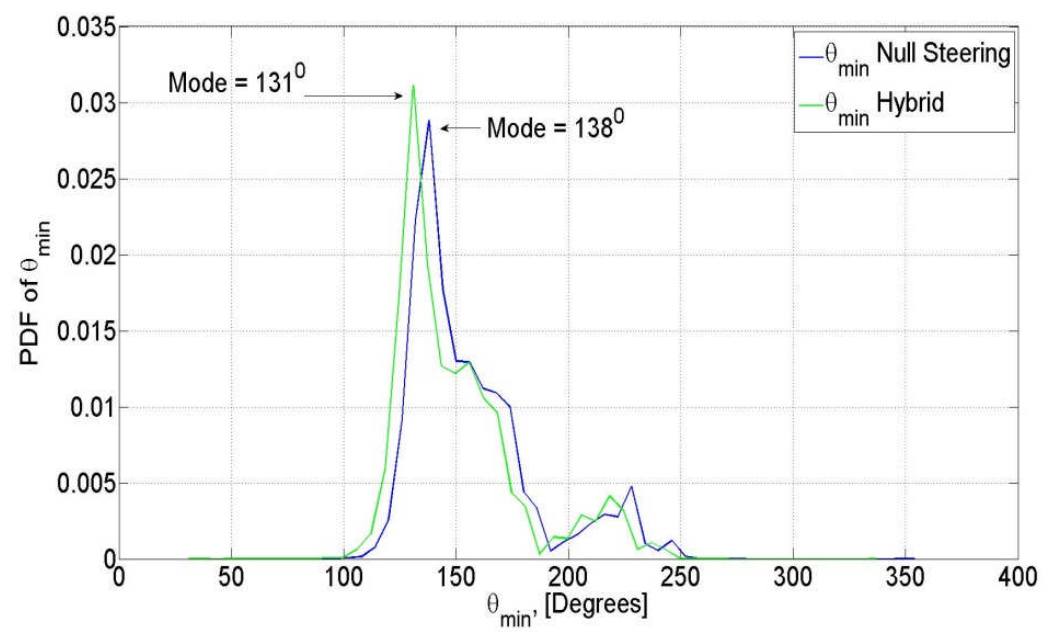


Figure 28. First order statistics of  $\theta_{min}$ , the angle that minimises exposure.

The effect of the hybrid technique on the AP receive power is now considered and compared with null steering in Figure 29. The point 0 dB should be understood to mean no effect while positive values indicate a gain and negative indicate a loss in receive power. In either case, 'AP pair 1', is the channel between the AP and one pair of transmit antennas and similarly, 'AP pair 2', is the channel between the AP and a second pair of transmit antennas. It is clear that there can beat times a small penalty of reduction in power at the AP when the technique is applied, however it is also apparent that there can be a gain and this provides a degree of compensation. When this technique is applied to the scenario, 'Far Bench', the reduction in power to the AP is at its most severe. This is logical since the user, the laptop device and the



AP are all in a line here. This simply highlights the rather simple caveat that users should not operate their devices in this way, i.e. the user should not be in line with the AP when operating their device as the AP itself will be in the null.

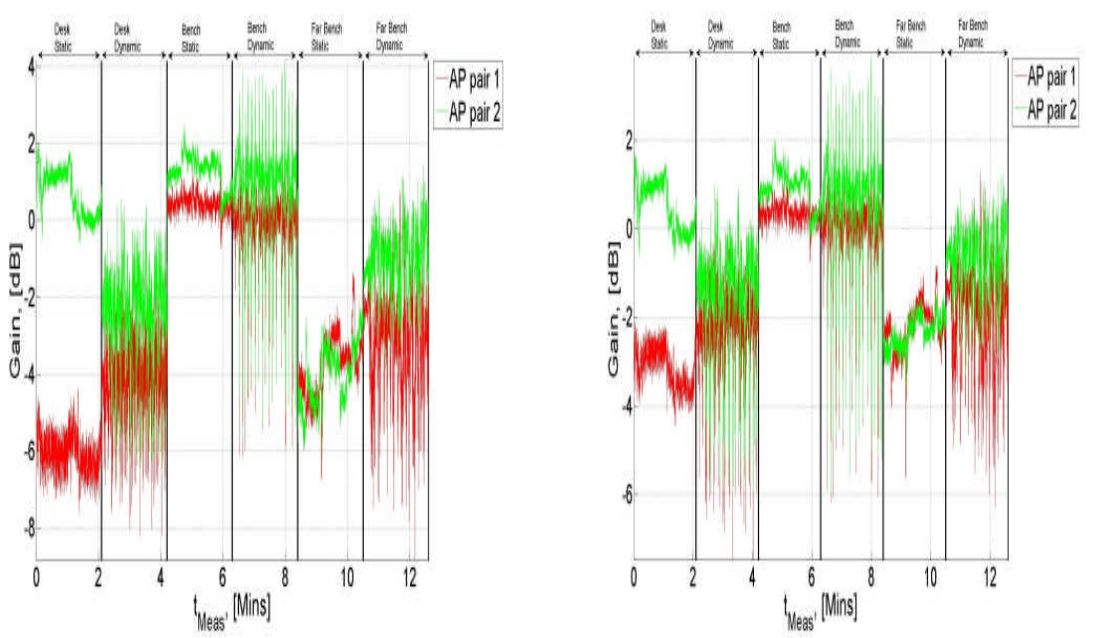


Figure 29. The effect of null steering (left) and the hybrid technique (right) on the AP power gain in the UL based on two channels, 'AP pair 1' and, 'AP pair 2'.

Finally, the impact of the hybrid technique on neighbouring users is considered. To do this, the technique is applied and the receive probe power is measured at 6 positions around the laptop beginning at 1 with the user facing the laptop and rotating anti-clockwise around through 5 more positions. The hybrid technique is compared with null steering in this regard in Figure 30. It is clear that both techniques exhibit a similar behaviour and that neighbouring users, particularly in positions 2-4, would benefit from reduced exposure even though they would not be exactly aligned with the null. Users in positions 1 and 5 would exhibit little or no difference in exposure.

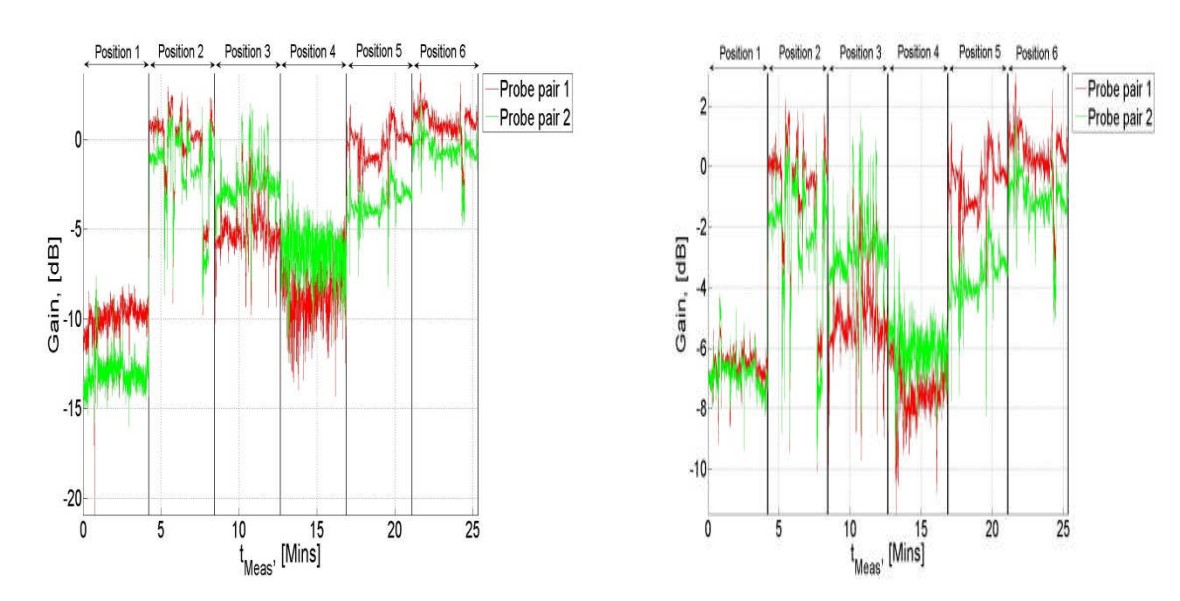




Figure 30. The effect of null steering (left) and the hybrid technique (right) on neighbouring users for 6 positions, 1-6 depicted.

# 3.3.4.2 Specific scenario inputs

The work uses a 5 MHz bandwidth LTE (MIMO-OFDM) signal with the AP router transmitting at 30 dBm (~1 Watt) and the MIMO laptop terminal transmitting 23 dBm across its two Tx antennas. The carrier frequency is 2.4 GHz.

#### 3.3.4.3 Evaluation on exposure reduction

The EI is considered in terms of two constituent components:  $D^{DL}$ , the DL part and,  $D^{UL}$ , the UL part both measured in W/kg.

DL component ( $D^{DL}$ ): Assuming a 30 dBm AP transmit power, an indoor path loss model at 5m is used to calculate the power at the user:  $P_{User}$ . Then, the DL power density at the user,  $P_{D,i}(0)$ , may be calculated from:  $P_{D,i}(0) = 4\pi \frac{P_{User}}{\lambda^2}$ wavelength), and is: 0.0019 V/m. This in turn gives rise to a DL EI component,  $D^{DL}$ of  $D^{DL} = 8.3 \times 10^{-10}$  W/kg based on the k-factor approach of [3] for the Wi-Fi scenario. This remans constant throughout as the work does not address altering of the DL EI component.

<u>UL component</u>  $(D^{UL})$ . This is a three step process that has been defined to suit the experimental nature of this work as follows:

- Compute the Rx power at probes with and without either technique. (i)
- Calibrate these Rx powers to SAR using the approach in [40]. (ii)
- Compute the UL EI,  $D^{UL}$ , with and without either technique according to: (iii)

$$D^{UL} = T \times SAR_{wb} \times P_{Tx(AP-User)}$$
 (3.22)

(i) is achieved by calculating the average of the measured power at each of the four body mounted probe antennas. In relation to (ii), a calculation of the whole body SAR,  $SAR_{wh}$ , is required. To do this, consider the SAR at a point where the EM wave just impinges on the human body, i.e., SAR(0), may be written as:

$$SAR(0) = -\frac{\sigma}{\rho} Z_i |t|^2 P_{U,i}(0), \tag{3.23}$$

Where  $\sigma$  is the conductivity of the medium into which the EM wave is about to impinge and  $\rho$  is its density. In both cases, this medium is the human body with  $\sigma$ being frequency dependent and derivable from scientific tables while  $\rho$  for the human body is generally accepted to be 1000 kg/m<sup>3</sup>.  $Z_i$  is the characteristic impedance of the medium in which the EM wave has propagated, most likely air, and t is the transmission coefficient of the medium into which the EM wave is about to impinge (the body) and is calculated from:

$$t = \frac{2}{1 + \sqrt{\epsilon_r}}, (3.24)$$



Where  $\epsilon_r$  is the complex permittivity of that same medium.  $P_{U,i}(0)$  is the UL power density at the point of EM impingement on the body and is given by:  $P_{U,i}(0) = 4\pi \frac{P_{Probe}}{\lambda^2}$ , ( $\lambda$  is wavelength), where  $P_{Probe}$  is a measurement of the received power made by omnidirectional probes on the user's chest. Using this definition for SAR(0) in conjunction with the statistical approach of [40] allows for the calculation of conservative values of  $SAR_{wb}$ . Finally with regard to (iii), a figure of 34 nW for  $P_{Tx(AP-User)}$  is used based on the 3G indoor femtocell transmitting at 23 dBm at a carrier frequency of 2150 MHz scenario. Computations of EI, i.e. the sum:  $D^{UL} + D^{DL}$ , when the null steering and the novel hybrid technique are applied are tabulated in Table 25. The absolute value of EI is calculated when no technique is applied.

Table 25. Els for null steering and hybrid techniques. The absolute El is when no technique is applied

Technique	EI, [W/Kg]
None (absolute value)	1.6998e-06
Null steering	3.0666e-07
Hybrid	5.8143e-07

Table 26. % El reduction from absolute El for the null steering and hybrid techniques.

Technique	% EI reduction
Null steering	82%
Hybrid	66%

#### 3.3.4.4 Conclusions, analysis

In this work, a novel communication system has been proposed that consists of simple phase weighted null steering in combination with modulation alphabet design that can successfully steer a null to reduce user exposure and transmit two data streams. This provides a significant advantage over conventional exposure reduction techniques that rely on null steering in literature [36]-[39]. A full experimental treatment of the idea has been given that concludes that the system will provide reasonable QoS at the AP and will not induce any significant added exposure to neighbouring users. Future work should consider the possibility of expanding the modulation alphabet at higher SNRs to include symbols in between those at:  $\exp\{j\theta_{SAR}\}$  and  $\exp\{j-\theta_{SAR}\}$ . Furthermore, although the complexity of the proposed system should be very low, the possibility of steering the null in the hybrid system using antenna parasitic rather than baseband signal processing would provide reduced system complexity.

# 3.3.5 Solution H - Sleep/idle mode in a mesh gateway deployment

In this section, we quantify the EI reduction we can achieve through idle mode for Wi-Fi gateways deployed in a hot-spot fashion, to serve a shopping mall area for instance. We model the behaviour and capabilities of the Wi-Fi gateways based on



the ones used in WP6 [41]. The Wi-Fi gateways are Dual-Band Dual-Concurrent (DBDC) devices which simultaneously provide services (e.g. Internet access) to the users on the 2.4GHz ISM band using IEEE 802.11n technology and communicate with each other through a mesh network on the 5GHz ISM band using also IEEE 802.11n technology. The advantage of such network topology is that only one gateway needs to be effectively connected to the Wide Area Network (WAN) Internet, while the others will route their external traffic toward it. Under such deployment, the idle mode will essentially consist in reducing the transmission power of the 2.4GHz radio of the DBDC Wi-Fi gateways based on the load or the traffic conditions.

# 3.3.5.1 Remind on solution concept

Switching-off the transmitting part one radio of a DBDC Wi-Fi Access Point (AP) means that services through this radio cannot be offered anymore. If this mode clearly produces no EMF exposure at all, it is only suitable for (predictable) periods of time when services are not needed.

The idea behind the idle (or sleep) mode is to operate the radio of an AP in a "degraded" mode characterised by a transmit power reduced by a factor  $\Delta_{idle}$ . By being able to broadcast the Wi-Fi beacons, the AP is still able to advertise its presence to the Stations (STAs) which are in the AP's (reduced) range. In case a STA cannot find any AP beacon through passive scan, it usually enters an active search state where it periodically broadcasts frames (Probe Request) waiting for an AP to reply (Probe Response).

In our investigations, we considered two idle mode approaches based on this concept:

- In the first approach, the AP runs by default with its maximum transmit power. The AP activates the idle mode (power reduced by  $\Delta_{\rm idle}$  dB) only when no traffic is monitored during  $T_{\rm exp}$  seconds. When the AP in idle mode receives a Probe Request from a STA, it increases its transmit power to its maximum value to serve the STA. In this approach, the AP reduces its transmit power only when no STAs are connected to it.
- In the second approach, the AP always runs in idle mode (power reduced by Δ<sub>idle</sub> dB). If a STA successfully manages to detect and associate to an AP in dle mode, the AP keeps its transmit power reduced. The AP increases its transmit power only when it receives a Probe Request from a distant STA. The AP will activate the idle mode again when no traffic will be monitored during T<sub>exp</sub>. In this approach, the AP increases its transmit power only when a STA triggers it through a probe request. Note that the STA behaviour is implementation-dependent since it is not standardised. There are cases where after a successful passive scan (beacon found) an STA will still actively trigger an AP response (through Probe Request) before attempting an association request. Such implementation is not considered here, but a selection through the received power level (above a given threshold) and/or the parsing of the probe request (which can contain a Wi-Fi network identifier) may be used to discriminate a probe request coming after a beacon detection or not.

Version: V1.1



In both approaches, the idle mode is resumed after no traffic is observed during  $T_{\rm exp}$  seconds. We suspect the second approach to be more efficient in terms of EI, but the QoS may suffer more.

### 3.3.5.2 Specific scenario inputs

In order to assess the EI reduction achievable by our approaches in such hot-spot deployment, we rely on a system-level evaluation. In system-level simulations, a Monte-Carlo procedure is used to drop (randomly or not) APs/STAs within a layout capturing a standard environment. Compared to D4.2 [1], we refined our simulation assumptions and used a dynamic drop of the STA and their traffic per run.

In terms of layout, we use a modified version of the ITU-R Indoor Hotspot (InH) layout [42]to capture a shopping centre environment. We consider 3 APs equally separated at fix positions on the ceiling (6 meters high) as shown in Figure 31. Each AP uses a different 20MHz primary channel on the 2.4 GHz ISM band. In each run, the STAs are dropped according to an exponential law of parameter  $\lambda$  (arrival rate) based on the time of the day.

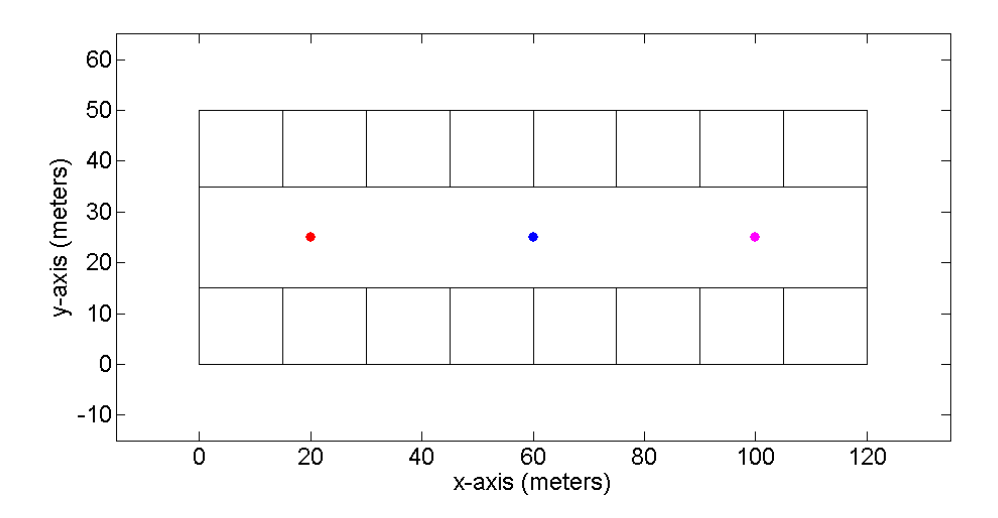


Figure 31. ITU-R InH-based layout with 3 APs

Going for a 24h evaluation, we divide the day into three distinct periods capturing a shopping centre activity as shown in Figure 32: a closing period (CP), a middle-affluence opening period (MA) and a high affluence opening period (HA).



Figure 32. Day segmentation

Users are dropped only during the opening hours with the mean arrival time given in Table 27.



Table 27. Average arrival time per period of day

Period	Mid-Affluence	High-Affluence	Closing Hours
Arrival $\frac{1}{\lambda}$ (s)	30	6	N/A
Hour	08:00-11:00 19:00-22:00	11:00-19:00	22:00-08:00
Ratio over 24h	0.25	0.3333	0.4167

We assume that each arriving STA managing to access the WLAN network will generate an average traffic of 50 Megabytes split in 90% DL and 10% UL. During the passive scan, the STA will search for the best AP in range in terms of received signal also known as Received Signal Strength Indicator (RSSI). If the STA finds one AP, it can start its traffic based on the DL and the UL throughput values derived from the sensitivity given in Table 28 for 20MHz in the SISO case [43]. The association/authentication process is not modelled, the data exchanged during this phase representing a low proportion compared to the data traffic.

Table 28. IEEE 802.11n physical throughput for one spatial stream on 20MHz

MCS	PHY Throughput (short guard interval)	Sensitivity (20MHz)
0	7.2 Mbps	-82 dBm
1	14.4 Mbps	-79 dBm
2	21.7 Mbps	-77 dBm
3	28.9 Mbps	-74 dBm
4	43.3 Mbps	-70 dBm
5	57.8 Mbps	-66 dBm
6	65.0 Mbps	-65 dBm
7	72.2 Mbps	-64 dBm

As a reminder a Basic Service Set (BSS) represents the AP and all its associated STAs. Since Wi-Fi relies on the Carrier Sense Multiple Access with Collision Avoidance (CSMA/CA) mechanism, when a device of the BSS transmits, the others devices in range defer their transmissions on this channel. In our layout, one different channel is associated to one AP, so we do not have overlapping BSS.

For the traffic simulation within the BSS, we assume for simplicity that the time is divided in Transmit Opportunity (TXOP) of duration 4 ms [43]. In each TXOP, one STA can either receive or transmit data with the assurance that other STAs will not compete for the medium access. A TXOP is gained using the classical CSMA/CA mechanism. We apply an overhead of 50% of the physical throughput derived from Table 28 to capture the MAC procedure leading to this slot reservation. We also simulate the beacon transmission which occurs every 100 ms between TXOPs. For backward compatibility reasons with the older IEEE 802.11b amendment, the beacon is sent using the lower data rate of 1 Mbps. Beacons typically carry between 150 and 250 bytes. Based on the arrival time in the BSS, a round-robin approach is assumed



between all STAs for the TXOP allocation. Once a STA has finished its traffic it leaves the BSS.

The STA will try during 20 seconds to associate to the best AP in its range through passive scan. If the STA fails to find a valid AP, it will send a Probe Request frame asking for any AP in range to respond with a Probe Response frame which has content usually equivalent to the one found in a beacon (for association purpose). Typical Probe Request carries around 100 and 150 bytes of information, while Probe Response carries between 150 and 250 bytes. Both are encoded at the lower IEEE 802.11b rate of 1 Mbps. If no AP is found after 20 seconds, the STA is declared in outage and is removed (representing a user changing position to detect a Wi-Fi signal).

# 3.3.5.3 Evaluation on exposure reduction

#### 3.3.5.3.1 Evaluation methodology

For our two affluence scenarios, we simulate around 3 hours of STA arrival per run. For each STA, we log its session time and its aggregate average throughput (in UL and DL) needed to consume its 50 Megabytes of data. For each AP, we collect the time when STAs are associated or not. For each of this period, we also collect the time when the idle mode is engaged on the 2.4GHz radio. The idle mode corresponds to a power reduction of the 2.4GHz radio by a factor  $\Delta_{idle}$  after the expiration of the timer  $T_{exp}$ . This timer starts as soon as the last associated STA leaves the BSS and is reset either when a STA is associated (first approach) or when a probe request is received (second approach). Table 29 gives the main simulation assumptions, where the channel model is the one currently adopted in the IEEE 802.11 TGax [44] (TGn channel D [45] with 7dB of wall attenuation).

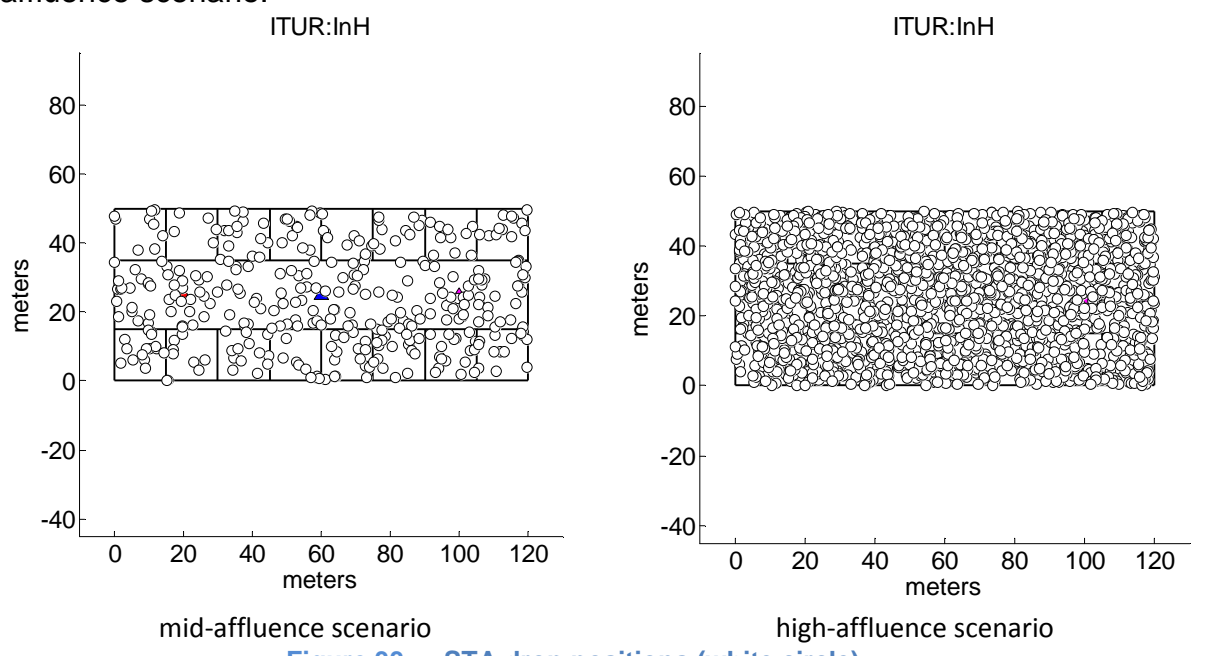
Table 29. Main simulation assumptions

Propagation							
Layout			ITU-R InH				
Channel model			IEEE TGn Channel D with 3D distance				
Shadowing			3dB LOS, 5dB NLOS				
Wall modelling	Modelling		Enabled				
wan modelling	Attenuation		7 dB per wall				
AP parameters							
Number			3 (fixed position)				
	Antenna	Number	1				
2.4GHz radio		Gain	0 dBi				
2.4GHZ Taulo	Tx Power		20dBm (maximum)				
	Bandwidth		20 MHz				
Beacon	Period		100 ms				
Deacon	Duration		2 ms (250 bytes)				
Probe Response Duration			2 ms (250 bytes)				
5GHz mesh update			1 s				
Idle mode timer $T_{\rm exp}$			5 s				



STA parameters							
Number			Exponential arrival with rate $(1/\lambda)$				
	Antenna	Number	1				
2.4GHz radio		Gain	-2 dBi				
	Tx Power		15 dBm				
	Data		50 Mbytes				
Traffic	DL		90 %				
	UL		10 %				
Probe Request Duration			2 ms (250 bytes)				
Outage timerTout	•		20 s				

Figure 33 shows the position of all nodes when dropped over the simulation for both scenarios (white circle), indicating that we completely cover the area in the highaffluence scenario.



#### **STA** drop positions (white circle) Figure 33.

# 3.3.5.3.2 Results

Table 30 and Table 31 give simulation results for different power reductions with the first approach (power reduced only when no stations are associated after a timer expires) for the mid-affluence and high-affluence setup, respectively. The case  $\Delta_{idle} = 0 dB$  corresponds to the baseline scenario. The results include the average session time and the average instantaneous UL throughput of the STAs. For the AP, we consider two states:

- at least one STA is associated to the AP (AP is assumed to transmit almost continuously);
- no STA is associated to the AP (AP only transmits one beacon every 100 ms). The results give the average time ratio an AP is in one of these states. For each of these states, we measure the average time ratio when idle mode is engaged.



Table 32 and Table 33 show the same performance indicators but for the second approach, where the idle mode is always engaged and only a Probe Request can trigger the transition to a transmission at the maximum power.

As a general comment we can notice that the session time increases with the STA density. In the base line setup, the average session time goes from 13.99s to 34.52s when the arrival rate goes from 30 to 6. In the mid-affluence scenario, the average data transmission air-time is around 14%, while this value is around 65% in the high affluence scenario which was expected.

Table 30. Mid-Affluence scenario results (1<sup>st</sup> approach)

		STA		AP			
		Session Time (s)	UL Throughput (Mbps)	Without STA		With STA	
$\Delta_{\mathrm{idle}}$	Outage Ratio (%)			Time ratio (%)	Idle ratio (%)	Time ratio (%)	Idle ratio (%)
0 dB	0	13.99	33.14	86.41	0	13.59	0
3 dB	0	14.55	33.12	86.08	94.63	13.92	0
6 dB	0	15.50	33.07	85.53	94.74	14.47	0
9 dB	0	16.83	33.00	84.58	94.82	15.42	0
12 dB	0	17.19	32.95	82.81	94.87	17.19	0

Table 31. High-Affluence scenario results (1<sup>st</sup> approach)

	STA			AP			
				Without STA		With STA	
$\Delta_{ m idle}$	Outage Ratio (%)	Session Time (s)	UL Throughput (Mbps)	Time ratio (%)	Idle ratio (%)	Time ratio (%)	Idle ratio (%)
0 dB	0	34.52	33.30	34.84	0	65.16	0
3 dB	0	36.49	33.27	34.40	77.07	65.60	0
6 dB	0	38.73	33.19	34.12	78.34	65.88	0
9 dB	0	41.85	33.14	32.99	79.02	67.01	0
12 dB	0	46.24	33.03	31.41	80.03	68.59	0

Version: V1.1 71



Table 32. Mid-Affluence scenario results (2<sup>nd</sup> approach)

	STA			AP			
				Without STA		With STA	
Δ <sub>idle</sub>	Outage Ratio (%)	Session Time (s)	UL Throughput (Mbps)	Time ratio (%)	Idle ratio (%)	Time ratio (%)	Idle ratio (%)
0 dB	0	13.99	33.14	86.41	0	13.59	0
3 dB	0	14.47	33.14	86.01	100	13.99	100
6 dB	0	15.36	33.14	85.28	100	14.72	100
9 dB	0	17.14	33.14	83.87	100	16.13	100
12 dB	0	20.67	33.14	81.31	100	18.69	100

Table 33. High-Affluence scenario results (2<sup>nd</sup> approach)

		STA		AP			
				Without STA		With STA	
$\Delta_{ m idle}$	Outage Ratio (%)	Session Time (s)	UL Throughput (Mbps)	Time ratio (%)	Idle ratio (%)	Time ratio (%)	Idle ratio (%)
0 dB	0	34.52	33.30	34.84	0	65.16	0
3 dB	0	37.59	33.28	33.04	100	66.96	100
6 dB	0	44.80	33.29	29.54	100	70.46	100
9 dB	0	65.73	33.29	23.58	100	76.42	100
12 dB	0	201.49	33.29	13.16	100	86.84	100

# 3.3.5.3.3 Uplink throughput

In the first approach, the UL throughput decreases as the DL transmit power decreases due to idle mode. Indeed, there are cases where a STA will detect an AP that is farther away (in terms of link budget) than a closer one due to the latter having its idle mode engaged, while the former transmits at its maximum power. Since there is no re-scanning of APs once the association is done, the transmission occurs with a worst DL quality, hence the decrease in UL throughput and the increase in the session time. With a 90%-10% DL-UL ratio, the session time is greatly dependent on the DL conditions.

Version: V1.1



However, in the second approach, we do not observe such behaviour for the UL throughput. Indeed, the results show that all APs are always transmitting with a reduced power. Therefore, a STA associating to a farther AP (in terms of link budget) is unlikely to happen as there is no power difference in the APs. As we used well-accepted (transmission friendly) assumptions for the channel model (channel TGn D and 7dB of wall attenuation [44]), the APs never received a frame requesting an increase in their transmit power. This is a point we may investigate for further studies.

#### 3.3.5.3.4 Session time

As mentioned earlier, the session time is greatly impacted by the DL quality.

In the first approach, the average session time can go up by 20% in a mid-affluence scenario for a power reduction of 12dB (from 13.99s to 17.19s), mainly due to an association with a farther AP based on the beacon scan. In the high-affluence scenario, this penalty can reach 34% (from 34.52s to 46.24s).

In the second approach, the average session time is greater than the one in first approach for the high power reduction factors (from 9dB). Under such conditions, the DL budget link forces the AP to select smaller MCSs leading to a higher transmission time for a given data quantity.

It is worth noting that for 3 and 6dB of power reduction, the second approach tends to provide better results than the first approach. In the first approach, we are more likely to observe an association with a farther AP, the difference in powers being less pronounced, while this does not occur in the second approach since all APs transmits with the same reduced power.

### 3.3.5.3.5 Exposure index computation

When computing the EI in our scenario, only the indoor components of the equation are adapted to reflect our time separation. The day components are mapped to the mid and high influence period, while the night ones are mapped to the closing period, during which there are no Wi-Fi users. The following equation is then derived to compute the EI:

$$EI = r_{mid} \left( k5 \frac{P_{TX}^{mid}}{Th^{mid}} + k9 P_{TXWLAN}^{mid} \right) + r_{high} \left( k5 \frac{P_{TX}^{high}}{Th^{high}} + k9 P_{TXWLAN}^{high} \right)$$

$$+ r_{clo} \left( k7 \frac{P_{TX}^{closed}}{Th^{closed}} + k11 P_{TXWLAN}^{closed} \right)$$
(3.25)

where  $r_{\text{clo}}$ ,  $r_{\text{mid}}$  and  $r_{\text{high}}$  represent the proportion per day of time of the closing, the mid-affluence and the high affluence period, respectively. These values are taken from the last row of Table 27. We can neglect the closing period part since no users will be present.

The average throughput  $Th^{mid}$  and  $Th^{high}$  can be found in the UL Throughput column of the previous tables. Since we did not assume any power control in the STA, we have  $P_{TX}^{mid} = P_{TX}^{high} = 15 \ dB$  based on Table 29. The AP transmit power is the weighted sum of the transmit power when a STA is connected (assumed to be continuous, the overhead factor being already considered in the throughput) and when no STA is connected (beacon transmission only, 2ms every 100 ms).



Let  $r_{WoSTA}^{mid}$  be the time ratio when no STAs are associated to the AP,  $r_{WoSTA,P_{idle}}^{mid}$ the time ratio during the "no connected STA" period when the AP transmits at its maximum power reduced by the  $\Delta_{idle} factor$  and  $r_{WiSTA,P_{idle}}^{mid} be$  the time ratio during the "connected STA" period when the AP transmits at its maximum power (23dBm from Table 29) reduced by the  $\Delta_{idle}$  factor. Those values can be deduced from the columns "Without STA/Time Ratio", "Without STA/Idle Ratio" and "With STA/Idle Ratio", respectively. We have:

$$EI_{mid} = r_{WoSTA}^{mid} \left(1 - r_{WoSTA,P_{idle}}^{mid} + r_{WoSTA,P_{idle}}^{mid} \Delta_{idle}\right) P_{max} \frac{2}{100}$$

$$+ \left(1 - r_{WoSTA,P_{idle}}^{mid}\right) \left(1 - r_{WiSTA,P_{idle}}^{mid} + r_{WiSTA,P_{idle}}^{mid} \Delta_{idle}\right) P_{max}$$
(3.26)

The same computation can be derived for the high-affluence scenario  $P_{TXWLAN}^{high}(dB)$ .

Table 34 gives the EI table per population with different transmit power reduction factors for the first approach based on Table 30 and Table 31. The "Session Increase" row represents the average increase in terms of session time from the base line and is computed using a weighted sum of the session times from the mid and high-affluence scenario. It is used to assess the QoS.

Children Young people **Adults** Seniors Baseline EI [W/kg in a day] 0.3514 0.2161 0.2140 0.1966 3dB 0.3505 0.2156 0.2134 0.1961 +0.26%  $\Delta_{idle}$ El Reduction +0.26% +0.26% +0.26% Session Time Increase +5.31% 6dB 0.3516 0.2162 0.2141 0.1967 El Reduction -0.05% -0.05% -0.05%  $\Delta_{idle}$ -0.05% Session Time Increase +11.87% 9dB 0.3589 0.2207 0.2185 0.2008 -2.13 -2.13% El Reduction -2.13 -2.13  $\Delta_{idle}$ Session Time Increase +21.01% 12dB 0.3716 0.2285 0.2262 0.2079 El Reduction -5.73% -5.73% -5.73% -5.73%  $\Delta_{idle}$ Session Time Increase +31.37%

El evaluation (step 5) (1<sup>st</sup> approach) Table 34.

Even though the "without STA associated" state may represent a significant part of the air time, the effective transmission only represents 2% of this period (beacon only), leading to negligible impact on the EI. Dividing the power by 2 ( $\Delta_{idle} = 3 \text{ dB}$ ) brings only 0.26% of EI reduction. Worst dividing event more the power ( $\Delta_{idle} = 6 \text{ dB}$ and above) deteriorates the EI significantly (up to a 5.73% increase).

This can be explained by the session time which drastically increases as the idle mode factor increases (from 5% up to 31%). Due to a bad STA association decision (based on RSSI only and without AP handover), the effect on the beacon power reduction is completely overshadowed by the increased time where the AP will have to transmit at its maximum output power, thus the counter intuitive results.

Version: V1.1

Dissemination level: PU



As a conclusion, the first approach is not something to recommend for reducing the EI of the active users.

Table 35 gives the EI table per population with different transmit power reduction factors for the second approach based on Table 32 and Table 33. This approach keeps a reduced transmit power until a probe request is received. With our setup and the range of power reduction factors investigated, the probe request is never sent since one of the three AP is always in range of a STA.

Children **Adults Seniors** Young people Baseline EI[W/kg in a day] 0.1966 0.3514 0.2161 0.2140 3dB 0.1808 0.1112 0.1101 0.1012 El Reduction +48.54% +48.53 +48.54 +48.53%  $\Delta_{idle}$ Session Time Increase +7.62% 6dB 0.0580 0.0952 0.0586 0.0533 EI Reduction +72.90% +72.91% +72.9% +72.90%  $\Delta_{idle}$ Session Time Increase +25.12% 9dB 0.0516 0.0318 0.0315 0.0289 EI Reduction +85.30% +85.28% +85.29% +85.30%  $\Delta_{idle}$ Session Time Increase +74.58% 12dB 0.0294 0.0181 0.0179 0.0164 El Reduction +91.64% +91.62% +91.63% +91.64%  $\Delta_{idle}$ Session Time Increase +382.07%

Table 35. El evaluation (step 5) (2<sup>nd</sup> approach)

Since the transmit power is always kept at a low level with and without STA, the EI is also reduced. However, this reduction does not go linearly with the transmit power reduction factor. As the DL quality goes down, the session time is increased (by a significant margin with a high power reduction). There is no dynamic correction of the transmit power unless a probe request is received. With a power divided by 2, we are able to reduce the EI by 48% with a slight increase in the session time of 7.62%. If we reduce the power by a factor 4, then the EI is reduced by 72% and the session time increased by 25%. In our opinion, this represents the upper limit in terms of acceptable QoS and EI reduction we can obtain. Decreasing even more the power leads to unacceptable session time with this current approach.

Note that the absolute EI average over one day can be computed by doing a weighted sum of the EI per population and dividing by result by one day duration expressed in seconds. Using the population repartition defined in D2.8 [3], we can reduce the global EI from 2.67 10<sup>-6</sup> W/kg to 1.38 10<sup>-6</sup> with the second approach and an idle factor of 3dB (Table 35).

# 3.3.5.4 Conclusions, analysis

As surprising as it can be, dividing the transmit power of an AP by more than a factor 2 when no stations are associated to it, does not generally lead to an EI reduction. The unbalance in the APs beacons can lead to a bad AP selection by the STA. Since there is no standardised ways to move a STA to another AP currently implemented and supported without performing an explicit de-association procedure, one can only



recommend keeping the beacon transmit power at the same level for all APs within the same network.

The second approach does that and keeps the low power level even during communications. The results tend to demonstrate that a power divided by two brings a clear EI reduction (48%), while the session time on average is not too much impacted (+7%).

# 3.3.6 Solution I - Interference mitigation in Zigbee & Wi-Fi

### 3.3.6.1 Remind on solution concept

Radio access technologies operating in the same frequency range manifest interference with one another. In this section we study the interference between Wi-Fi and Zigbee-like devices, an umbrella for wireless sensor networks. Different wireless sensor networks will differ in radio access technology, protocol stack and application type, but interference with Wi-Fi will always be present in the 2.4GHz band. In this section we consider the EI reduction as result of mitigation of interference between Wi-Fi and Zigbee.

The proposed solution works on one of our WSN platforms with the current protocol stack, but we believe it is sufficient proof of concept on the importance of dynamic channel switching in the context of El reduction. Channel switching has been selected as the method of mitigation, and the dynamic nature of the protocol should allow sensor networks to always avoid specific Wi-Fi networks.

Each node periodically takes measurements of RSS (Received Signal Strength). Every high RSS measurement taken when the node is not transmitting or receiving packets (or physical symbols part of WSN transmission) is a sign of a different radio access technology. On high sustained levels of interference, the node will choose a different channel. The decision to change channels is local, but the effects must be network-wide. Because of this, a node that decides to change the current transmitting channel will send a few repeated broadcast packets to notify immediate neighbours of this change. Short, repeated packets have a greater chance of being successfully transmitted at least once. We have chosen avoid the issue of obtaining consensus on a channel to switch the entire network, since it is difficult to achieve when many packets are lost. As such, the deciding node switches to the next channel by jumping over three channel numbers (e.g. 11 to 15, 15 to 19, 25 to 13), depending on the number of Zigbee channels available to the transceiver hardware.

## 3.3.6.2 Specific scenario inputs

The home Wi-Fi scenario is used for this work. It is presumed that a WSN network is also present and will be aggregated into EI along with Wi-Fi. The Wi-Fi and the WSN networks have both a DL component. The Wi-Fi also has an UL component, for when a user is actively using a Wi-Fi device. This is the component that will be the most affected one by this work. The WSN network is in the same 2.4GHz band as Wi-Fi, with 2.2mW (3.4dBm) transceivers. For Wi-Fi we considered commodity hardware with 84mW (19.25dBm) transmit power.

The solution aims to reduce EI through interference mitigation. While maintaining QoS, a lower number of retransmissions of the same content on Wi-Fi and WSN will



decrease the dose received by a nearby user. Departing from classic low-power research, we find that Wi-Fi retransmissions make a greater contribution to the EI and thus should be prioritized over WSN retransmissions.

Table 36. Scenario breakdown

Time	Population	Environment	RAT	Cell Type	User Profile	Posture	Usage
Day	Children	Indoor	Wi-Fi	N/A	N/A	Sitting	Data tablet
Night	Young people		WSN				Data, laptop on a lap
	Adults						Data, laptop on a desk
	Seniors						

#### 3.3.6.3 Evaluation on exposure reduction

For Wi-Fi, a duty cycle of 1.4% is considered for the DL component (meaning the average percentage of time a Wi-Fi signal is detected in a single channel over a period of time), as research suggests this is the median duty cycle of home networks[46].  $P_{TXWiFi}$  is an average power considered to include this duty cycle. For the purposes of this evaluation, it will also include the number of retransmissions needed, so it is in fact  $P_{TXWiFi} = P_{TX}$  \* Duty / PRR (Packet Reception Rate).

For WSN, a starting duty cycle of 1% is also considered, which then expands based on the PRR (the amount of transmissions needed remains the same, but with added retransmissions). In the EI formula, we expand the sum of RATs:

$$EI^{SAR} = \frac{1}{T} \sum_{t}^{N_T} \sum_{p}^{N_P} \sum_{e}^{N_E} \sum_{pos}^{N_{pos}} f_{t,p,e,pos} \cdot (d^{DL} \bar{S}_{RXinc,Wi-Fi} + d^{UL} \bar{P}_{TX,Wi-Fi} + d^{UL} \bar{P}_{TX,Wi-Fi})$$

$$+ d^{UL} \bar{P}_{TX,WSN}) \left[ \frac{W}{kg} \right]$$
(3.24)

El is the summation over  $N_T$  time periods of the day, over  $N_P$  population categories, over  $N_E$  environments and over  $N_{pos}$  postures of the emissions in this scenario. We consider the  $d^{DL}\bar{S}_{RXinc,\,Wi-Fi}$  coefficient, associated with the download component of Wi-Fi transmissions, as well as  $d^{UL}\bar{P}_{TX,\,Wi-Fi}$ , the upload coefficient. For WSNs we only consider the upload coefficient  $d^{UL}\bar{P}_{TX,\,WSN}$ , because the download coefficient is negligible at the transmitted power that WSNs commonly have.

As we have shown in D4.2, interference conditions can lead to PRR of 50% or more. El Reduction greatly depends on the initial conditions of the interference, and we have provided in the following tables an El reduction for different situations.



El Percentage Improvement considering Wi-Fi

	Baseline		PRR <sub>IM,Wi-Fi</sub>	
	Daseille	0.5	0.7	0.9
Absolute EI[W/kg]	3.97E-07	2.24E-07	2.23E-07	2.22E-07
El Reduction[%]		43.62%	43.87%	44.01%

Table 38. El Percentage Improvement considering WSN

	Baseline	PRR <sub>IM,WSN</sub>				
	Daseille	0.5	0.7	0.9		
Absolute El[W/kg]	3.97E-07	3.43E-07	3.41E-07	3.40E-07		
El Reduction[%]		13.60%	14.03%	14.27%		

In the case of the WSN network, often a single application will be running in the network. This allows for a more fine-grained approach to EI calculation and can be customized for specific applications.

### 3.3.6.4 Conclusions, analysis

Channel switching WSN networks have a positive impact on EI, since interference is avoided. The time it takes for the WSN network to detect and switch is negligible compared to time they operate during the day. QoS for Wi-Fi is improved, but QoS for the WSN network is not affected much.

While this specific channel switching done on our networks will not be applicable to all WSNs due to diversity in structure and functioning, from the EI reduction we can conclude that it is more important to maintain a low number of retransmissions on the Wi-Fi side. As such, in a wireless sensor network where channel switching proves more difficult, a case can be made to choose the solution which is more disruptive for the WSN, but less disruptive for the Wi-Fi network (an example would be a sensor network forced to split momentarily).

## 3.3.7 Solution J - Radio link allocation

### 3.3.7.1 Remind on solution concept

Typical deployments of wireless sensor networks in a Smart Home application exhibit special communication patterns that differentiate them from normal data-carrying wireless networks. An important difference between WSNs and data-carrying wireless networks is that most WSN applications use a single-sink model where data is gathered from a multitude of sensor nodes and must be sent to a special node called the sink (or coordinator). In this model, transmission is usually done in a tree fashion with intermediate nodes gathering data from leafs and forwarding it towards the sink [47]. Another difference between WSNs and traditional networks is that, in most WSN applications, delays in data transmission are tolerated.

Considering that real-time delivery of data is not critical in most WSN scenarios we can schedule node transmissions at appropriate times, by locally buffering data, in order to reduce user exposure to EMF radiation. This can be achieved for example by limiting the transmit power of sensor nodes to a single room and scheduling data

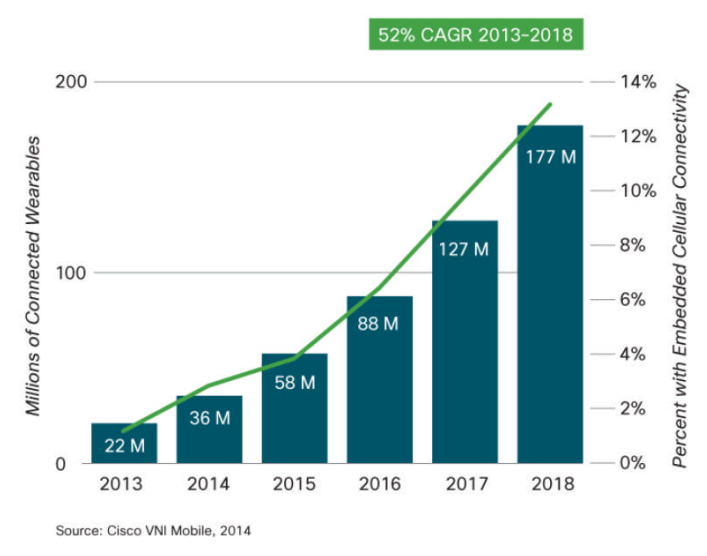


transmission when no users are detected in the room, using presence sensors or static and/or dynamic schedules.

# 3.3.7.2 Specific scenario inputs

Considering the predicted growth of WSN deployments, it is important to not only compute the exposure from WSNs in the present, but also consider their impact as more WSNs are deployed. An important input for this, that is not captured in the El formula, is represented by the number of WSN deployments.

Currently, the number of deployed WSNs is small, making the percentage of the population affected by WSN exposure also small, in comparison with exposure from cellular networks or Wi-Fi. However, this number is expected to rise as more and more buildings are equipped with environment monitoring systems and intelligent climate control. As a source of data for WSN deployments and their growth we will consider the Internet of Everything adoption study presented in [48]. The growth of WSNs is not explicitly considered as a category so we assume their growth is similar to that of connected wearable devices, presented in Figure 34.



Growth of connected wearable devices Figure 34.

Using this trend we assume only a fraction of buildings are equipped with WSNs and the same fraction of population is affected by WSNs. This gives us the following percentages extrapolated to 2025 to apply to our affected population (Table 39).

Percentage of population affected by WSNs Table 39.

2015	2016	2017	2018	2019	2020	2021	2022	2023	2024	2025
4.0%	6.0%	8.7%	12.1%	16.3%	22.0%	29.2%	38.3%	50%	65%	82.7%

It should be kept in mind that once WSN deployments become ubiquitous and affect 100% of the population, the EI contribution of WSNs as computed in this study will reach its maximum, and further increases in exposure can only come from multiple WSNs operating in the same space and at the same time.



### 3.3.7.3 Evaluation on exposure reduction

The EI evaluation of the solution is based on the general formula for the EI. Considering the scenario inputs, the sums over c (Cell Type), l (User Profile) and u (Usage) can be eliminated as they are not applicable to a WSN solution. We will also ignore the sum over RATs for this evaluation, as we consider only one RAT: WSN. We will keep the sum over pos (Posture), even though the category only has one element, in order to have a complete formula defining the EI for WSNs. With these simplifications and by removing the  $close\ devices$  term, which is not considered by LEXNET, the formula becomes:

$$EI^{SAR} = \frac{1}{T} \sum_{t}^{N_T} \sum_{p}^{N_P} \sum_{e}^{N_E} \sum_{pos}^{N_{pos}} f_{t,p,e,pos} \cdot d^{DL} \bar{S}_{RXinc} \left[ \frac{W}{kg} \right]$$
(3.27)

For the fraction  $f_{\rm t,p,e,pos}$  of the total population that corresponds to category p in environment e and posture pos during time period t we consider the population repartition presented in D2.8 [3]. This fraction only depends on the population category (child, young people, adult and senior) and not on the environment (100% of the category is both indoor and outdoor, but at different times), posture (100% of the category is considered to be standing) or time period (100% of the category is considered during each time period).

For computing the  $d^{DL}$ term we extract the time durations  $TD^{DL}_{t,p,e,pos}$  of posture pos in environment e for the population category p during time period t by considering the life segmentation data [3]. We include the percentage of time spent in Transportation as being Outdoor and compute the number of seconds spent in each situation from the given percentages.

The second part of the  $d^{DL}$ term consists of the  $SAR_{p,pos}^{DL}$  values, which we also extract from D2.8 [3]. We consider the SAR values for 2600MHz frequency band (which is the closest match for the 2.4GHz used in WSNs) for children and adults in a standing position and using data. Furthermore we use the adult values for young people, adult and senior categories and the child values for the children category.

Our final requirement of assessing the EI is computing the average received power density before and after applying the solution. We begin with assessing the received power density without any LEXNET improvements. Our main formula is the relation between power density and received power, with G being the antenna gain at the receiver and  $\lambda$  being the signal wavelength:

$$S_{RX} = \frac{4\pi}{\lambda^2} \frac{1}{G} P_{RX} \tag{3.28}$$

We consider the signal wavelength of the 2.4GHz band  $\lambda \approx 0.125m$  and the antenna gain G = -0.5dBi or  $G \approx 0.8912$  of a small wireless sensor node [49]. The received power is computed in a simplified way with the basic Friis transmission equation, (with exponent 2) and considering an average distance between users and deployed sensor nodes of 5m (the size of a medium room). For the actual transmitted power



we again refer to the mentioned sensor nodes [49] which have a maximum transmitted power  $P_{TX\,ERP}=2.4dBm~{\rm or}P_{TX\,ERP}\approx 1.74mW$ . If we also take into consideration a duty cycle for transmission (derived from the monitoring application proposed in D4.2 [1]), we obtain a received power at the receiver (after the antenna) of  $P_{RX} = 7.037 \cdot 10^{-11} mW$  and a power density before the antenna of  $S_{RX(w_0 LEX)} =$  $6.351 \cdot 10^{-11} \frac{W}{m^2}$ 

Using the previous value we can create the table of power densities (Table 40) given the population category, time period and environment. We consider that the outdoor exposure is negligible given the greater distances and low transmission power of WSNs.

c	Day (8a	m-6pm)	Night (6pm-8am)		
$S_{RX(wo\ LEX)}$	Indoor	Outdoor	Indoor	Outdoor	
Children	6.351·10 <sup>-11</sup>	0	6.351·10 <sup>-11</sup>	0	
Young	6.351·10 <sup>-11</sup>	0	6.351·10 <sup>-11</sup>	0	
Adult	6.351·10 <sup>-11</sup>	0	6.351·10 <sup>-11</sup>	0	
Senior	6.351·10 <sup>-11</sup>	0	6.351·10 <sup>-11</sup>	0	

Table 40. **Power density without LEXNET solution** 

Applying the EI equation for WSNs (Eq.(3.25)) we obtain the following predicted exposure caused by WSNs without the LEXNET solution (Table 41).

2015 2016 2017 2018 2019 2020 2021 2022 2023 2024 2025 1.04 1.57 2.27 4.30 5.77 7.64 3.16 1.00 1.30 1.69 2.17 10<sup>-14</sup> 10<sup>-13</sup> 10<sup>-14</sup> 10<sup>-14</sup> 10<sup>-13</sup> 10<sup>-13</sup> 10<sup>-14</sup> 10-14 10<sup>-14</sup> 10<sup>-14</sup> 10<sup>-13</sup>

**Exposure Index from WSNs without LEXNET** Table 41.

In order to obtain the average received power density with the LEXNET solution we employ the relative improvement in received power described in D4.2[1]. Considering that the transformation from received power to power density is linear in the received power term, the same reduction obtained previously can be applied to the received power density in Table 40to obtain the received power density with the LEXNET solution (Table 42).

This reduction however cannot be applied to all situations. We consider that only children, young people and adults exhibit the behaviour of being in different buildings at different time periods and thus the reduction only applies to them. Furthermore, we must keep in mind that this reduction is computed for the particular WSN scenario described in [1] for an update rate of 1 packet every other minute and a buffer size of 8KB.



Table 42. Power density with LEXNET solution

c	Day (8a	m-6pm)	Night (6pm-8am)		
$S_{RX(wo\ LEX)}$	Indoor	Outdoor	Indoor	Outdoor	
Children	2.990·10 <sup>-11</sup>	0	2.990·10 <sup>-11</sup>	0	
Young	2.990·10 <sup>-11</sup>	0	2.990·10 <sup>-11</sup>	0	
Adult	2.990·10 <sup>-11</sup>	0	2.990·10 <sup>-11</sup>	0	
Senior	6.351·10 <sup>-11</sup>	0	6.351·10 <sup>-11</sup>	0	

Again, applying the equation (3.25) we obtain the following predicted exposure caused by WSNs, but reduced by applying the LEXNET solution (Table 43).

Table 43. Exposure Index from WSNs with LEXNET

2015	2016	2017	2018	2019	2020	2021	2022	2023	2024	2025
	8.50· 10 <sup>-15</sup>									

Table 34 presents the predicted growth of the EI values from WSNs, with and without the proposed solution.

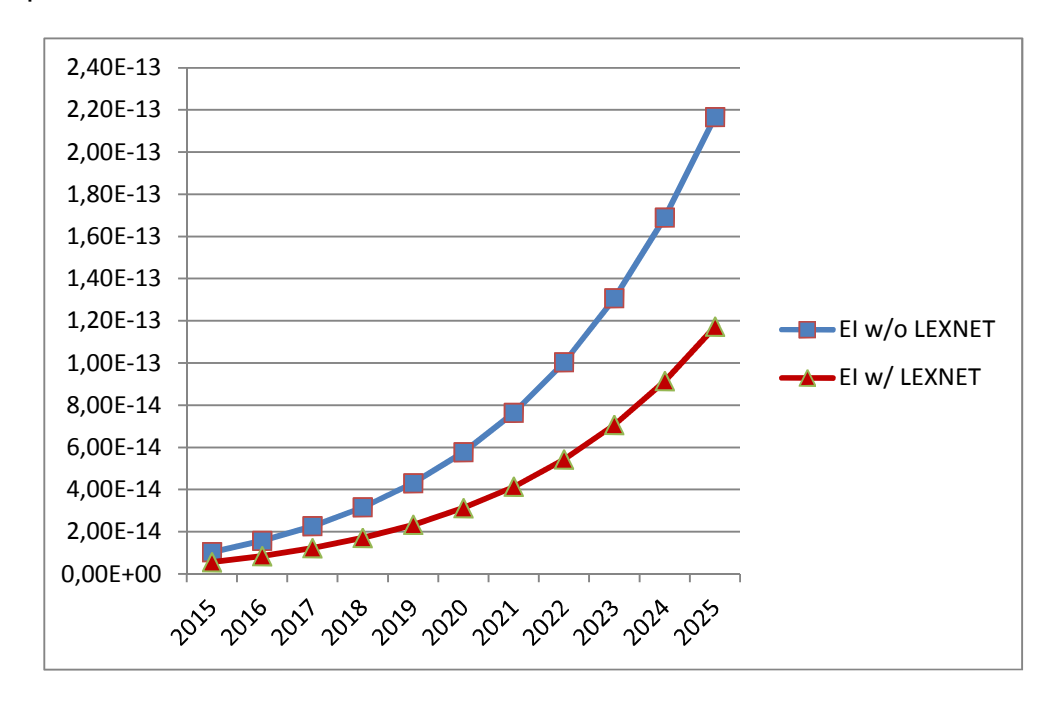


Figure 35. Growth of El values for WSNs

In order to get a better characterization of the EI reduction achievable with this solution with respect to the available parameters, we can compute the reduction based on the relative improvement of the received power, presented in[1]. Table



44shows a better estimate of the reduction, that takes the population distribution and different behaviour of population categories into account. This estimate is necessarily smaller than the one in [1] as not all population categories are covered by the proposed solution as assumed previously.

Table 44. Potential El improvement as a function of buffer size and update rate

$Ratio_{EI-RLA}(\%)$	Update rate (packets/min)						
Buffer	0.1	0.2	0.5	1	2	5	10
1 Kbytes	-28.69	-14.35	-5.74	-2.87	-1.43	-0.57	-0.29
2 Kbytes	-57.39	-28.29	-11.48	-5.74	-2.87	-1.15	-0.57
4 Kbytes	-86.75	-57.39	-22.96	-11.48	-5.74	-2.30	-1.15
8 Kbytes	-86.75	-86.75	-45.91	-22.96	-11.48	-4.60	-2.30
16 Kbytes	-86.75	-86.75	-86.75	-45.91	-22.96	-9.18	-4.60
32 Kbytes	-86.75	-86.75	-86.75	-86.75	-45.91	-18.36	-9.18
64 Kbytes	-86.75	-86.75	-86.75	-86.75	-86.75	-36.73	-18.36

In order to have a real world evaluation a prototype was built and tested during the course of the project. The prototype was built on the Dresden Elektronik sensor nodes [49] using the default 6LoWPAN network stack (Figure 36). The solution implemented a static schedule based on the LEXNET reference scenario of two time periods: day (8am-6pm) and night (6pm-8am). The evaluation consisted of scheduling the transmissions of an office environment monitoring application and was conducted in a real office environment over the course of multiple days using 5 sensor nodes: a gateway node, a router node and three leaf nodes. The application parameters were chosen to be as close as possible to the theoretical evaluation: packets of 42 bytes and an update rate of 1 packet every 2 minutes.





Figure 36. Example of sensor nodes used in solution evaluation

Figure 37 presents the average power density throughout the day, computed from the transmit powers and time of transmission recorded using the methodology described in [1]. As can be seen the computed values are higher than estimated using the application traffic alone. This is caused by the signalling of the lower stack protocols which adds network traffic and thus induces more exposure. Moreover, this traffic is also present during the day, when application traffic is buffered for later transmission. The spike in average power density at the end of working hours represents this buffered traffic being transmitted by the solution when users are not affected by the transmission.

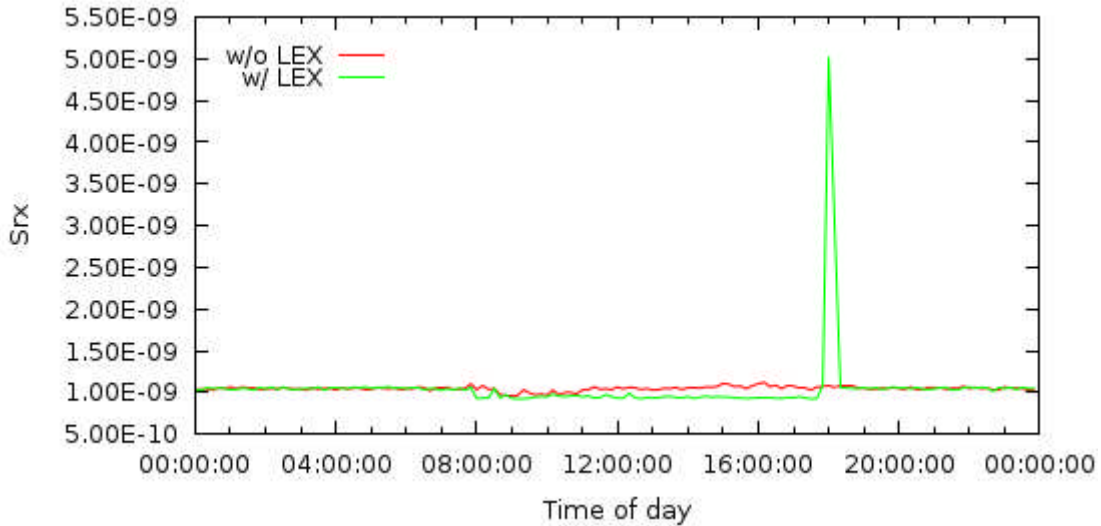


Figure 37. Power density throughout the day

Using the power density we can compute the EI before and after applying the solution to this office environment. Only adults are covered by this evaluation and we consider the fraction of the population affected by WSNs in 2015. We obtain an EI of 2.315·10<sup>-14</sup>W/kg for adults without the solution and 2.102·10<sup>-14</sup>W/kg with the proposed solution, which implies a reduction of -9.18%.

# Document ID: D4.3: Final validation and recommendations for smart low exposure index FP7 Contract n°318273



An important part of any EI reduction solution is not decreasing the QoS level together with reducing the exposure. For the current study we have chosen the PRR as the QoS metric, meaning that we count the packets received during the application's required transmission delay. This imposed requirement is achieved trivially, through the design of the solution, as packets are buffered only until this deadline expires. If a WSN application which is not tolerant to delays is deployed using our solution, no QoS degradation will be observed, but the EI reduction obtained will be decreased.

### 3.3.7.4 Conclusions, analysis

In this work we analysed the EMF exposure coming from WSNs running environment monitoring applications and proposed a method for reducing the impact of the exposure to the population. The method works by buffering data packets from application in the network stack, and delaying their transmission until such a time comes that the impact from that transmission will be reduced. In the prototype implementation the delaying decision is done statically based on the day/night cycle assumed for population activities, but more dynamic decisions based on real-time sensor data can be implemented.

Our evaluation shows that the EI contribution of WSNs is relatively small when compared to cellular technologies or Wi-Fi, which is mostly attributed to the smaller, transmit powers employed in WSNs and the reduced data traffic. However, predictions of future WSN deployments can increase this ratio, and together with an increase in data traffic carried by WSNs, attributed to the need for a more accurate picture of our environments, can make WSNs relevant in the total EI calculation. It can be envisaged that future sensors will transmit more data, but will also have better hardware making buffering still possible. This, coupled with equipping nodes with sensors capable of detecting persons, can make the solution scale even if future applications require more data and have stricter delay requirements.

Another area of future development revealed by the practical evaluation is reducing the network stack protocol signalling, which, for the measured stack implementation was responsible for a significant part of the total EI from the WSN. This could be done similarly as with the buffering solution, but reducing the signalling frequency during office hours or, if the hardware is available, when users are in the proximity.



# 4 WP4 TECHNOLOGIES POSITIONING ON ABSOLUTE EI (STEP 5)

This section proposes a synthesis and preliminary analyses about absolute and relative EI evaluations for all the WP4 studied solutions.

Table 45 gives a relevant overview of the exposure improvement for each technologies by showing on the one hand the absolute EI without (EI ref.) and with (EI LEXNET) the solution implementation; and on the other hand the relative improvement (EI ratio). A last column focuses on specific points concerning the evaluation. This last point is crucial not to misinterpret the presented EI figures; This topic has already been raised in section 2.2.

# Analysis of positionning:

At a first glance, the positioning approach on a common axis shows that the absolute EI can present a large range of values spanning a scale more than 3 decades as shown in Figure 38. Obviously, it is important to remind that the scenario (including population usage, data volume, RAT and mean transmit power) drives the absolute EI level (before LEXNET solution implementation). Moreover some solutions could not be associated with a single EI scenario. Additionally some of the analysed radio component technologies could be applied another scenario. This is the case for the metamaterial antenna, which has been applied to the WiFi scenario but could be applied to a mobile terminal in a high band LTE scenario where the benefit in terms of exposure reduction should be comparable because wavelengths are of the same order of magnitude.

The rural scenario and WiFi deployement in a very dense user distribution present the highest absolute EI before the implementation of associated solutions. The distanceto the eNB for the ruralcase and the density plus the lack of power control management for the WiFi could explain this positionning (EI>10<sup>-6</sup> W/kg).Onthe other side of the axis the WSN solution presents an absolute EI below 10<sup>-9</sup> W/kg dueto a combinaison of very low duty cycle and Tx power and a important distance between the source and the body. LTE technologies show absolute EI around 10<sup>-8</sup> W/kg in a urban scenario. Finally the WiFi scenario (when a high density of user is typical) presents an EI around 5×10<sup>-7</sup> W/kg.

## Role of absolute vs relative EI evaluation:

Some solutions, like WSN radio link allocation, can present a large EI ratio reduction (46%) meanwhile their absolute EI are very low (below 10<sup>-9</sup> W/kg). At the opposite end, other solutions, like the dual-hop OFDM in LTE-A relay deployement in rural scenario, reach as low as 8% on DL absolute EI but starting from a higher level (higher than 10<sup>-6</sup> W/kg). Therefore the evaluation of a given low EMF technology needs to propose not only relative exposure reduction (EI ratio (step-3 and 4 of the common evaluation methodology)) but also wheter the absolute reduction (in W/kg) or the EI evaluated with and without the solution implementation (step-5 of the common evaluation methodology). Notice that as relative EI evaluation is significantly simpler, it can be used to compare two technologies that share the same scenario with the same inputs parameters used for the evaluation.

Version: V1.1

Dissemination level: PU

Document ID: D4.3: Final validation and recommendations for smart low exposure index FP7 Contract n°318273



# Role of the input parameters:

It's crucial to stress the major impact of the input parameters on the absolute obtained EI figures. For instance at a first glance, it seems rather conterintuitive that LTE solutions for urban scenario show an EI ten times lower than WiFi solutions. But when input parameters are detailled, in the former solutions, a very low penetration of LTE users have been considered (early adopter in France in 2014). This results in decreasing of the absolute EI compared to WiFi usage which is already largely spread in the population.

A second reason that explains very low EI of the SCBS miniature & directive antenna is that, in this specific case, the evaluation makes the assumption that 80% of the users are connected with a small cell for whom Tx power is quite low due to the relative proximity. This results in low EI UL values, also compared to the two other LTE solutions in urban scenario. A last remark concerns the fact that the best benefit of such a solution is reached for high traffic load where the interference impact is the main limiting factor compared to the budget link. Thus the relative improvement figure is dependent of the selected traffic load.

### Possible improvements:

If the goal is to be able to compare two low EMF technologies, animportant point is to evaluate both of them with exactly the same scenario input parameters (usage, data volumes,...). The setting of some standardized exposure scenarios could be highly relevant as has been done for wireless propagation channel models. The idea is to simplify the ICT scenario with only 2 or 3 input parameters that could be experiment with,for instance the ratio between voice and data and the ratio between UL/DL. The Tx power and Rx power density could be derivated from the existing channel models. Thus the statistical distribution of EI could be assessed by giving more complete information than only the mean exposure. A example of this approach is effectively adopted in section3.2.2.3.

Finally in order to take into account the RAT efficiency in terms of exposure, one could normalize the EI by the Tx data volume for the UL, and by the Rxdata volume for the DL.

## Possible associations:

Additional exposure reduction can be expected by simply considering aggregation of the analysed individual solutions when they are compatible. This is usually the case because the solutions do not belong to the same ISO layer or to the same RAT and can be considered as independent from each other. The exception concerns the solution based on relay deployement that is only envisaged in rural area. This corresponds to a case where scenarios are considered as mutually exclusive; which is not the case for LTE urban, WiFi and WSN scenarios. Unfortunatly WP4 hasn't carried on this global EI assessment by aggregating the different RAT exposures because of the heterogeneity of the individual evaluations.

To conclude, the global analysis of suchabsolute EI figures can only be carried outby knowing the details of the EI evaluation context. Nevertheless this kind of analysis is able to point out the absolute exposure for a given situation that corresponds in the

Version: V1.1 87

Dissemination level: PU



current case, to the population ICT usages in 2014. From an absolute point of view, the most promising solutions to reduce exposure are those which both present a hight level of absolute EI before the LEXNET implementation even if their relative reduction is low. That concerns the technologies which addresses the WiFi and LTE rural scenario. However this last point could change in future years while LTE penetration will have reached a dominant positionamong the different RATs.

Table 45. Overview of absolute and relative El evaluation for the different solutions

Solution	El ref. (10^-8 W/kg)	EI LEXNET (10^-8 W/kg)	El ratio (%)	Comment
Low exposure cooperative communication techniques (Dual hop OFDM based on relay)	110	102	7.7%	Only DL exposure is considered. See details in section 3.1.2.
SCBS miniature & directive antenna	0.04	0.03	25%	El is assessed with a low proportion of LTE adopters among the population. In this evaluation +6 dB on SINR reached for the UL, is not converted into exposure reduction. Thus this solution brings both 25% El ratio and significant UL QoS improvement. See details in section 3.2.2
Enhanced SC DTX for low EMF	0.3	0.06	80%	Only DL exposure is considered. See details in section 3.2.3
Low Noise receiver architecture	3.3	2.3	30%	Considering 1.5 dB improvements on noise figure. See details in section 3.2.4.
Enhanced efficiency in reference symbol usage	20.2	18.3	9.1%	See details in section 3.2.5.
Antenna on terminal for low El	0.25	0.18	28.7%	Only UL exposure is considered. Solution using the monopole antenna with RHIS back to the PCB. See details in section 3.3.3
Beamforming technique	170	58	66%	For the novel 'hybrid' solution proposed.  See details in section 3.3.4.
Sleep/idle mode in a mesh gateway deployment	270	140	48%	while the session time on average is not too much impacted (+7%) See details in section 3.3.4.
Interference mitigation in Zigbee & Wi-Fi	40	22	44%	El reduction depends on initial interference conditions. This solution improves QoS for Wi-Fi and WSN as well.  See details in section 3.3.6
WSN radio link allocation	2.32 ·10-6	2.10 ·10-6	9.2%	For typical 2015 WSN deployment. Value from real measurements. See details in section 3.3.7



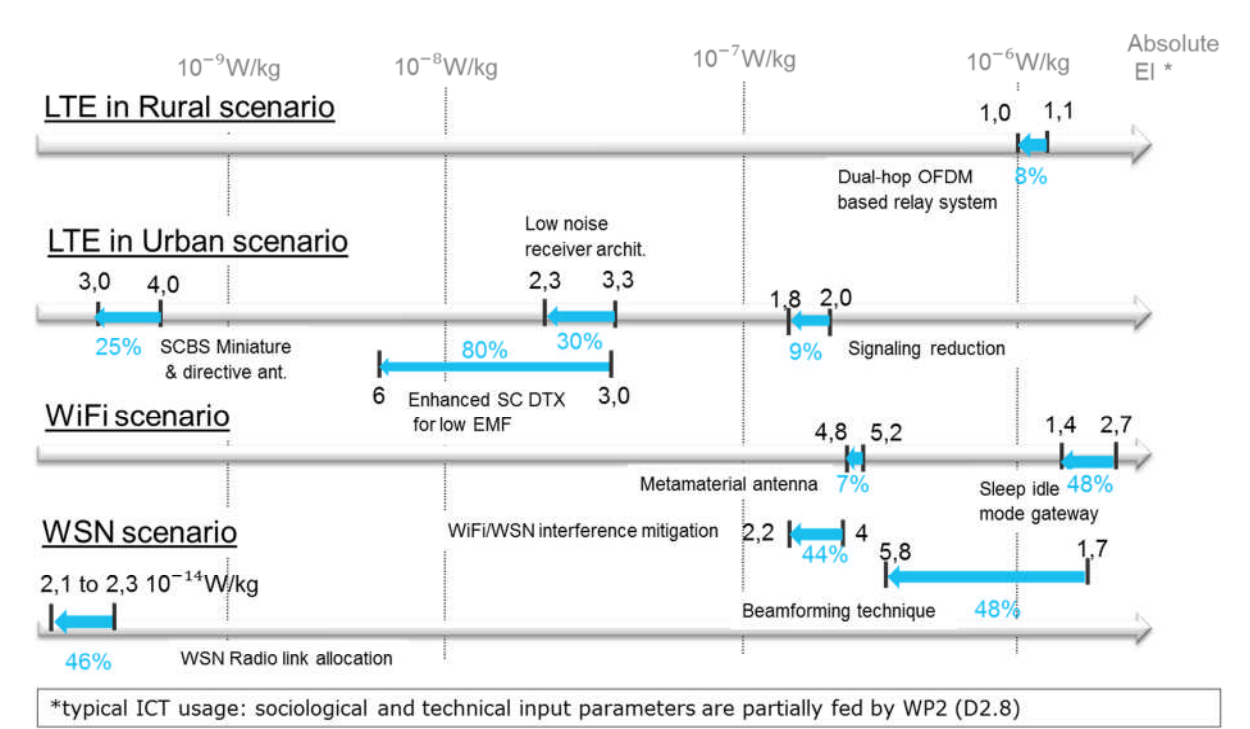


Figure 38. Synthesis of the WP4 solutions to reduce EMF positioned on a common absolute EI axis for 4 scenarios based on 2014-2015 ICT usages detailed in LEXNETD2.8



# 5 CONCLUSIONS AND RECOMMENDATIONS FOR SMART LOW EXPOSURE INDEX

The three main goals of the WP4 consist of identifying, developing, and analysing the radio components and transmission techniques that allow reduction of global exposure while preserving QoS. The SotA review presented in D4.1 [50] has allowed listing of a dozen promising Low EMF technologies. They have been developed and characterised through their relative improvement (EI ratio) in D4.2 [1]. This report consolidates the studies with final development updates and also with the absolute EI assessment for each of the solution analysed in their associated scenario taking into account population ICT usages. Practically the LEXNET project EI metric is implemented to analyse performance and relevancy of low EMF technologies. This has been possible through important cross-communication between telecom engineering (WP4) and EM dosimetry (WP2/3) communities in the project.

# WP4 achievements and promising solutions:

El ratio results (El reduction vs. QoS) are proposed for each solution regarding a specific scenario. The relative exposure reductions vary from 7.7% to 80% depending on the solutions while checking QoS is preserved. For technologies that tend to control the near or far EM field, most often based on antenna or transmission techniques, a disruptive amount of El reduction (more than 50%) can be reached because this aspect had not been identified in classical radio link optimisation. For instance beamforming (miniature & directive) antenna at Small Cell BS has shown both +6 dB SINR increasing and 25% El ratio reduction. However these improvements bring an additional complexity, or are optimized for a given usage. More generally, except for specific usage (laptop), low EMF technologies will have to support and be optimized for different contexts and usages. Thus they will need to support dynamic configurations (e.g. tunable filter) in order to keep their benefit whatever the scenario. This is a general trend in communications as 5G standards are in preparation.

# WP4 innovation:

The WP4 innovation beyond the SotA is twofold. On the one hand, the novelty of this work is in the analysis itself of a global assessment of the exposure (UL and DL, over a population) through modified or specifically developed tools. By considering the daily ICT usages, WP4 studies have evaluated the impact of a given technological solution in a given scenario. Before LEXNET, works that presented exposure reduction only showed one performance indicator (e.g. SAR) without taking into account both UL & DL, or any ICT usage dilution effect. However WP4 has demonstrated that relative improvement is not sufficient, while simpler to assess. By introducing both relative and absolute EI assessment methodology, a positioning of different solutions regarding their exposure for a given scenario has been made possible. This justifies retrospectively why low relative EI ratio (<10%) solutions have not been down selected after end of year 2. Actually some of them can already be effective to reduce exposure in a scenario where the initial absolute EI is high (e.g. LTE-A Dual hop OFDM on relay system).

On the other hand some of the proposed solutions for EI reduction present the cutting edge of research in their domain (e.g. miniature and directive antenna for

Document ID: D4.3: Final validation and recommendations for smart low exposure index FP7 Contract n°318273



SCBS), while the other analysed radio components and transmission solutions are partially (re)using known physical mechanisms developed to solve other issues in wireless communication systems (energy consumption, capacity increasing, antenna decoupling). Their innovation is first in the adaptation of these mechanisms to the EM exposure lowering.

## WP4 Key learning and suggested improvements:

El is also a relevant metric to compare the benefit of a given technology analysed in a given context or scenario. Positioning several technologies from different RATs on a common El axis is relevant but their ranking is delicate. Even if the methodology is common, one should ensure that the input parameters and the evaluations of all these technologies are homogeneous; which has not been the case in this 3-years long work. In fact some partners have exploited system-level evaluations or laboratory testbeds, those are both local and large scale.

The impact of scenario inputs and the ICT usages is crucial. It positions the absolute EI of a technology. On the one hand, this is an advantage when the solution exposure assessment needs to be analysed over a middle or long period (e.g. new RAT penetration, introduction of voice over IP). On the other hand, this sensitivity to the input scenario must be handled if the objective is to compare the EI of two technologies. In that specific case, the setting of some standardized exposure scenarios has been suggested. The idea is to simplify the ICT scenario with only 2 or 3 inputs parameters that could be play with (for instance the ratio between voice and data, the ratio between UL/DL). The Tx power and Rx power density could be derivated from the existing channel models. Thus the statistical distribution of EI could be assessed by giving complete information than only the mean exposure. A example of this approach is more or less adopted in section 3.2.2.3.

## Future research works & actions:

The proposed EI evaluation methodology should be disseminated in the communications research and development community. This has been initiated through scientific communications but also thanks to inter-projects collaboration, particularly with FP7 MiWaves project that tends to compare EI reduction of a millimetre waves offloading regarding the microwave LTE case in a high throughput indoor scenario. The proposed methodology could be reuse to evaluate the impact on EI of coming low frequency LTE bands (below 700 MHz) known to present higher SAR values. Finally the next steps will consider additional trade-off (energy consumption, deployment cost, robustness). An important future works should consist to increase the TRL of some promising low EMF technologies.

Version: V1.1 91

Dissemination level: PU



# 6 REFERENCES

- [1] LEXNET, Project Deliverable D4.2, "Performance evaluation of low exposure index solutions for components and transmission techniques", http://www.lexnet.fr/, November 2014.
- [2] LEXNET, Project Deliverable D2.3, "Scenarios", http://www.lexnet.fr/, November 2013.
- [3] LEXNET, Project Deliverable D2.8, "Global wireless exposure metric definition", http://www.lexnet.fr/, November 2015.
- [4] 3GPP TR 36.826 v11.3.0 (2013.07), "Relay radio transmission and reception", Release 11.
- [5] E. Kocan, M. Pejanovic-Djurisic, S. Bories, "Downlink Exposure Reduction in Dual-Hop OFDM Decode-and-Forward Relay Systems", special session on Low-EMF Radio-Link Technologies and Wireless Networks Management, in the frame of IEEE ISWCS conf., Brussels, Belgium, August 2015.
- [6] M. Pigeon, C. Delaveaud, L. Riudant, and K. Belmkaddem, "Miniature directive antennas," Intern. J. Microwave Wireless Techn., Feb. 2014.
- [7] J. E. Hansen, "Spherical Near-Field Antenna Measurements," IET, 1988.
- [8] A. Clemente, M. Pigeon, L. Rudant, and C. Delaveaud, "Super directive compact antenna design using spherical wave expansion," IEEE Antennas Propag. Soc. Int. Symp. (APS 2014), Jul. 2014.
- [9] R. F. Harrington, "On the gain and beamwidth of directional antennas," IEEE Trans. Antennas Propag., vol. 6, no.3, pp. 219-225, Jul. 1958.
- [10] R. F. Harrington, "Effect of antenna size on gain, bandwidth and efficiency," J. Res. Nat. Bur. Stand, vol. 64-D, pp 1-12, Jan./Feb. 1960.
- [11] 3GPP TSG RAN, "TR 36.872, Small cell enhancements for E-UTRA and E-UTRAN-Physical layer aspects (Release 12)," V12.1.0, Dec. 2013.
- [12] 3GPPTSG RAN, "TR 36.814, Evolved Universal Terrestrial Radio Access (E-UTRA); Further advancements for E-UTRA physical layer aspects (Release 9)," V9.0.0, Mar. 2010.
- [13] I. Guvenc, et al., "Range expansion and inter-cell interference coordination (ICIC) for picocell networks," in IEEE Vehicular Technology Conference (VTC Fall), pp. 1–6, Sep. 2011
- [14] EARTH, Project Deliverable D4.2, Green Radio Technologies, https://www.ict-earth.eu/publications/ deliverables/deliverables.html, December 2011.
- [15] P. Frenger, P. Moberg, J. Malmodin, Y. Jading, I. Godor, "Reducing Energy Consumption in LTE with Cell DTX," IEEE 73rd Vehicular Technology Conference (VTC Spring), pp.1,5, 15-18 May 2011.
- [16] H. Holtkamp, G. Auer, S. Bazzi, and H. and Haas, "Minimizing Base Station Power Consumption," IEEE Journal on Selected Areas in Communications, Vol. 32, No. 12, December 2014.
- [17] C. Hoymann, D. Larsson, H. Koorapaty, and J.F. Cheng, "A Lean Carrier for LTE," IEEE Communications Magazine, vol. 51, no. 2, pp. 74–80, 2013.
- [18] H. Ishii, Y. Kishiyama, H. Takahashi, "A novel architecture for LTE-B:C-plane/U-plane split and Phantom Cell concept," IEEE Globecom Workshops, 2012 pp.624,630, 3-7 Dec. 2012.



- [19] A. Mohamed, O. Onireti, M. Imran, A. Imrany, R. Tafazolli, "Correlation-based adaptive pilot pattern in control/data separation architecture," in Communications (ICC), 2015 IEEE International Conference on , vol., no., pp.2233-2238, 8-12 June 2015.
- [20] 3GPP TR 36.104 "Evolved Universal Terrestrial Radio Access (E-UTRA); Base Station (BS) radio transmission and reception", (Release 12), 2013.
- [21] O. Kivekas, J. Ollikainen, T. Lehtiniemi, P. Vainikainen, "Bandwidth, SAR, and efficiency of internal mobile phone antennas", Electromagnetic Compatibility, IEEE Transactions on, Vol. 46, No. 1, 71-86, 2004.
- [22] A. H. Kusuma, A.-F. Sheta, I. M. Elshafiey, Z. Siddiqui, M. A. S. Alkanhal, S. Aldosari, S. A. Alshebeili, S. F. Mahmoud, "A new low SAR antenna structure for wireless handset applications", Progress In Electromagnetics Research, Vol. 112, 23-40, 2011.
- [23] M.I. Kitra, C.J. Panagamuwa, P. McEvoy, J.C. Vardaxoglou, J.R. James, "Low SAR Ferrite Handset Antenna Design", IEEE Transactions on Antennas and Propagation, vol. 55, no. 4, pp 1155-1164, April 2007.
- [24] R. Ikeuchi, A. Hirata, "Dipole Antenna above EBG Substrate for Local SAR Reduction", IEEE Antennas and Wireless Propagation Letters, Vol. 10, pp 904-906, 2011.
- [25] S. Lee, N. Kim, S.Y. Rhee, "Design of Novel Artificial Magnetic Conductor Reflector and Its SAR Analysis", Progress In Electromagnetics Research Symposium Proceedings, Moscow, Russia, pp 325-328, August 2012.
- [26] A. C. Lepage, X. Begaud, and J. Sarrazin, Microwave and Millimeter Wave Circuits and Systems: Emerging Design, Technologies and Applications, chapter 3: Wideband directive antennas with High Impedance Surfaces. Wiley, 2012.
- [27] M. Grelier, F. Linot, A. C. Lepage, X. Begaud, J. M. Le Mener, and M. Soiron, "Analytical methods for AMC and EBG characterizations", Applied Physics A: Materials Science & Processing, 102(2), Feb.2011.
- [28] F. Linot, X. Begaud, M. Soiron, C. Renard, and M. Labeyrie, "Characterisation of a loaded high impedance surface", International Journal of Microwave and Wireless Technologies, 1(9):483–487, Dec. 2009.
- [29] Y. Pinto, X. Begaud, A. C. Lepage, "Monopole Antenna with Metamaterial Structures", EuCAP 2014 -The 8th European Conference on Antennas and Propagation, April 2014.
- [30] Y. Pinto, X. Begaud, "Monopole antenna with metamaterials to reduce the exposure", Applied Physics A: Materials Science & Processing, May 2015. http://dx.doi.org/10.1007/s00339-015-9230-0.
- [31] Y. Pinto, X. Begaud, "Mobile phone model with metamaterials to reduce the exposure", META15 -The the 6th International Conference on Metamaterials, Photonic Crystals and Plasmonics. New York, USA, August 2015.
- [32] S. Leng, W. Ser, C.C. Ko," A simple constrained based adaptive null steering algorithm," in Proc. 2008 16th European Signal Processing Conference, Aug. 2008.
- [33] R.A. Qamar, N.M. Khan, "Null steering, a comparative analysis," in Proc. IEEE 13th International Multitopic Conference, 2009.INMIC 2009.Dec. 2009.
- [34] M.R.R. Khan, V.Tuzlukov,"Null-steering beamforming for cancellation of Cochannel interference in CDMA wireless communication system," in Proc. 2010

- 4th International Conference on Signal Processing and Communication Systems (ICSPCS), Dec. 2010.
- [35] S. Leng, W. Ser, "Adaptive null steering beamformer implementation for flexible broad null control", Elsevier Signal Processing, pp. 1229–1239, vol. 91, 2011.
- [36] K-C.Chim, K. C. L. Chan, R. D. Murch, "Investigating the impact of smart antennas on SAR", IEEE Transactions on Antennas and Propagation, vol. 52, no. 5, May 2004.
- [37] K.-C. Chim R.D. Murch, "Investigating the effect of smart antenna on SAR," IEEE Antennas and Propagation Society International Symposium, 2002, pp.432-435 vol.1, 2002.
- [38] B.M. Hochwald, D. J. Love, S. Yan, J. Jin, "SAR codes", Information Theory and Applications Workshop (ITA), 2013, pp.1-9, 10-15 Feb. 2013.
- [39] B.M. Hochwald, D.J. Love, S. Yan, P. Fay, J-MJin, "Incorporating specific absorption rate constraints into wireless signal design," in Communications Magazine, IEEE, vol.52, no.9, pp.126-133, September 2014.
- [40] M.-C. Gosselin, G. Vermeeren, S.-V. Kuhn, V. Kellerman, S. Benklar, and T. M. I. Uuitupa, W. Joseph, A. Gati, J. Wiart, F. J. C. Meyer, L. Martens, T. Nojima, T. Hikage, Q. Balzano, A. Christ, N. Kuster "Estimation formulas for the specific absorption rate in humanexposed to base-station antennas," IEEE Trans. Electromagn. Compat., Vol. 53, No. 4, Nov. 2011, pp. 909-922.
- [41] LEXNET, Project Deliverable D6.1, "Validation platform framework and initial assessment", http://www.lexnet.fr/, April 2014.
- [42] ITU-R, report M2135, "Guidelines for evaluation of radio interface technologies for IMT-Advanced", 2008.
- [43] IEEE 802.11-2012, "IEEE Standard for Information technology Telecommunications and information exchange between systems Local and metropolitan area networks Specific requirements, Part 11: Wireless LAN Medium Access Control (MAC) and Physical Layer (PHY) Specifications", 2012.
- [44] IEEE 802.11 TGax, "TGax Simulation Scenarios", doc: IEEE 802.11-14/0980r3, Jul 2014.
- [45] IEEE 802.11 TGn, "TGn Channel Model", doc: IEEE 802.11-03/0940r4, May 2004.
- [46] W. Joseph, D. Pareit, G. Vermeeren, D. Naudts, L. Verloock, L. Martens & I. Moerman, "Determination of the duty cycle of WLAN for realistic radio frequency electromagnetic field exposure assessment", Progress in biophysics and molecular biology 111.1, (pp.30-36).
- [47] J. Zheng, A. Jamalipour, "Wireless sensor networks: a networking perspective", Wiley-IEEE Press, 2009.
- [48] Cisco, "Cisco Visual Networking Index: Global Mobile Data Traffic Forecast Update, 2013–2018", 2014.
- [49] Dresden-Elektronik, "Radio modules deRFmega128", <a href="https://www.dresden-elektronik.de/funktechnik/products/radio-modules/adapter-boards-oem-modules/?L=1">https://www.dresden-elektronik, "Radio modules deRFmega128", <a href="https://www.dresden-elektronik.de/funktechnik/products/radio-modules/adapter-boards-oem-modules/?L=1">https://www.dresden-elektronik, "Radio modules deRFmega128", <a href="https://www.dresden-elektronik.de/funktechnik/products/radio-modules/adapter-boards-oem-modules/?L=1">https://www.dresden-elektronik.de/funktechnik/products/radio-modules/adapter-boards-oem-modules/?L=1</a>.
- [50] LEXNET project D4.1 deliverable "D4.1: Promising Low Exposure Index Solutions for Components and Transmission Techniques", http://www.lexnet.fr/, November 2013.

Document ID: D4.3: Final validation and recommendations for smart low exposure index FP7 Contract n°318273



95

# 7 APPENDIX 1: INTERNAL REVIEW

	Reviewer	1:Filipe Cardoso (INOV)		Reviewer 2: Yann Toutain (Satimo)			
	Answer	Comments	Type*	Answer	Comments	Type*	
1. Is the deliverable	e in accordan	ce with					
(i) the Description of Work?	Yes ☐ No		□ M □ m □ a	⊠ Yes □ No		□ M □ m □ a	
(ii) the internation State of the Art?	al ⊠ Yes □ No		☐ M ☐ m ☐ a	⊠Yes □ No		☐ M ☐ m ☐ a	
2. Is the quality of	he deliverabl	e in a status					
(i) That allows to send it to EC?	⊠ Yes □ No		□ M □ m □ a	⊠ Yes □ No		□ M □ m □ a	
(ii) that needs improvement of the writing by the editor of the deliverable?		Eliminate typos and obtain a consistent writing/formatting style through the whole document	∐ M ⊠ m	☐ Yes ☑ No		□ M □ m □ a	
(iii) that needs further work by the partners responsible for	. No		□ M □ m □ a	⊠ Yes □ No	Some minor clarifications are required, in particular on some numbers.	☐ M ⊠ m ☐ a	

<sup>\*</sup> Type of comments: M = Major comment; m = minor comment; a = advice



# 8 APPENDIX 2: El FORMULA & ASSOCIATED INPUT DATA

The general formula of the EI is reminded hereafter:

$$EI^{SAR} = \frac{1}{T} \sum_{t}^{N_{T}} \sum_{p}^{N_{P}} \sum_{e}^{N_{E}} \sum_{r}^{N_{R}} \sum_{c}^{N_{C}} \sum_{l}^{N_{L}} \sum_{pos}^{N_{pos}} f_{t,p,e,r,l,c,pos} \left[ \sum_{u}^{N_{U}} (d^{UL} \bar{P}_{TX}) \right]$$

$$+ d^{DL} \bar{S}_{RXinc} + d^{DL,closedevices} S_{RXinc}^{DL,closedevices} \left[ \frac{W}{kg} \right]$$

### where:

- EI<sup>SAR</sup> is the Exposure Index value, the average exposure of the population of the considered geographical area over the considered time frame T. SAR refers to whole-body SAR, organ-specific SAR or localized SAR.
- N<sub>T</sub> is the number of considered periods within the considered time frame (e.g., single day);
- N<sub>P</sub> is the number of considered Population categories;
- N<sub>E</sub> is the number of considered Environments;
- N<sub>R</sub>is the number of considered Radio Access Technologies;
- N<sub>C</sub> is the number of considered Cell types;
- N<sub>L</sub> is the number of considered user Load profiles;
- N<sub>pos</sub> is the number of considered Postures;
- N<sub>U</sub> is the number of considered Usages with devices
- P̄<sub>TX</sub> is the mean TX power transmitted by the users' devices during the period
  t, in usage mode u, connected to RAT r, in environment e. For example, when
  EI is computed from simulation tools, the TX power can be predicted over a
  map that covers the whole considered geographical area and the average
  value is extracted for the EI evaluation.
- $\bar{S}_{RXinc}$  is the mean incident power density on the human body during the period t, induced by RAT r, in environment e. A distribution of the incident power density for the whole considered geographical area is considered and the average value over this area is taken into account for the EI evaluation.
- $S_{RXinc}^{DL,close\,devices}$  is the incident power density on the human body during the period t, induced by a wireless device connected to RAT r of a user in the proximity, in environment e. This term is important when the exposed person is the user itself; it can also be significant for persons in the proximity of users of a wireless device, for instance in a crowded meeting room, in public transportation, etc. In the applications discussed in this paper, this term is neglected. We also remark that  $S_{RXinc}^{DL,close\,devices}$  depends on the orientation of the user of the wireless device with respect to the body of the people in its proximity.
- $d^{\text{UL}}(\frac{ws}{kg}/W)$ ,  $d^{\text{DL,close devices}}(\frac{ws}{kg}/\frac{w}{m^2})$ , and  $d^{\text{DL}}(\frac{ws}{kg}/\frac{w}{m^2})$  are the normalised raw dose values for UL, the DL from the user in the proximity, and DL from



base stations and access points, respectively, all multiplied by the time spent in the configuration.

• f<sub>t,p,e,r,l,c,pos</sub> is the fraction of the total population that corresponds to population category p, user load profile I, in posture pos, connected to RAT r, for a cell type c, in environment e, during the time period t.

In the following, we explain the different terms used in the EI formula in more detail.

# Coefficients d<sup>UL</sup> and d<sup>DL</sup>

The coefficient  $d^{\mathit{UL}}$  is associated to the exposure induced by the UL and expressed as an absorbed dose normalised to a transmitted power of 1 W:

$$d_{\left[\frac{S}{\lg}\right]}^{UL} = \frac{TD_{t,p,l,e,r,c,u,pos[s]}^{UL}SAR_{p,r,u,pos[W/\lg]}^{UL}}{P_{TX[W]}^{ref}} \left[\frac{Ws}{\lg}/W\right]$$
(2)

where:

- $TD_{t,p,l,e,r,c,u,pos}^{UL}$  is the time duration of usage u, and a user profile load l, when connected to the RAT r, operating in cell type c, in the environment e, for the population category p, in the posture pos, during the time period of the day t.
- $\frac{SAR_{p,r,u,pos}^{UL}}{P_{TX}^{ref}}$  can be the whole body or an organ-specific or tissue-specific SAR value for the usage u and the posture pos, in the frequency band of the RAT r, and the population category p, calculated for an incident emitted power of  $P_{TX}^{ref}$  and normalized to this power.

The coefficient  $d^{DL}$  is associated to the exposure induced by the DL and also expressed as an absorbed dose normalised to an incident power density of 1 W/m<sup>2</sup>:

$$d_{\left[\frac{S}{\lg g}\right]}^{DL} = \frac{TD_{t,p,e,r,c,pos[s]}^{DL}SAR_{p,r,pos[W/\lg g]}^{DL}}{S_{RX[W]inc}^{ref}} \left[\frac{Ws}{kg} / \frac{W}{m^2}\right]$$
(3)

where:

- $TD_{t,p,e,r,c,pos}^{DL}$  is the time duration of posture pos, when connected to the RAT r, operating in cell type c, in the environment e,for the populationp,during the time period of the day t.
- $\frac{SAR_{p,r,pos}^{DL}}{S_{RXinc}^{ref}}$  can be the whole body or an organ-specific or tissue-specific SAR value induced by the base station or access points of the RAT r, in the population p, for the posture pos, normalized to the received power density  $S_{RXinc}^{ref}$ .



Based on WP2 global scenario for July 2014; the hypothesis is that, in 2014, 48 % of the connections will be 3G connections, 44% will be 2G and 8 % 4G connections. And considering the existence of four telecom operators in France we assumed that only 25 % of these percentages will use the Orange network.

## El\_global=

(%children\*El\_children+%young\_people\*El\_youngpeople+%adults\*El\_adults+%seniors\*El\_seniors)/(24\*3600); [W/kg]

EI\_adults = k1 x PTX\_indoor\_day\_voice + k2 x PTX\_outdoor\_day\_voice + k3 x PTX \_indoor\_night\_voice + k4 x PTX \_outdoor\_night\_voice +

k5 x PTX\_indoor\_day\_data / Th\_indoor\_day\_data + k6 x PTX\_outdoor\_day\_data / Th\_outdoor\_day\_data + k7 x PTX\_indoor\_night\_data / Th\_indoor\_night\_data + k8 x PTX\_outdoor\_night\_data / Th\_outdoor\_night\_data +

k9 x SRX\_indoor\_day + k10 x SRX\_outdoor\_day + k11 x SRX\_indoor\_night + k12 x SRX\_outdoor\_night;

(transmitted power values in W, received power density values in W/m2and throughputs in kB/s)

## Rural macro 2G scenario

k coefficients	Children	Young people	Adults	Seniors
k1	0.1127	0.2328	0.2304	0.1698
k2	0.0483	0.0998	0.0988	0.0728
k3	0.0673	0.1389	0.1375	0.1013
k4	0.0289	0.0595	0.0589	0.0434
k5	0.0247	0.0719	0.014	0.0012
k6	0.0096	0.0197	0.0052	4.36e-4
k7	0.0269	0.0574	0.0153	0.0013
k8	0.0105	0.0215	0.0057	4.8e-4
k9	243.54	168	166.32	152.88
k10	52.92	31.2	32.76	45.24
k11	405.9	265.44	263.76	263.76
k12	7.56	15.6	17.16	17.16

# Urban macro 2G scenario

k coefficients	Children	Young people	Adults	Seniors
k1	0.1427	0.2797	0.2768	0.2039
k2	0.0612	0.1199	0.1186	0.0874
k3	0.0849	0.1662	0.1645	0.1212
k4	0.0364	0.0712	0.0705	0.0520
k5	0.0303	0.0645	0.0180	0.0019
k6	0.0118	0.0242	0.0068	7.1e-4
k7	0.033	0.0704	0.0197	0.0021
k8	0.0129	0.0264	0.0074	7.8e-4
k9	243.54	168	166.32	152.88
k10	52.92	31.2	32.76	45.24
k11	405.9	265.44	263.76	263.76
k12	7.56	15.6	17.16	17.16





# Rural macro 3G scenario

k coefficients	Children	Young people	Adults	Seniors
k1	0.0736	0.2175	0.1032	0.0761
k2	0.0287	0.0932	0.0442	0.0326
k3	0.0524	0.1635	0.0735	0.0542
k4	0.0204	0.0701	0.0315	0.0232
k5	0.9974	2.4916	0.9762	0.4691
k6	0.2389	0.3580	0.0510	0.0080
k7	1.9094	3.7024	1.6268	0.6442
k8	0.3137	0.47	0.0646	0.0097
k9	210.87	159	157.41	144.69
k10	48.51	28.2	29.61	40.89
k11	351.45	251.22	249.63	249.63
k12	6.93	14.1	15.51	15.51

# Urban macro 3G scenario

k coefficients	Children	Young people	Adults	Seniors
k1	0.0666	0.1970	0.0935	0.0689
k2	0.0260	0.0844	0.0401	0.0295
k3	0.0507	0.1566	0.0712	0.0525
k4	0.0198	0.0671	0.0305	0.0225
k5	0.79	1.97	0.9	0.4565
k6	0.1672	0.2505	0.0352	0.0054
k7	1.5649	2.8367	1.5048	0.6251
k8	0.1944	0.2913	0.034	0.0058
k9	210.87	159	157.41	144.69
k10	48.51	28.2	29.61	40.89
k11	351.45	251.22	249.63	249.63
k12	6.93	14.1	15.51	15.51

# Rural macro LTE scenario

k coefficients	Children	Young people	Adults	Seniors
k1	0	0	0	0
k2	0	0	0	0
k3	0	0	0	0
k4	0	0	0	0
k5	0.5492	1.0528	0.8031	0.3634
k6	0.0652	0.1552	0.0788	0.0100
k7	1.4271	1.7294	1.3342	0.4987
k8	0.0773	0.2035	0.1	0.01
k9	196.02	147	145.53	133.77
k10	45.36	25.2	26.46	36.54
k11	326.7	232.26	230.79	230.79
k12	6.48	12.6	13.86	13.86

Dissemination level: PU



# Urban macro LTE scenario

k coefficients	Children	Young people	Adults	Seniors
k1	0	0	0	0
k2	0	0	0	0
k3	0	0	0	0
k4	0	0	0	0
k5	0.4932	0.9144	0.7315	0.3531
k6	0.044	0.1087	0.0548	0.0066
k7	1.3438	1.5	1.2194	0.4849
k8	0.0458	0.1266	0.0620	0.0061
k9	196.02	147	145.53	133.77
k10	45.36	25.2	26.46	36.54
k11	326.7	232.26	230.79	230.79
k12	6.48	12.6	13.86	13.86

# WiFi scenario

k coefficients	Children	Young people	Adults	Seniors
k1	0	0	0	0
k2	0	0	0	0
k3	0	0	0	0
k4	0	0	0	0
k5	6.8569	16.1083	13.4286	6.4898
k6	0	0	0	0
k7	8.7125	17.2282	14.4512	6.7819
k8	0	0	0	0
k9	6.8310	4.2	4.1580	3.8220
k10	45.36	25.2	26.46	36.54
k11	11.3850	6.6360	6.5940	6.5940
k12	6.48	12.6	13.86	13.86

Version: V1.1

Dissemination level: PU